DEMAND SIDE MANAGEMENT FOR BUILDING ENERGY EFFICIENCY THROUGH HYBRID DAYLIGHTING SYSTEM AND BATTERY ENERGY STORAGE SYSTEM

by

Tonghui Li

A Dissertation Submitted in

Partial Fulfillment of the

Requirements for the Degree of

Doctor of Philosophy

in Engineering

at

The University of Wisconsin-Milwaukee

May 2018

ABSTRACT

DEMAND SIDE MANAGEMENT FOR BUILDING ENERGY EFFICIENCY THROUGH HYBRID DAYLIGHTING SYSTEM AND BATTERY ENERGY STORAGE SYSTEM

by

Tonghui Li

The University of Wisconsin-Milwaukee, 2018

Under the Supervision of Professor Chris Y. Yuan

This dissertation aims to investigate demand side management (DSM) to improve building energy efficiency and reduce on-peak electricity demand. Daylighting device and battery energy storage system (BESS) for peak shaving are proposed and studied. To reduce the cost and improve the efficiency of building lighting, an innovative parabolic trough solar lighting and thermal (PTL/T) system is designed and analyzed. In the proposed system, a parabolic trough collector (PTC) controlled by two-axis solar tracking system is used as solar collector. The collected sunlight is split by a cold mirror into visible light and infrared light. The visible light is reflected by the cold mirror, re-concentrated by a second-stage Fresnel lens, and then delivered by plastic optical fiber to the buildings for daylighting. The infrared light goes through the cold mirror, reaches the thermal system, and is used for heat generation. An economic and efficiency model of the PTL/T system is built to optimize the system parameters. A case study is conducted to get a specific optimized illumination area and PTC area. Its maximum energy savings, and simple payback period in the US are calculated to demonstrate its economic feasibility. The results show the proposed PTL/T system is competitive compared with traditional solar energy systems.

Peak demand charge is a significant portion of building utility cost, and battery energy storage system (BESS) is recognized as an effective technology for peak demand reduction. In this research, a mathematical model is developed to analyze the economic benefit of using lithium-ion BESS for peak shaving. The impacts of four key factors including BESS capacity, battery degradation, operation temperature, and utilization rate are quantified and compared for the first time. The simulation results show that the Net Present Value of Unit BESS (NPVU) decreases with the increase of Normalized Size Percentage (NSP). The benefit from optimizing the BESS capacity is limited by relatively low NPV because only around 4% NSP can be chosen. Due to the extremely low Utilization Rate (UR), the final cycling loss is at a super low level. The average NPVU can be improved by around 7.8% through the optimization of operation temperature in the US. In contrast, a 69.9% increase of NPVU is obtained through the increase of UR by peak-time charging. Through the comparison of all the analyzed factors, the UR is recognized as the most significant factor.

After, two new DSMs based on sharing economy are proposed to maximize the utilization and savings of BESS. Peak shaving is the base function of all proposed sharing network. The simple sharing, which shares one BESS among multiple customers, is capable to work as a cloud service. The demand reduction for each customer is optimized using genetic algorithm (GA). Simulation results show the sharing among six customers can increase max NSP, optimized NSP, NPVU and UR by 97.9%, 102.5%, 515.3% and 180.6% respectively without significant battery life impact. The comprehensive sharing, which shares one BESS for different services, works in modularized method. All the services that can be conveniently applied on the customer side are evaluated, which include TOU peak load shifting, integration of

PTL/T, power factor correction and combine meter effect. Economic analysis shows all the modules can provide considerable additional savings to the DSM system.

TABLE OF CONTENTS

LIST OF FIGURES

LIST OF TABLES

ACKNOWLEDGEMENTS

First and foremost, I want to thank my advisor, Professor Chris Yuan, to work with him has been a fantastic journey for me. He has provided all the supports, both academic and life, during the whole Ph.D. career. He has been always inspiring me in times of research ideas and approaches. His research standard and work attitude set a great example to me. It is really appreciated that I can work for him as a Ph.D.

I would also like to thank all the professors in the Industrial Assessment Center in University of Wisconsin Milwaukee (IAC-UWM), Professor Benjamin Church, Professor John Reisel, Professor Ryoichi Amano, Professor Wilkistar Otieno. They taught me so much during the assessments in the last several years. Many of my research ideas were inspired by assessments in the IAC-UWM.

In addition, I would like to thank all my colleagues in the IAC-UWM, and the colleagues from Laboratory for Sustainable and Nano-Manufacturing (LSNM) at the University of Wisconsin Milwaukee, especially the help from Yadan Zeng, Fan Yang, Yelin Deng, Junling Xie, Xianfeng Gao, Jianyang Li, who are always willing to help.

Finally, I would like to thank my family. Their love, understanding, and support has always been there to support me, help me to get through tough days.

1. Introduction and Research Objectives

Demand Side Management (DSM) is the energy consumption management on demand side including load management, energy efficiency and energy savings, etc.[1, 2]. DSM has become popular in recent years due to the rapid growth of electricity demand and renewable energy. According to the international energy outlook 2016 from the U.S. Energy Information Administration (EIA), the net electricity demand in the Organization for Economic Cooperation and Development (OECD) countries is projected to increase by 38% from 2012 to 2040. Meanwhile, the total world net electricity generation including non-OECD countries is predicted to increase by 69% during the same period. The growth of electricity demand already has put heavy burden on the grid. The share of renewable energy in the grid power accounted for more than 15% in 2016 [3]. Volatile renewable energy sources and electro-mobility added extra challenges to the grid. Normally, the grid capacity is designed to satisfy the peak power demand rather than the average demand, which requires expensive operation of peak-load plants during peak hours. With the rapid development of smart grid, energy storage system and energy efficiency technology, DSM has become another cheaper alternative to managing the peak power demand. In this thesis, three topics are researched to achieve an affordable and efficient DSM system for buildings: 1) development of a novel daylighting/thermal system to increase the efficiency of solar lighting system, 2) economic analysis of using battery energy storage system (BESS) for peak shaving, 3) new business models of sharing BESS.

1.1 Daylighting

The sunlight was the main source for the lighting of buildings until the end of 19th century. Due to the invention and development of electric lamps, the artificial light takes the place of sunlight and becomes the main lighting source in the modern buildings. The Energy consumption

from lighting contributes about 7% of the total electricity generated in the U.S. in 2017 [4]. Because of the overwhelming energy price, energy savings for lighting system has attracted substantial research interests recently. There are mainly two research directions in this field: one is inventing more efficient artificial lights such as T5 lamps, LED, etc.; the other one is using daylighting system to eliminate the usage of electricity for lighting in day time. This dissertation focuses on daylighting and aims to propose an optimum novel parabolic trough lighting and thermal system.

Daylighting is a lighting approach which uses natural sunlight to light the interior spaces of buildings during the day time. It is important for sustainable buildings because of its psychological and physiological benefits to the worker and its great potential in electricity savings [5]. Daylighting exists in most of buildings with windows and skylights as the most common approaches. The traditional daylighting systems usually have the problem of glare, heat loss and light transmission limitation etc. Many new daylighting devices and systems were developed in the last several decades to overcome these problems.

Daylighting can be categorized by many methodologies. The devices can be divided into: side-daylighting systems and top-daylighting systems based on system locations; passive and active daylighting systems based on harvesting approach of sunlight; traditional and integral hybrid daylighting systems based on their relationships to artificial lighting. The main purpose of this research is to find an efficient method to gather and transmit the sunlight. When considering how the sunlight is gathered and transmitted, the daylighting systems include the following three main categories:

1) Skylight. Skylight systems are one of the simplest and effective approaches to bring in sunlight into interior spaces. Nevertheless, some obvious drawbacks affect the application of this

system. The presence of a skylight results in the direct transmission of sunlight into the interior space which causes glare and heat loss problems. Skylights are typically easy and cheap to be installed for new buildings, but difficult to be added to the existing buildings. Meanwhile, a skylight is limited to only provide daylight to the top floor of a multi-story building or for a single-story building [6]. Tubular guidance daylight systems (TGDS) are more advanced than the traditional skylight system. TGDS uses a domed light collector to collect sunlight and passes the light through a tube. A diffuser is utilized at the end of the tube to deliver the light to an interior space. This system is capable to reduce the glare and heat loss problems from skylights. However, it is still difficult to be installed and has limited lighting capability.

2) Beam (or redirection) systems. Beam systems includes light shelves, light reflectors, and prismatic glazing systems etc. [7]. They use simple reflective or refractive elements to bring the sunlight into a room close to the outside. Similar to the skylight, it has drawbacks of glare, heat transfer, and changing light levels.

3) Optical fiber daylighting (OFD) systems. These systems transmit concentrated sunlight to interior space using plastic optical fiber (POF). A typical representative of this system is the hybrid lighting system (HLS). In HLS, sunlight is concentrated by a solar collector, delivered into a building through non-image optical fiber, and then distributed by a diffuser to the end use. In order to provide sufficient and consistent lighting, the transmitted daylight in HLS is usually integrated with dimmable artificial lights [8]. There are many significant benefits in this system: a) evenly lighting without glare is achieved by using diffuser; b) high solar collector efficiency is obtained through the use of active solar tracking system; c) daylight can be distributed to deeper inner space of buildings using optical fiber; d) it is easy to be installed on the existing building due

to no extra construction work requirement. All these advantages make the OFD one of the most promising technologies in the daylighting systems.

The OFD system has been studied worldwide due to its significant application potential. This concept was initially proposed in early 1970s. The first OFD system was HIMAWARI which was developed in Japan [9]. Hybrid Solar Lighting (HSL) was developed by Oak Ridge National Laboratory (ORNL) in the United States [10] as shown in Figure 1. HSL uses parabolic dish as solar collector, which is controlled by a two-axis solar tracking system. The concentrated ray is reflected and re-concentrated to the optical fiber bundle by an elliptical cold mirror. The visible light is then delivered and utilized. The daylighting is integrated with a dimmable electric lighting system to achieve constant lighting levels and simultaneously save electrical energy. The primary parabolic concentrator and the secondary reflector of the HSL are optimized by using the principles of the telecommunications antennas [11]. A successful commercialized HLS system called Parans was invented in Sweden [12] as shown in Figure 2. The main difference between Parans and HSL is that Parans uses many small Fresnel lenses as solar collectors. Also, a primary cost-effective HLS was developed in China [13] aiming to bring down the cost of HLS. An exegetic analysis model was established in [14] to study the performance of the OFD system. An OFD design guideline was proposed based on the proposed model. A comparative study was done in [15] for a light pipe and an OFD system. The results showed more daylight could be harvested and the evenness of the lighting is better when using the OFD system. Two sample OFD devices were developed and analyzed in South Korea [16]. They focused on obtaining uniform illumination at the entrance of optical fibers. Shao et al. researched the feasibility of using optical rods for daylighting [17]. Couture et al. suggested another novel daylighting system by combining the dome collector and optical fiber together [18]. It showed a special well-designed dome is possible

to act as an effective and cheap collector for optical fiber daylighting system. The transmission efficiency of optical fiber is critical for fiber daylighting system. The straight and bent optical-loss of optical fiber was modelled and validated by Tekelioglu et al. [19]. The same research group [20] divided the transmission losses of the optical fiber into basic three sources: effect of interface roughness, effect of interface defects and cladding absorption. The losses were theoretically modelled. The results were validated by literature data. The light transmission characteristic of optical fiber bundle was analyzed by [21]. It revealed that the fiber numbers and combination approach greatly influence the transmission capacity of light by fiber bundle. Due to the high concentration of sunlight, the heat problem at the entrance of fiber bundle is severe. Cheadle et al. modelled this heat generation and transfer process [22]. Some possible solutions were proposed according to the simulation results. Overall, OFD system is technically powerful enough to provide sufficient lighting to interior buildings but its cost is prohibitive which hinders its popularization. Public data shows that HSL system costs $330 to illuminate 1 m^2 when launched in 2007 [23].

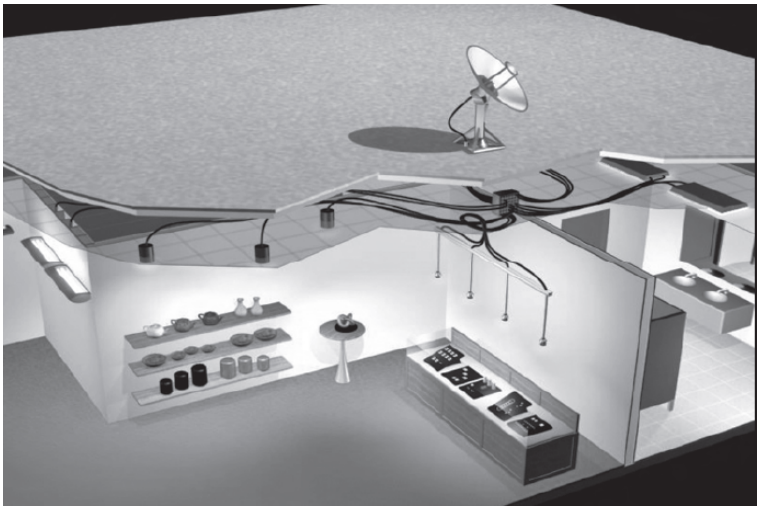

Figure 1. Hybrid Solar Lighting (HSL) System

Figure 2. Parans System

Solar collector system is one of the most important and expensive parts in OFD. It will be convenient and cheap to use successful commercial solar collector in OFD. The parabolic trough collector (PTC) is a state of art product and is always set as a benchmark for solar collector. The success of this technology is mainly indicated by the operation of nine commercial scale solar power plants, such as SEGS and Nevada Solar One [24-28]. However, no systematic study about the utilization of PTC in OFD system has been done so far. This thesis proposes a novel structure which uses PTC in OFD. The advantage of this application not only lies in the cost effectiveness, but also in its ability to increase the overall system efficiency. Infra-red (IR) is treated as harmful for OFD system because of heat problem. Due to the structure and cost limitation, IR is usually split and abandoned in existing OFD system. Nonetheless, this part of energy can be easily used for heating purpose if a PTC is applied in OFD system, which means full spectrum solar energy utilization can be achieved and the system energy efficiency can be increased. Actually, full spectrum solar energy utilization was already employed by many solar energy projects. The concentrating photovoltaic/ thermal (CPV/T) system was developed in Australian National University [29]. In this system, the sunlight is split into visible light and infra-red for different

purposes. This system electrical and thermal performance was analyzed through modelling in TRNSYS [30]. The thermal and electrical efficiencies were found to be around 58% and 11% respectively. Therefore, it is proposed to use PTC in optical fiber daylighting system to realize the combination of daylighting and heating using full spectrum technology in this research.

1.2 Battery Energy Storage System (BESS) for Peak Demand Reduction

Peak demand is the highest power consumption at a specific time interval during a billing period. The utility charging rate of the peak demand may be more than 100 times higher than that of the electricity usage rate because of the high generation cost during peak demand periods [31]. Electricity rate is still increasing quickly year by year as shown in Figure 3. According to the data from Industrial Assessment Center (IAC) [32], the peak demand charge takes 31.8% of the total electricity bill in small and medium sized US manufacturers in 2015. The detailed demand charge percentage in the total electricity bill in small and medium sized US manufacturers is shown in Figure 4.

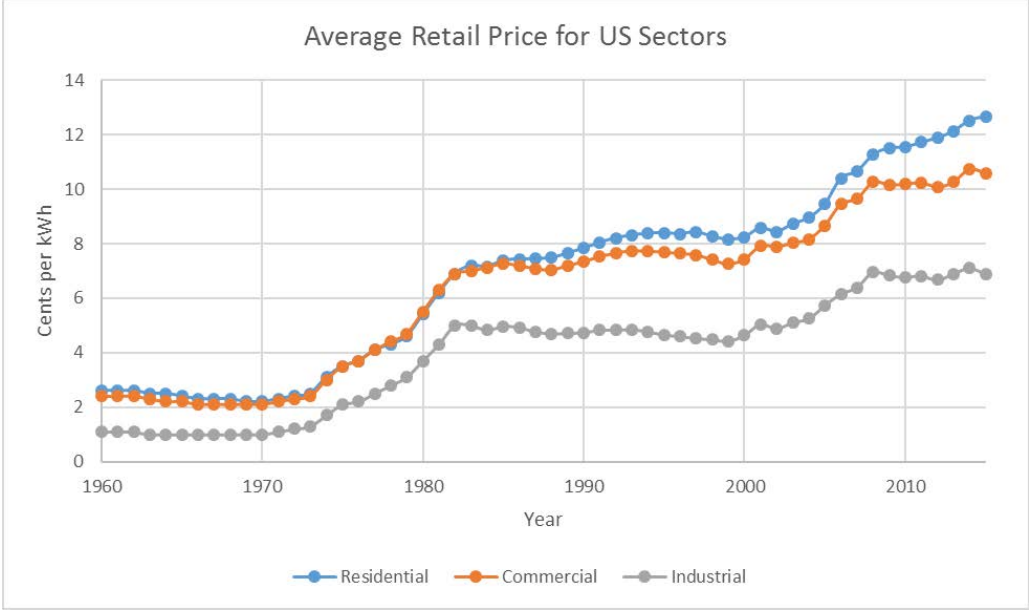

Figure 3. Growth of Electricity Rate

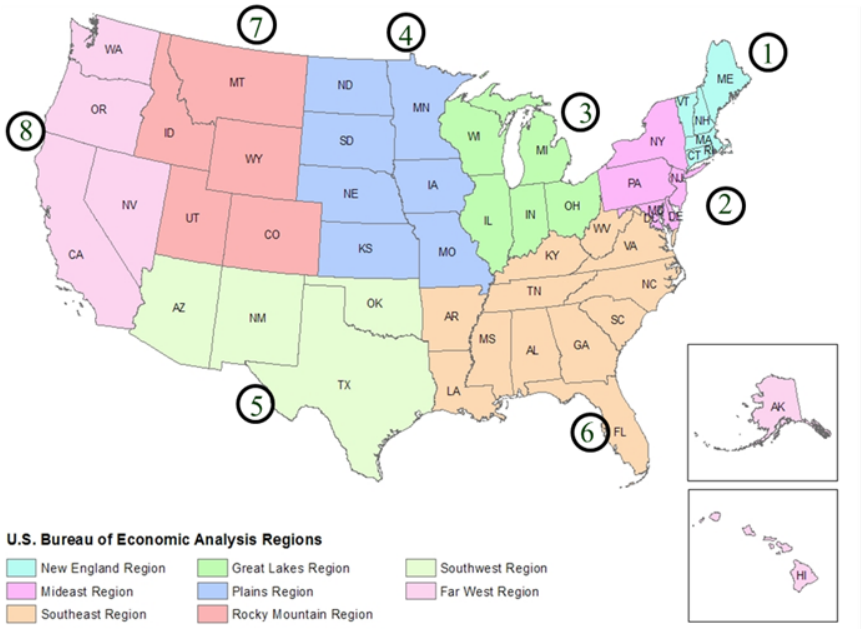

Region Code	Demand %
1	21.6%
2	24.2%
3	33.6%
4	29.0%
5	29.9%
6	23.4%
7	39.2%
8	24.3%

Figure 4. Demand Charge Percentage of Small and Medium Sized US Manufacturers

Peak demand is typically met by peak generators, which are costly, low utilized, less efficient, and with high GHG emissions. An alternative approach is to adopt demand response (DR) programs, which is to shift power loads from peak time to lower power demand periods to avoid power supply shortage. The DR programs could benefit both the utility companies and the consumers by balancing power supply and demand. It also encourages the deployment of new technologies, such as distributed generation and energy storage, and improves the efficiency and reliability of the electric system [1]. Traditional DR often causes interruption of production or curtailing of appliances for the participated customers. Over the past decades, the economics and technologies of the battery energy storage system (BESS) have been improved [33, 34], which makes the BESS based DR popular. Compared with traditional DR, the advantages of BESS based system includes instantaneously response, no interruption, precise control, dependability, and managing over-generation etc. Behind-the-meter (BTM) BESS has drawn particularly more

attention because of its flexibility and possible ability to integrated with other services [35-37], such as BTM BESS is also capable of shifting peak load to off peak time for time-of-use (TOU) customers, improving the power quality and regulating the frequency for industrial facilities. Furthermore, BESS is an essential support for the grid or facilities with renewables because of its capability to reduce intermittent behaviors of renewables caused by changing environmental conditions [38]. The renewable energy share has been growing quickly in all sectors in the US in the last decade, as shown in Figure 5.

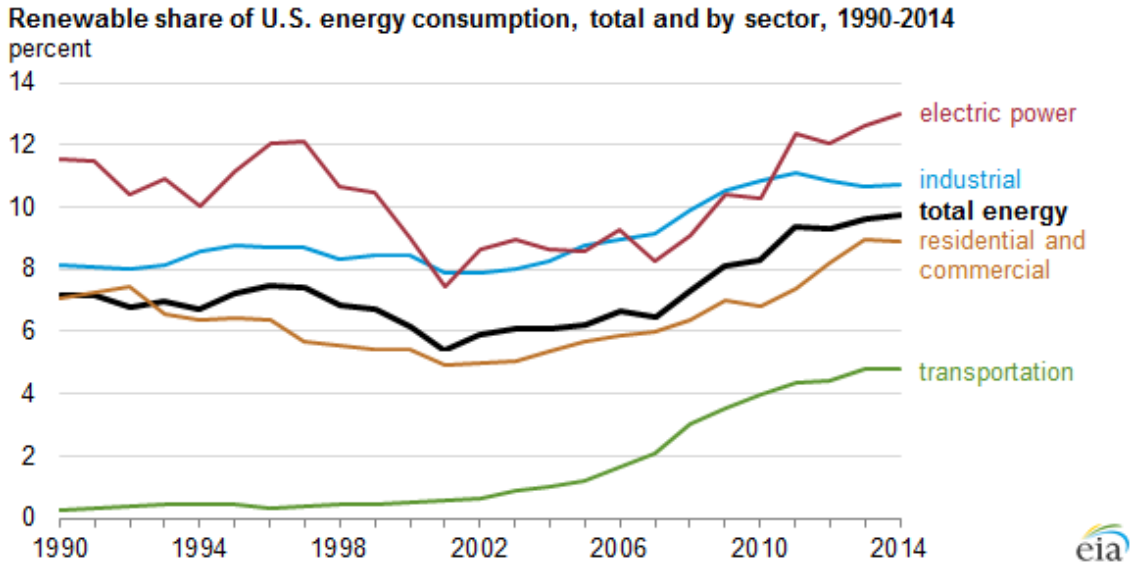

Figure 5. The Growth in Renewables

The price of the battery used to be a key factor that draws back the application of BESS, but it is its price is dramatically decreasing every year as shown in Figure 6, which makes its application more and more attractive [39]. Most recent research from NREL reveals that the demand reduction by BESS is economically possible for nearly 5 million commercial customers in the US [40]. There is already 3.375GW reported battery system operating in the world according to DOE database [41].

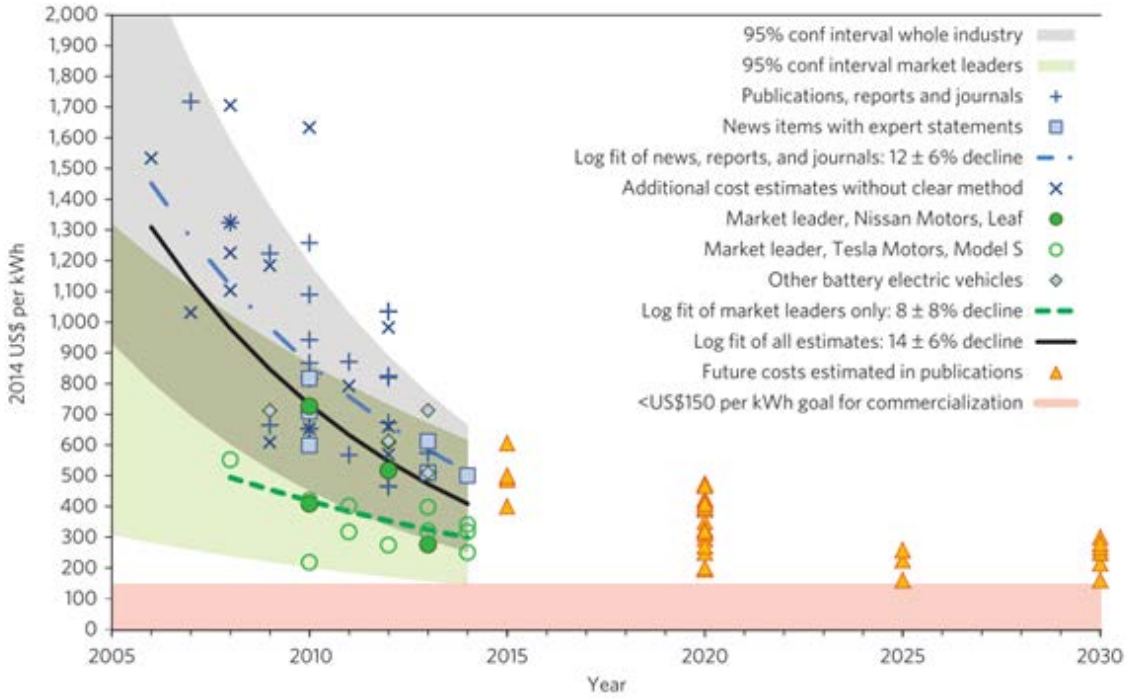

Figure 6. Reduction in Battery Price [39]

Because of its promising potential, the use of BESS for peak shaving has been widely researched in recent years, [31, 35, 38, 42-46]. Early research focused on the sizing of the BESS. An optimal sizing model was proposed to investigate the application of limited BESS capacity to achieve better peak load shaving performance [45]. Dynamic programming method was used to find optimal battery capacity and power for BESS [35]. Although the payback could reach as low as three years when applying a small-size BESS, the average payback is around ten years when using relatively large BESS [47]. Some case studies showed the payback periods of BESS were too long to be applied in industrial field even with optimized size [44, 48]. Due to the long payback time and high unit cost of the BESS, many research have been done to increase its utilization rate [49, 50] and reduce its ownership cost. A stochastic framework was proposed to size a sharing-based BESS for peak hour utility applications [46]. The results showed sharing one BESS in a community or increasing its utilization can substantially improve the cost savings compared with

using dedicated storage system for each individual user. Case studies of multi-using BESS were introduced, which revealed the economic potential and regulatory challenge of increasing the utilization of the BESS [51].

Among various battery technologies available, lithium ion battery is recognized as the best technology for BESS [52]. In particular, lithium manganese-oxides batteries have been considered as a popular candidate for energy storage systems because of its low cost and good technical performance in terms of both energy density and power density [53, 54]. During BESS operations, the battery degradation can significantly reduce the available capacity of the BESS [55], and hence limit the peak shaving potential. The approaches of reducing lithium ion battery degradation have been discussed in some earlier publications [56, 57]. The battery life can be prolonged by optimizing charge/discharge schedule and depth of discharge of the BESS [43]. However, the real economic impact of battery degradation for peak shavings remains unclear because the capacity of the battery was assumed to be unchanged [43, 45, 58-60] or only simplified battery model was used during system modeling [61]. Moreover, battery performance strongly depends on operation temperature [62], which affects battery degradation, charge/discharge efficiency, and battery capacity [63]. Nonetheless, the economic impact of the temperature on the BESS for peak shaving has not been researched to the best of our knowledge.

1.3 Comprehensive Demand Side Management (DSM) System

The stability of the power grid relies on the balance between the supply side and the demand side (i.e. customers). It is not an easy task since there is very little control on the demand side [64]. Strbac reported that the utilization of the power generation capacity is below 55% [65]. Adding new GHG-intensive generation capacity (in supply side) is neither economical nor environmentally friendly as the peak power demand happens infrequently and has no time pattern.

To address the imbalanced energy demand and supply, DSM has emerged and endorsed by both utility company and government [66]. By shifting the peak demand to off-peak periods or reducing the peak demand directly, DSM could economically and effectively reduce the generation capacity needs and increase the utilization rate.

DSM also known as demand side response (DSR), has extensive applications and is defined in a variety of methods. It is an integration of approaches to plan, monitor and implement utility activities or features that could change the electricity use patterns of the consumers in [65]. The main objective of DSM is to encourage the consumers to use less energy during peak hours or to shift the time of energy use to off-peak times to alleviate the burdens on the grid during peak demand periods [67]. However, DSM can also be defined in a more general method. Warren [68] divided the DSM into three categories according to the application methods (energy efficiency, demand response and on-site backup). Energy efficiency focused on reducing the overall demand. Demand response, mainly motivated by energy price or incentive programs, aims to shift the demand to off-peak periods. On-site backup, including generation and storage, is used to smooth the load shape and reduce the demand peaks. Similarly, Lund et al. [69] categorized DSM into reducing, increasing and rescheduling. “Reducing” aim to obtain peak demand clipping or strategic usage conservation; “increasing” would achieve strategic usage growth in all times or during off-peak periods (valley filling). “Rescheduling” usually applies flexible load shape or load shifting techniques. Therefore, DSM in this thesis is a comprehensive portfolio of measures to improve the energy system at the side of consumption [70]. It ranges from improving energy efficiency by using better materials, over smart energy tariffs with incentives for certain consumption patterns, up to sophisticated real-time control of distributed energy resources. A typical DSM system is shown in Figure 7 [71]. The proposed DSM systems in this research include most of the

components at the customer end, such as advanced metering, energy efficiency, renewables, and distributed storage etc.

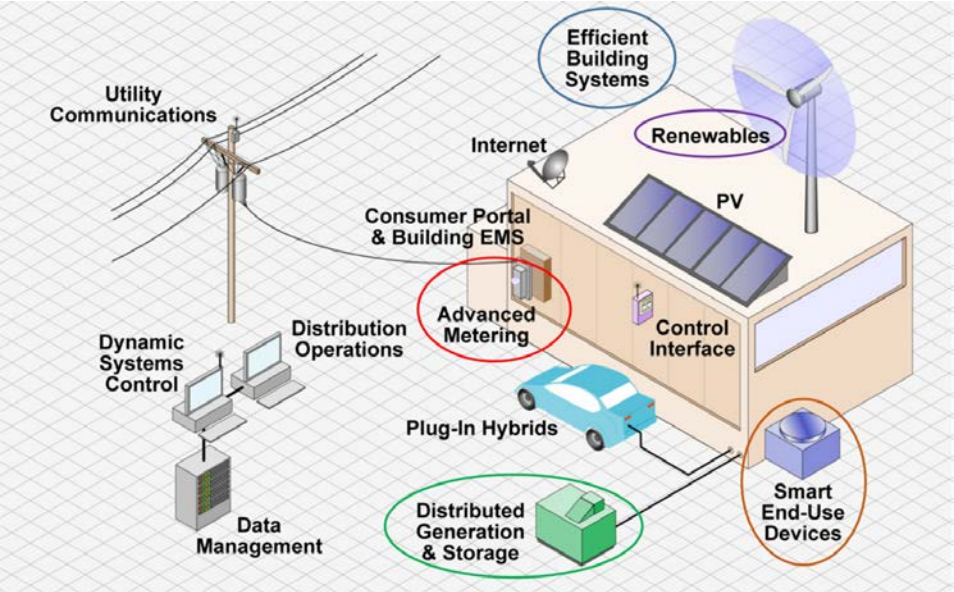

Figure 7. Typical Demand Side Management System [71]

BESS is the core component of the DSM systems proposed in this thesis. Its ability is not only limited to the peak demand reduction as mentioned in the above section, it is also a key component of DSM in modern smart grid. The entire US is embracing the BESS with an incredible speed. A 70 MW of battery energy storage was installed within 6 months to cover a major gas leak at Aliso Canyon in California in 2016 [72]. California has signed bill AB 2868 into law in 2016 to deploy a total 500 MW of energy storage within three major utility companies and required a total of 1.3 GW of storage by 2020 under bill AB 2514. Massachusetts has signed House Bill H.4568 into law in 2017 to deploy 200 MW of storage by 2020. Oregon has required its main utility companies to have a minimum 5 MW of storage in service by January 2020 [73]. A variety of incentives are also available across states. California's most successful incentive program, the Self-Generation Incentive Program (SGIP), plans to provide $166 million every year through 2020

for energy storage and other technologies; it also provides about $1.6/W incentive to battery energy storage installation [74]. New York is also enthusiastic in battery storage promotion. A $2,100/kW battery storage incentive is planned to cover half of the project cost aimed at summer peak demand reduction. New Jersey's Renewable Electric Storage Program offers $300/kWh for storage projects [75]. BESS is also playing an important role in global energy storage market. A 100 MW battery storage was built in South Australia within 100 days in 2017 [76]. Japan has announced a BESS incentive program in 2014 worth more than $700 million [77], which could cover up to 67% of BESS costs. It also provides additional incentives to support stand-alone renewable energy generation with batteries. Germany has a high penetration rate of renewable energy implementation. BESS is an ideal method to supplement the renewable energy generation to supply the power demand fluctuations. The German government has supported the BESS installations coupled with solar PV panels since 2013. It also provides incentives that could cover up to 30% of the battery cost [78]. China is the world's largest energy producer and consumer. China has installed the highest wind capacity and the second highest solar PV capacity, which only account for less than 3% of total energy production in 2013. Energy storage is listed as one of the top 100 national strategic projects in 2016 and will be actively promoted during the 13th Five-Year Planning Period (2016-2020) on both the grid-side and behind-the-meter side [79].

The function and the economy of the BESS are closely related with the type of BESS. Based on the installation location, BESS can be divided into Utility-Scale system owned by utility company, Behind-the-Meter (BTM) system operated by individual customer, and Remote Storage that works as isolated system [37]. Due to the fact that DSM investigated in this thesis is typically the behaver of the end-use customer, the BTM system is the focus of the research. BTM systems can provide most services to all stakeholders as shown in Figure 8 [80]. Besides of peak demand

reduction for customer, it can also relieve the grid burden and improve electricity quality. It is proposed to share BESS in comprehensive DSM systems to maximize its benefits. BTM storage is typically owned by the customers, the other stakeholders could be only free riders in this ecosystem. To make the venture economically viable, the customers must have a viable and visible value stream from the use of BESS. The values that can be easily received by the customer are peak shaving, load shifting, integration of renewables, and power quality services etc.

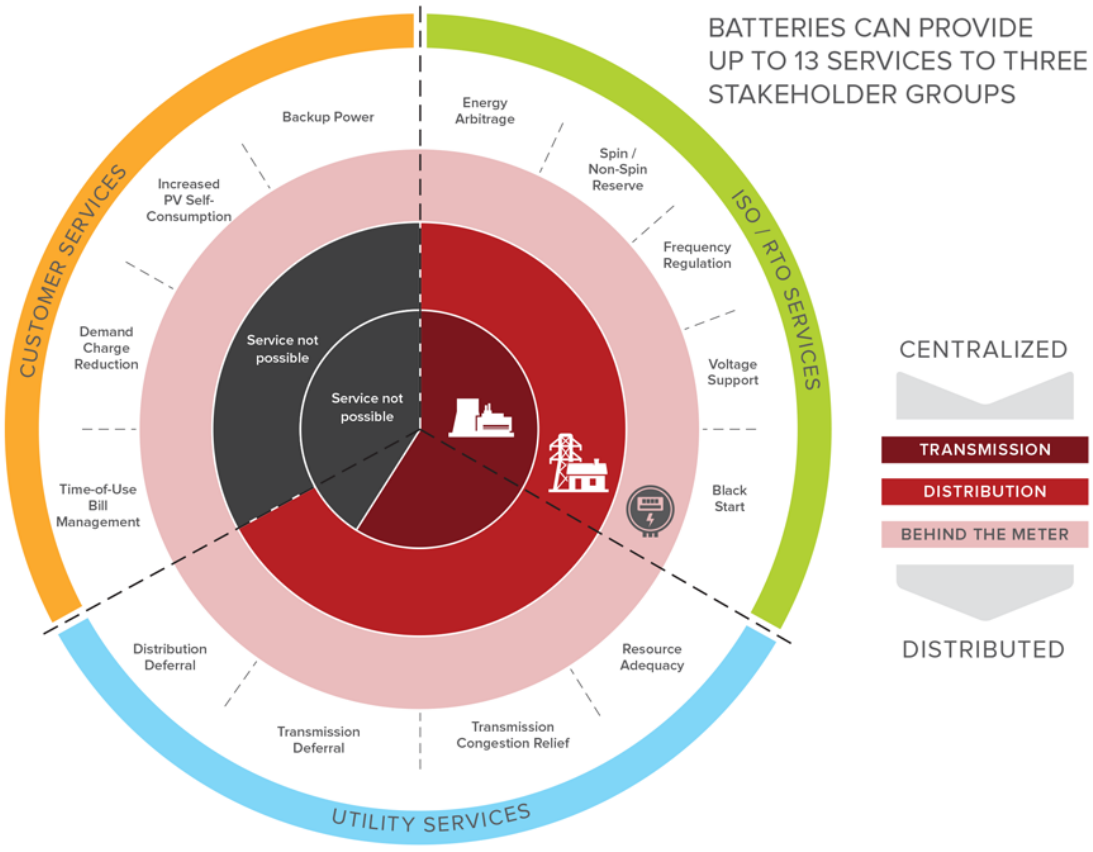

Figure 8. Overall Battery Energy Storage Functions [80]

Many studies have been devoted to maximizing the benefit of BESS. Sharing and integration with renewables and are two popular directions. Considering the variety services BESS can provide, many new business models were developed [81-84]. A cloud energy storage (CES)

concept which allowed the users to store and withdraw electrical energy from cloud BESS was proposed in [84]. Simulation results showed CES was capable of providing energy storage services at a substantially lower cost. Similar energy hub concept was proposed to integrate decentralized energy systems at community scale. The energy autonomy was between 64% and 92% in researched scenarios [85]. The feasibility of sharing one BESS in a community in real-time pricing structure was analyzed using Markov Decision method in [86]. An optimized policy was proposed to maximize its economic benefit. Distributed BESSs in the big community can simultaneously provide local services individually and system services in aggregate [87]. It is found that multitasking can almost double an BESS's profit as compared with a single-service approach. A novel dispatch strategy for shared ownership of BESS between customers and distribution network operators was developed to maximize the overall savings [88]. The jointed ownership was demonstrated to have higher profits and flexibility. Because of its ability to smooth out the power fluctuation in the renewable energy generation and improve the system reliability, the BESS is usually integrated together with renewables [89]. A grid connected PV plant with BESS in a university is modeled in [90]. In the proposed system the electricity demand is satisfied through the PV–BESS and the national grid serves as the backup source. The electricity cost can be reduced by 25% compared with using benchmark electricity pricing from the grid. A shared BESS management algorithm was proposed for renewable energy integration in a smart grid. The total profit of all participated users was increased by 10% over the case that customers own individual small-scale BESS [83]. Although improved performances and savings were observed in sharing and renewable integration systems, their deployments are still a challenge. More integrated services usually mean more savings, but the ownerships and controls are also more complex.

Therefore, it is critical to investigate the most valuable services and integrate them in the simplest method.

Sharing BESS among multiple customers or several services is the core concept of the proposed DSM system. It is essential to briefly introduce the red-hot sharing economy herein. Sharing economy, which is the collective term for peer-to-peer markets, offers appealing alternative options for consumers to obtain access to goods and services via community-based online services [91]. Emerging sharing companies, such as Airbnb and Uber, grow rapidly with innovating technologies and expanding market demands [92]. Some traditional industries, such as bike rental and car rental, rejuvenate and gain increasing attentions during this sharing economic era [93]. The booming of sharing economy is a challenge to traditional industries. It also inspires benign interactions with traditional business styles. The economic impact was analyzed between traditional hotel industry and the short-term accommodation platform (Airbnb) in Texas [92]. While the emerging sharing market took away 8-10% of hotel industry's revenue during peak demand, the hotels were more motivated to offer less aggressive room prices to benefit more consumers. A report from PwC revealed that 44% of US consumers were familiar with the sharing economy and 18% of the total population had involved in sharing economy activities [82]. It predicted that five key sharing sectors (travel, car sharing, finance, staffing and music and video streaming) have the potential to grow to $335 billion with an amazing expansion of more than 20 times [94-97]. Several different sharing strategies about BESS will be investigated in this thesis to maximize its benefits with least system complexity.

1.4 Research Objectives

The objectives of this dissertation research are to comprehensively investigate hybrid daylighting system, using BESS for peak shaving, and maximize their economic benefits in the modern DSM systems.

1). To bring down the cost and increase the efficiency of daylighting, a novel hybrid daylighting system which combines daylighting and solar thermal will be proposed and analyzed. The system specification will be optimized based on economic analysis. The overall system efficiency and cost savings will be evaluated by case studies.

2). To investigate how the economic performance of the BESS is affected by various parameters and operation conditions when used for peak shaving, a detailed battery model and simulation structure will be introduced. Case studies will be carried out to quantitatively compare the economic impacts of all key parameters and obtain the most significant impact factor.

3). To maximize the savings of DSM, several new operation models based on BESS and sharing strategy will be designed and simulated. System size and control strategy will be optimized based on economic analysis. Possible valuable services which can be integrated into the proposed DSM system will be investigated through case studies.

2. Parabolic Trough Daylighting/Thermal System

As one of the most important energy consumption source, lighting plays a major role in the global energy efficiency improvement. This chapter will introduce the structure and optimization of a novel daylighting system to increase the efficiency of solar lighting. A case study will be carried out to analyze the system efficiency, economic performance, and potential sustainability benefits.

2.1 Basic Structure of Parabolic Trough Daylighting/Thermal (PTL/T) System

An innovative PTL/T system is proposed based on the analysis in the introduction section. The proposed system aims to bring down the cost of OFD while increasing the utilization efficiency of concentrated solar energy. The system overall structure is shown in Figure 9. The ray tracing sketch is shown in Figure 10.

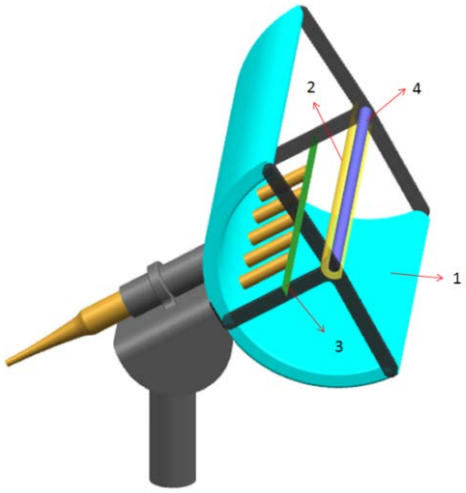

Figure 9. Overall Structure of Parabolic Trough Lighting/Thermal System

1, parabolic trough solar collector, which is controlled by a 2-axis solar tracking system; 2, cold mirror, which is used to split solar light. It is concentric with the PTC and have the same shape with the PTC; 3, Fresnel lens, which is connected with optical fiber lighting delivery system; 4, thermal system.

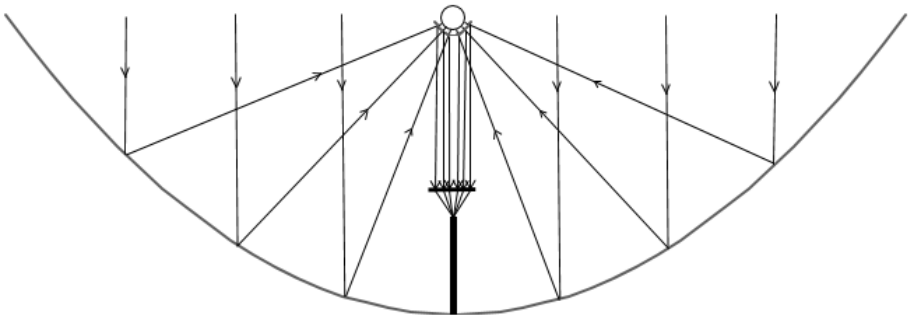

Figure 10. Layout of Ray Tracing

Based on the track of sunlight, the system can be divided into four stages: 1) the sunlight is concentrated by a parabolic trough solar collector (PTC) which is similar to other typical solar concentration system; 2) the concentrated sunlight is split by a cold mirror while the visible light is reflected to another Fresnel lens system and the IR transmits through the cold mirror and reaches the thermal system; 3) the visible light is re-concentrated by Fresnel lens to an optical fiber system and then delivered for daylighting; 4) the IR is absorbed by thermal system for heat generation.

The major advantages of the proposed system are concluded as:

1) PTC is used as solar collector. PTC is the most successfully commercialized solar collector, but has never been used for HLS. This is partly because the HLS needs all the sunlight to be concentrated to a small point and then delivered by optical fiber. However, the PTC can only concentrate the sunlight into a line. Another Fresnel lens system is used in the proposed PTL/T system to re-concentrate line light to point light, which can be delivered for daylighting. PTC also has the advantages of easy manufacturing, expansion and modularization compared with the parabolic dish. The conventional parabolic dish collector area of each HSL module is only about $1m^2$ and capable to provide lighting for about $93m^2$ indoor spaces [98]. It is technically not

convenient to expand the collector area because of manufacturing difficulty. Therefore, several modules are usually needed for a single building. Each module needs individual supporting and tracking system, which increases overall system cost. In the contrast, PTC can be easily made into any area. All sizes of PTCs are available in the market. It is possible to use only one PTC to serve a whole medium size space. Because of this high flexibility, it is possible to optimize the collector area for a specific case, which will be presented in the following sections.

2) Full spectrum energy from sunlight is utilized. The total efficiency of the existing HLS is relatively low because it has never taken use of IR. The spectrum split technology similar with that in PV/T system is used in the proposed daylighting system. The IR can be separated from sunlight and utilized for heating purpose using cold mirror. The thermal problem related to the lighting system can also be relieved benefitted from the use of the cold mirror. The split IR was initially proposed for electricity generation using solar panel or Stirling engine in HSL system. However, it has never been realized due to the high cost of the suitable electricity generation system. Meanwhile, it is difficult to establish a cheap heating system for HSL system because of the structure limitation. Therefore, the IR is currently separated but wasted in the existing HLS systems. PTC is initially designed for heat generation. Therefore, using IR for heat generation in the PTC-equipped PTL/T system is very cheap and straightforward.

2.2 Analysis of Critical Components and Overall Structure

2.2.1 Choice of Fibers

In PTL/T system, the solar light is concentrated from PTC surface, reflected by cold mirror, re-concentrated by Fresnel lens, transmitted through POF and then reaches end use space. There

are energy losses during each stage of this procedure. The biggest transmission loss is from POF, which is 4%-5% per meter. To adopt suitable fiber system is critical for the overall efficiency. Due to the transmission capacity limitation of a single fiber, fiber bundle is always utilized in the daylighting system. In order to achieve higher efficiency, fiber diameter and bundle combination method need to be optimized.

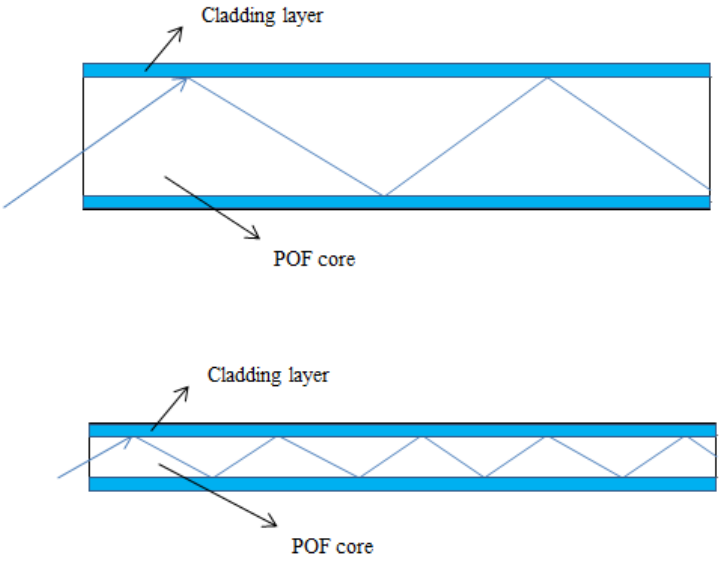

Figure 11. Illustration of Lighting Transfer Difference between Large and Small Fiber Diameter

The transmission of light in an optical fiber can be illustrated by Figure 11. Light propagates within the POF by total internal reflection. It is clear that a smaller diameter of the fiber means more reflection times of light compared with a larger diameter fiber, and hence more light losses. Shao et al. [17] researched the transmittance of the PMMA (Polymethyl methacrylate) rods with different diameters under regular sunlight. When using one-meter length rods for testing, the mean transmittance values were found to be 0.439, 0.596 and 0.649 for the 25mm, 50mm and 75 mm diameters respectively when all the other parameters are the same (the transmittance in this experiment was very low because the rods were only placed under regular sunlight. The

transmittance would be much higher when the sunlight is focused and the incident angle is smaller). Larger fiber diameter can also benefit heat release of the fiber bundle. The heat problem is a critical issue that limits the capacity of each fiber bundle, because the POF will deteriorate when the working temperature is higher than the required value. The thermal loads of the fiber can be divided into two components. First, the heat generation because of transmission loss, which is significant but doesn't cause big heating problem because of the long transmission distance and hence large heat release surface. Second, the radiation incident on the pores between optical fibers is absorbed by the cladding material and results in heat generation. This proportion is significant because the high level of solar flux on the end of fiber bundle and the relatively high pore ratio [22]. Larger fiber diameter means smaller surface to volume ratio and results in a reduction of the fraction of the area that is covered with cladding. This is helpful to reduce the porosity of the bundle, which can result in less heat flux on the cladding material of the fiber, and then less heat generation. In order to release the heat, Ullah et al. proposed to use a short section of silica optical fiber before the POF[16]. In this way, uniform light ray can be obtained at the entrance of POF, which can reduce the possibility of hot spot at the POF surface. Liang et al. introduced the utilization of polished fiber bundle, which was proved with a capability to tremendously limit heat generation[21]. The end of each fiber was polished to be hexagon. This eliminates the gaps among different fibers, which prevents the main heating source. The author also used forced air to cool the fiber bundle. The solar flux at the entrance can be as high as 8000kW/m^2. However, the entrance solar flux in [16] can only be around 650kW/m^2. It was tested that the bundle would melt if the flux was much higher.

Table 1. Optical Fiber Information

Item	Value
Diameter	3mm
Core material	PolyMethylMethAcrylate
Cladding layer material	Fluorinated polymer
Transmission	96.5% per meter

Based on the above analysis, a relatively large fiber diameter and the polished bundle structure are selected for the proposed PVL/T system. The fiber diameters range from 0.75mm to 3mm in some of fiber daylighting systems [10, 16, 23]. The larger diameter fibers also are available in the commercial market. Nonetheless, the larger diameter fibers are more expensive. They also lack flexibility, because the light can travel without major losses only when the bent radius is no less than 8 times the fiber diameter [99]. Therefore, the 3mm diameter POF is chosen for the proposed system. The detailed information is shown in Table 1. The fiber is polished to hexagon using the method described in [21] at the end to form a bundle. It is estimated that the solar flux at the entrance of proposed fiber bundle can be at least as high as 1000kW/m^2 because of the reduction of heat compared with that in [16].

2.2.2 PTC Geometric Parameters

Both optical efficiency and thermal efficiency highly depend on the optimal geometric parameters of the PTC. Theoretically, three parameters can absolutely define the performance of a PTC, namely, aperture, rim angle and concentration ratio. The optical efficiency of the collector highly depends on the aperture. The larger aperture leads to a lower optical efficiency because of the severer abnormal incident effect. Nonetheless, the larger collector aperture means a higher concentration ratio when the receiver diameter is fixed, which results in lower thermal losses [100]. Rim angle is closely related with tracking errors. An optimal rim angle is capable of providing

maximum error-tolerances for the whole system [101]. The design of the PTC is not the core part of this feasibility research, therefore, the optimized PTC is directly chosen according to the results in [100, 102], as shown in Table 2. It was proved the optimal dimensions were effective as long as the ratio of collector aperture to length and concentration ratio keep the same. It should be mentioned that the final optimal PTC parameters will be calculated based on the thermal and tracking system parameters.

Table 2. Optimal PTC Geometric Parameters

Item	Value
Ratio of collector aperture to length	0.64
Rim angle	90^0
Concentration ratio	21.2

2.2.3 Illumination Area Analysis

The area of solar collector module largely determines the capacity of optical fiber daylighting system, and further influences the illumination area and possible energy savings. For a specific area, the fundamental cost of using a single larger collector is less than that of a multi-collector system because only one supporting and control system is required. Nonetheless, due to the big capacity, long POF is needed to transmit the collected light to further space, which increases the fiber cost and reduces the overall transmission efficiency. A smaller collector area means a shorter fiber length and a higher transmission efficiency. However, the fundamental cost will take a big share in its overall price. Hence, the collector area needs to be optimized based on economic analysis. The optimization procedure is: a) list the basic assumptions related with the system cost; b) describe the service area and fiber arrangement method; c) express the total fiber length as a function of illumination area; d) calculate the required solar collector area based on system

efficiency and requirement; e) calculate the cost of illuminating unit area and get the optimum value.

The basic assumptions about the system cost are:

1) The cost of the whole system can be divided into three main sections: PTC system, fiber system, and other cost, as shown in:

$$\mathrm{C_t} = \mathrm{C_f} + \mathrm{C_p} + \mathrm{C_o} \quad (1)$$

where, C_f is the fiber cost, C_P is the PTC cost, and C_o is the other cost besides the fiber and collector. C_o includes all the other components costs and system installation cost.

2) Cost of fiber is proportional to its length:

$$C_f = C_1 L_{ft} \quad (2)$$

where, $C_1$is constant, L_{ft} is the total fiber length.

3) The PTC cost is proportional to its area:

$$C_P = C_2 A_P + C_3 \quad (3)$$

where, C_2, C_3 are constant, A_P is the PTC area. This relationship was gotten based on market price survey of PTC.

Other cost C_o is constant for each module. The other cost mainly includes the cost of tracking system, supporting structure, thermal system and installation. Because C_o only slightly changes when varying the collector area in a small range, it is treated as constant herein.

The PTL/T system is supposed to be installed closely to the geometric center of the serving area. Accordingly, only a very short fiber with a length of L_0 is needed before it enters a building.

To simplify the design, the illuminated area is supposed to be a square space. The fiber can be arranged in two ways: 1) the area is divided into many small spaces. Each fiber illuminates a small square, as shown in Figure 12. It is straightforward, requires least lengh of fiber and provides highest transmission efficiency, but it lacks flexibility and is very hard to manufacture and install; 2) the whole space is divided into "n" sections by "n" squares. The fiber is also divided into "n" bundles, each of which provides service for one section, as shown in Figure 13. In this way, a balance can be found between system efficiency and flexibility by optimization. Therefore, it is used in this research.

According to Figure 13, the bundle length in the buildings at each section equals to the production of "a" and "i". Fiber length for each divided area is:

$$L_{fi} = L_0 + ai \quad (4)$$

where, i is the section number, L_0 is the fiber length before it enters the buildings. The transmission efficiency of the fiber is exponentially related with fiber length, which is shown by:

$$E_f = {E_{fu}}^{L_{fi}} \quad (5)$$

where, $E_{fu}$is unit length efficiency. In this calculation, the major loss due to bending of fiber is ignored, which requires the bent radius of the fiber to be larger than 8 times of the fiber diameter during installation. The total length of fiber can be calculated by:

$$L_{ft} = \sum_{i=1}^{n} \frac{L_{fi} I_{ri} (2i-1) a^2}{IR_e E_d E_f} \quad (6)$$

where, I_{ri} is required luminance in the service space, IR_e is the maximum endurable amount of light at the entrance of each fiber decided by fiber bundle property, and E_d is distribution efficiency at the end use. Substituting (4) and (5) into (6), the total length of fiber is:

$$L_{ft} = \sum_{i=1}^{n} \frac{(L_0+ai)I_{ri}(2i-1)a^2}{IR_eE_dE_{fu}^{(L_0+ai)}} \quad (7)$$

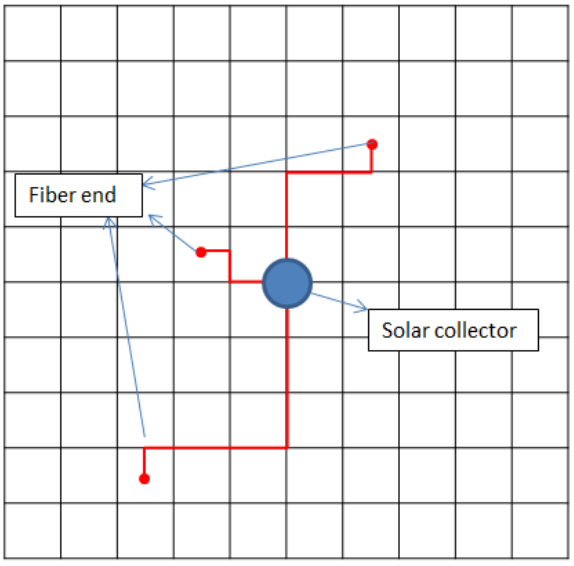

Figure 12. Illustration of Dividing Serving Space into Many Small Squares

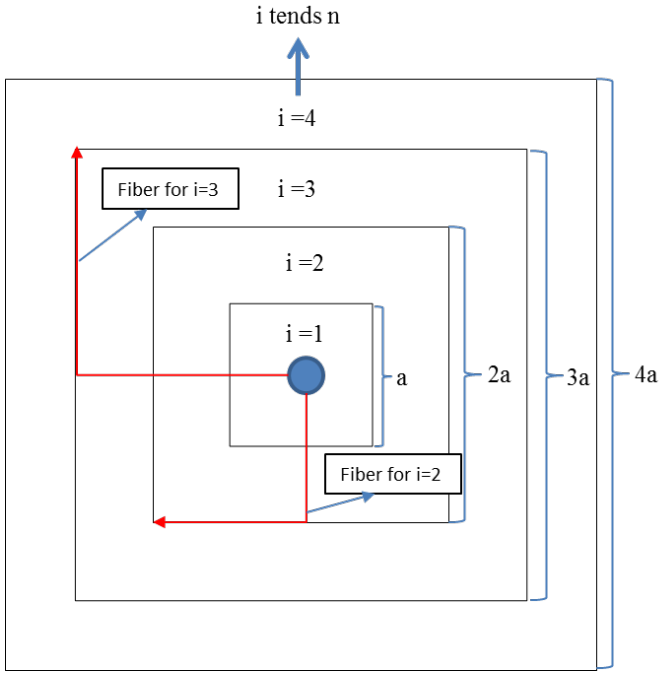

Figure 13. Illustration of Dividing Serving Space into Several Big Areas

The required solar collector area is related to the maximum intensity of solar radiation, required radiation at the end use, and system efficiency. The HLS is the combination of daylighting and artificial lighting. Due to the non-storability of light, the collector capability should be designed according to the maximum value of solar radiation intensity other than the average value. In this way, all the light can be utilized with no waste of collected light. During cloudy time, the insufficient lighting can be complemented by artificial lighting. Because the solar light is filtered by cold mirror before entering the POF, only the power and efficacy of visible light are considered in the calculation. Following these descriptions, the collector area can be expressed by:

$$A_p = IR_r / IR_{mi} \quad (8)$$

where, IR_{mi} is the maximum intensity of solar radiation in the service location, IR_r is the required total radiation from sun, which can be expressed by:

$$IR_r = IR_{re} / (VL_p VL_e E_d E_f E_{rp} E_{rc} E_{ft} E_{oe}) \quad (9)$$

where, VL_p is the power percentage of visible light in the solar light, VL_e is the efficacy of visible light, E_{rp} is the reflectivity of PTC, E_{rc} is the reflectivity of cold mirror for visible light, E_{ft} is the Fresnel lens transmittance, E_{oe} is the optical fiber entrance efficiency, $IR_{re} = \sum_{i=1}^{n} I_{ri}(2i-1)a^2$ is the required total radiation at the end use. Only key components efficiency was considered in this expression. The transmission efficiencies from one component to another were all assumed to be 1. Finally, we can get:

$$A_p = \sum_{i=1}^{n} \frac{I_{ri}(2i-1)a^2}{IR_{mi} VL_p VL_e E_d E_{fu}^{(L_0+ai)} E_{rp} E_{rc} E_{ft} E_{oe}} \quad (10)$$

The cost of illuminating unit area is:

$$C_u = C_t / (na)^2 \quad (11)$$

where, $(na)^2$ is the illumination area. Combining the equations together, the unit cost can be finally expressed by:

$$C_u = \frac{C_f + C_p + C_o}{(na)^2}$$

$$= \frac{\left(C_1 \sum_{i=1}^{n} \frac{(L_0+ai) I_{ri}(2i-1)a^2}{IR_e E_d E_{fu}^{(L_0+ai)}} + C_2 \sum_{i=1}^{n} \frac{I_{ri}(2i-1)a^2}{IR_{mi} V L_p V L_e E_d E_{fu}^{(L_0+ai)} E_{rp} E_{rc} E_{ft} E_{oe}} + C_3 + C_0\right)}{(na)^2} \quad (12)$$

2.3 Case Study

In this section, the efficiency, possible energy savings and sustainability benefits of PTL/T system are analyzed by a complete case study. Firstly, the cost and efficiency of critical components are estimated based on literature results. Secondly, the system detailed dimensions are decided by the above design analysis approach. Finally, the system energy savings and greenhouse gas reductions are calculated and presented.

2.3.1 Critical Components Parameters

The price of the PTC is estimated by a linear regression approach based on the price from [103], the result is

$$C_P = 272.7A_P + 1055.2 \quad (13)$$

The unit cost of fiber is \$0.47/m [104], therefore:

$$C_f = 0.47L_f \quad (14)$$

The average installation cost of HLS is \$3520 [105]. The tracking and thermal system cost around \$1000 [103]. Assume all the other small components cost \$1000, then the total other cost C_o is \$5520. All the cost related constants are shown in Table 3.

Table 3: Values of Cost Related Constants

Cost related constants	Values ($)
C_o	5520
C_1	0.47
C_2	272.7
C_3	1055.2

The system is supposed to be installed in the centre of the roof top and provide service for a big interior area. 3m of fiber is needed before it enters the buildings. The required luminance is 500lux. Assume the maximum irradiation intensity is 1000W/m^2. A fiber bundle composed by 7 fibers with 3mm diameter is employed. The maximum endurable intensity of solar radiation at the entrance of each single fiber is estimated to be at least 1000kW/m^2. Only visible light is reflected by cold mirror and reaches the entrance of the fiber. The efficacy of the visible light is at least 200lm/w [106]. Therefore, the maximum amount of light at the entrance of each fiber is around 1500 lumens. At the sea level, about 52% of the radiation is visible light, 42% is IR [107]. All the critical parameters used are listed in Table 4. Plugging in all the coefficients into Equation (12), we get:

$$C_u = \sum_{i=1}^{n} \frac{0.189(3+ai)(2i-1)+2.046(2i-1)}{n^2 0.965^{(3+ai)}} + \frac{6575.2}{(na)^2} \quad (15)$$

Table 4. Parameter Values of Critical Components

Fiber length before entering the buildings L_0	3m
Required luminance at the service space I_{ri}	500lux
Maximum amount of light at the entrance of each fiber IR_e	1500lumens
Maximum radiation intensity IR_{mi}	1000W/m^2

Reflectivity of PTC E_{rp}	92%
Reflectivity of cold mirror for visible light E_{rc}	93%
Fresnel lens transmittance E_{ft}	95%
Optical fiber entrance efficiency E_{oe}	95%
Distribution efficiency E_d	83%
Unit length efficiency of fiber E_{fu}	96.5%
Power percentage of visible light in the solar light VL_p	52%
Efficacy of the visible light VL_e	200lumens/W

2.3.2 Results

According to equation (15), division number "n" and section length "a" are the parameters that determine the cost of illuminating unit area. Therefore, the optimization work focus on choosing their values. Let n in the equation (15) change from 1 to 7. The optimization results are shown in Figure 14. It shows the overall optimum areas are between 500 m^2 and 700 m^2 when considering all the scenarios. The unit cost can be expressed as a function of illumination area as shown in Figure 15. It can be seen there is an optimum illumination area for each specific n. The unit cost decreases with the increase of illumination area until it reaches the optimum critical point. The reason is that the increased illumination area brings down the average constant cost for unit area, thus reduces the total unit cost. The unit cost increases slowly after the optimum point, because the transmission efficiency becomes lower and lower with the increase of fiber length. On the other hand, when illumination area is set as constant, the unit cost decreases with the increase of n. It means the illumination area should be divided into some small sections. The fiber length of each bundle should be adapted to the corresponding service area. Nonetheless, too many

divisions will severely harm the flexibility of the system. According to Figure 14 and Figure 15, the cost difference becomes negligible after the n reaches 4.

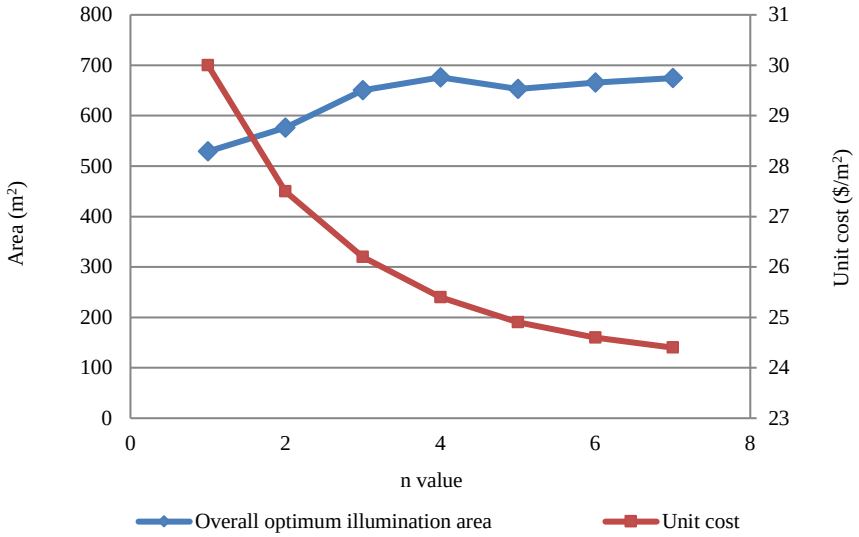

Figure 14. Relationship among Illumination Area, Unit Cost and N Value

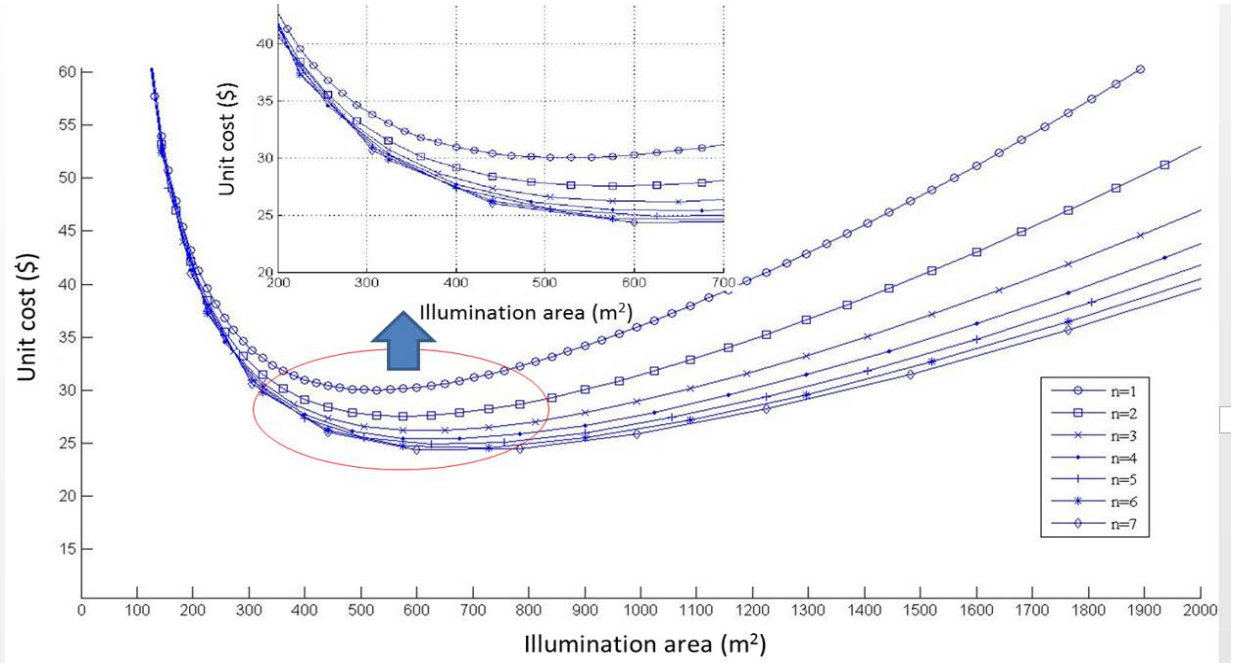

Figure 15. Detailed Results of Unit Cost

Therefore, n=4 is selected in this research. The partial view in Figure 15 shows the gain from increasing the illumination area is minimal after the area reaches 500, since the unit cost begins approaching a relatively steady-state value. Because the system flexibility decreases with the increase of illumination area, it is better to choose an illumination area considering both unit cost and system flexibility. Therefore, the value 500 is chosen in this case study.

The thermal subsystem has already been deeply investigated by many researchers and is also highly commercialized. The estimated efficiency of the thermal subsystem is used directly without the description of the detailed system specifications. The efficiency highly depends on the working temperature. It can reach 73% for high temperature usage [108], and is around 55% [109] at low temperature utilization. The proposed PTL/T system is a relatively small module when compared with big parabolic trough power plant. Thus, the low temperature thermal efficiency of 55% is used in calculation. Applying all the optimization and assumptions to the PTL/T system, the key components parameters are chosen and listed in Table 5.

Table 5. Critical Parameters of The Case Study

Item	**Value**
Illumination area	500 m^2
PTC aperture	2.26m
PTC length	3.54m
PTC rim angle	90^0
PTC concentration ratio	21.2
Receiver diameter	35mm
Cold mirror aperture	55mm
Fresnel lens length	58mm
Focal length	60mm
Shadow area	0.2 m^2

Effective solar capitation area	$7.8m^2$
Numerical aperture	0.4
Calculated acceptance angle	23.43
Fiber bundle number	61
Divided sections in illumination area	4
Fiber	3 of 8.6m with 73.6% efficiency
	9 of 14.2m with 60.3% efficiency
	18 of 19.8m with 49.4% efficiency
	31 of 25.4m with 40.5% efficiency
Combined fiber efficiency	49%
Lighting efficiency	16.3%
Thermal efficiency	23.1%
Total efficiency	39.4%

2.3.3 Energy Savings and GHG Reductions

The PTL/T system can contribute to the sustainable development of building systems by saving traditional energy and reducing greenhouse gas emission. Because the solar radiations and energy consumption structures are different in different places, the location-based sustainability benefits are calculated for the US.

Energy source to be substituted is closely related with the actual energy savings. Although the lighting subsystem of PTL/T only makes use of 16.3% of the total insolation, it is capable to save lots of electricity because the light delivered to the interior of the building is only visible light. The luminous efficacy of the visible light is over 200 lm/w, which is significantly high. The typical efficacy of fluorescent bulb is only around 60 lm/w. Because of its widely usage in commercial and industrial buildings, the fluorescent bulb is treated as the substituted energy source in our analysis. The analysis results reveal that 1 watt of visible light can save up 3.33 watts of electricity.

For the heating section, because the most economical traditional heating approach is natural gas heating, the absorbed IR energy by PTL/T is supposed to substitute gas usage.

The PTC is only capable of collecting the beam radiation. The data of direct normal solar radiation from NASA is used [110]. Ten typical cities where solar radiation gradually changes from 3.38 to 7.02 kWh/day were chosen. The local average electricity and gas rate from EIA were used [111]. Due to the rate difference among residential, commercial and industrial, the savings were calculated separately for each sector. The maximum savings and simple payback period were calculated based on 24/7 operation hours. The results are shown in Figure 16, Figure 17 and Figure 18.

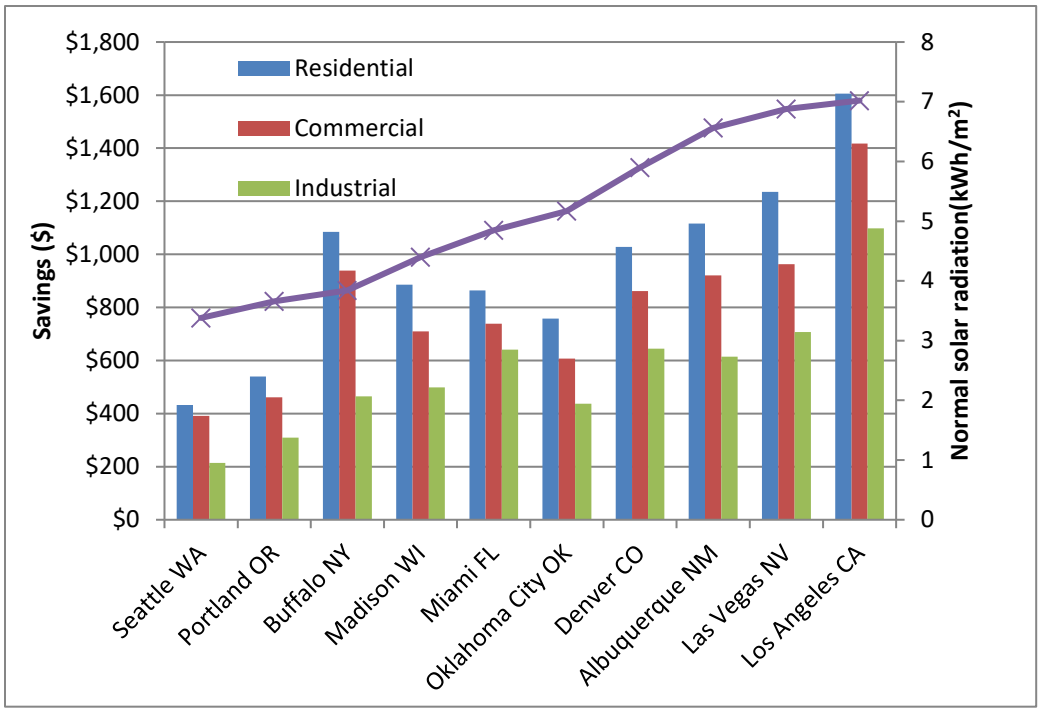

Figure 16. Maximum Electricity Savings in Each City

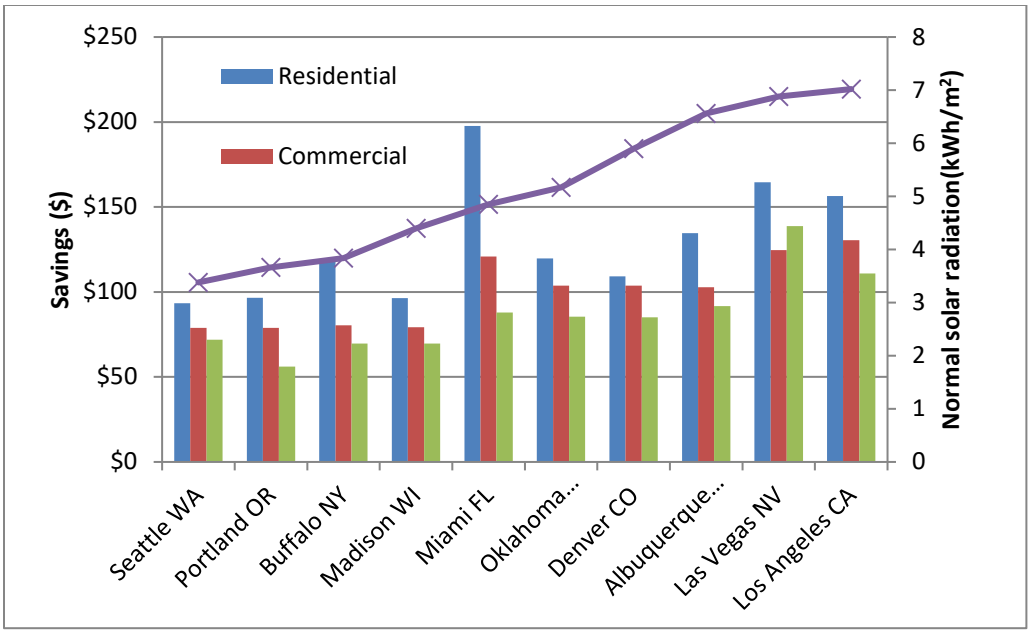

Figure 17. Maximum Gas Savings in Each City

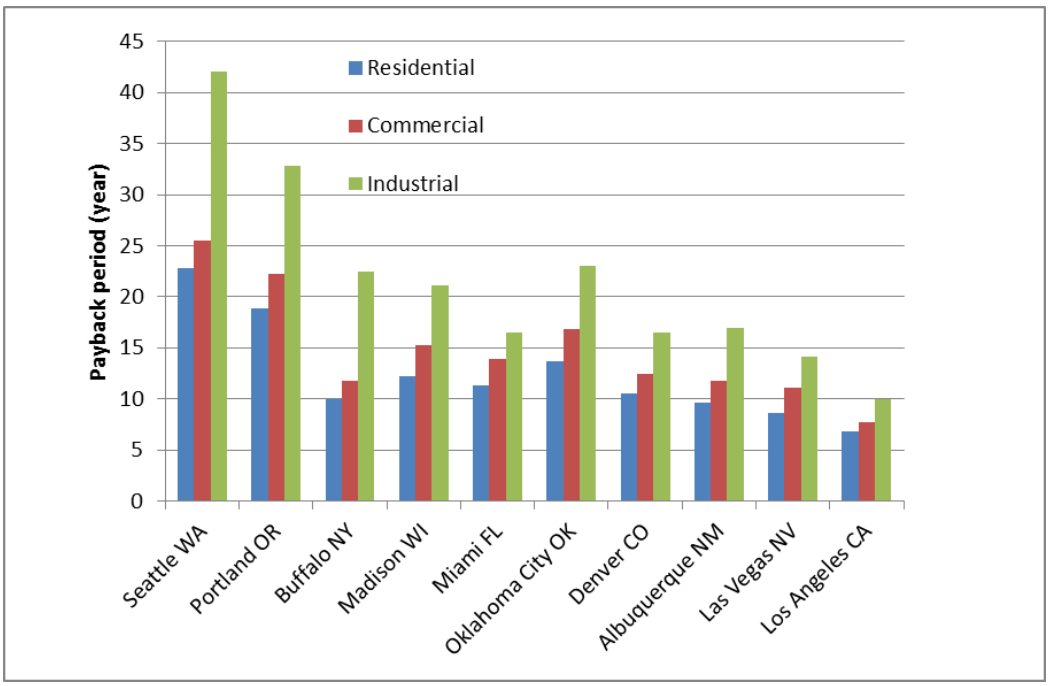

Figure 18. Simple Payback Period in Each City

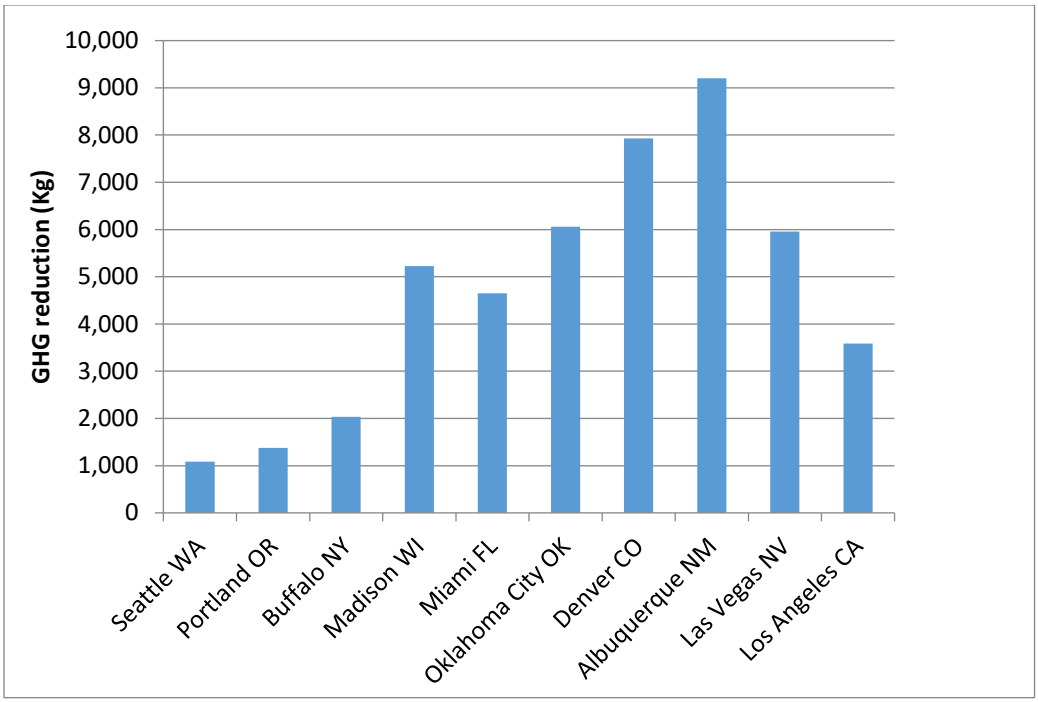

Figure 19. GHG Reduction in Each City

Overall, daylighting subsystem contributes most of the savings, which should be treated as the core subsystem in PTL/T. The thermal subsystem, which contributes about 10.0% of the total savings, is also a necessary complement for the improvement of the overall efficiency. In the cities where normal solar radiation is no less than 3.84 kWh/m^2, we can conclude:

1) The electricity savings is greater than $437/year. The gas savings is around $100/year.

2) The savings in Los Angeles is highest and the payback period is less than 10 years in all sectors.

3) The savings is greatest in residential because of the highest energy rate, which results in a payback period of less than 14 years.

4) The commercial building should be the best candidate for the proposed system due to the moderate payback period and the high coincidence of its operation hours with the daylighting time.

Although the simple payback of PTL/T for industrial sector is longest, the industrial buildings could still be good candidates. The reason is: the electricity usage rate is low for industrial customers. The results above only counted the usage savings. Nonetheless, the daylighting is also capable to reduce the electricity demand, which is more valuable in most cases. This effect is more related with demand management. Therefore, it will be separately investigated in the demand side management chapter. The savings and payback period in Honolulu HI is calculated because Hawaii has the highest utility rate in the US. The results show it has a payback period of less than 4 years. Based on the GHG emission rate of unit electricity and gas consumption in each city [112], the GHG reduction is calculated and the result is shown in Figure 19. In most of cities, the reduction is more than 4,500 Kg per year. To better illustrate the economic benefits of the PTL/T system, a maximum potential cost savings map of the whole US is created as shown in Figure 20. The normal solar radiation data from over 1,200 sites [113] is used to calculate the average solar radiation for each state. Because only commercial buildings are good candidates for this system, the annual average electricity and gas rate for commercial sector of each state is used.

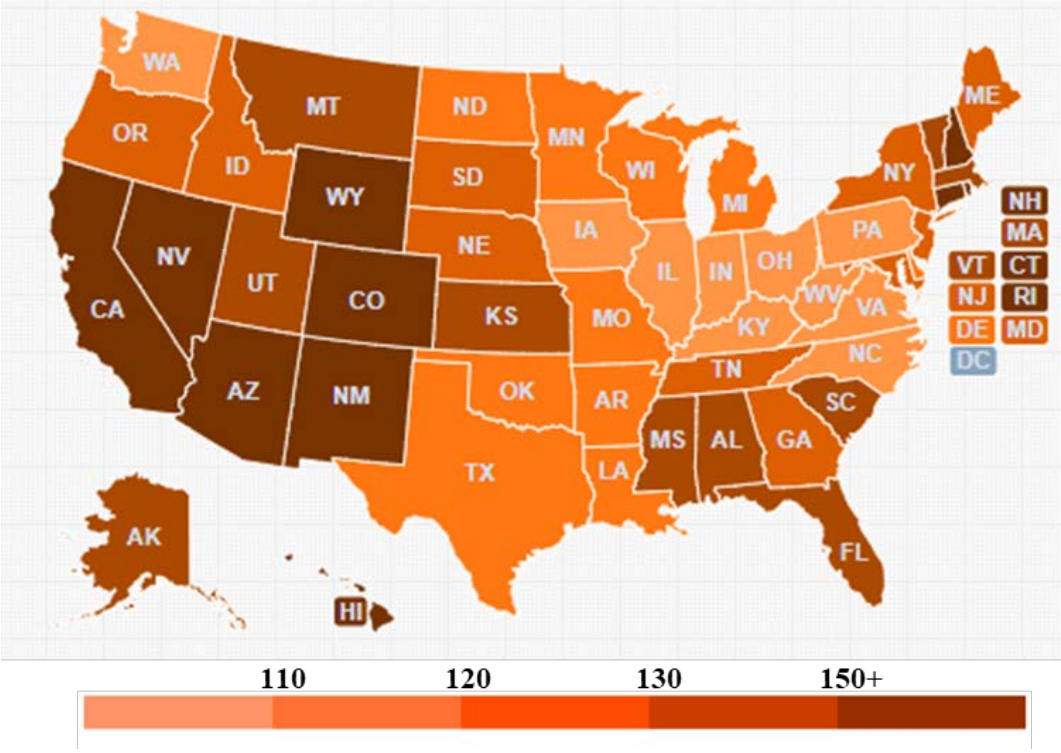

Figure 20. Cost Savings Potential in the US

3. Battery Energy Storage System for Peak Demand Reduction

As discussed in the introduction chapter, using BESS for peak demand reduction is a rapidly developing market. But high upfront costs are still a major barrier to its growth. BESS capacity, utilization rate, battery degradation, and operation temperature are the four critical factors for the demand reduction from BESS. However, previous research only focused on one or two specific factors. No comprehensive analysis and comparisons among the four key factors have been done yet. This research aims to build a mathematical model to thoroughly analyze all the factors by comparing their economic effects.

3.1 Battery Model

The available capacity of the BESS is a key factor that determines the performance of the peak shaving. For current BESS built on lithium ion battery, the battery capacity is continuously decreasing during operation due to the battery degradation which is primarily caused by the loss of cyclable lithium [114]. The battery capacity loss can be separated into cycling loss resulted from charge/discharge cycles and calendar loss due to self-discharge of batteries during energy storage time. Both cycling loss and calendar loss are significantly affected by the battery operation conditions. High temperature enhances the cycling loss because of the accelerated side reactions [63]. The Arrhenius Law is typically used to describe the temperature dependence of the calendar loss. A semi-empirical battery degradation model based on commercially available lithium-ion battery (Sanyo 18650 cylindrical cell) is adopted in this study to calculate the capacity loss [115]. This model combines both battery cycling loss and battery calendar loss in one equation. The general capacity loss is a function of temperature, charge throughput, and operation time:

$$Q_{i,loss,\%} = (a \cdot T^2 - b \cdot e^{-3}T + c)\exp\left[(d \cdot T + e) \cdot I_{i,cell}\right] \times \sum_{i=1}^{i=i} Ah_i + f \cdot t^{0.5} \cdot \exp(-E_a/(RT)) \qquad i = 1,2,3,\cdots \tag{16}$$

where, $Q_{i,loss,\%}$ is the general capacity loss, i is the month number, T is environmental absolute temperature in °K, t is the number of operation days, $I_{i,cell}$ is the overall average discharge rate (C rate) at the end of "i" month, $\sum_{i=1}^{i=i} Ah_i$ is the charge throughout of the battery till "i" month. a, b, c, d, e and f are constant coefficients.

The battery capacity is not only related to the battery degradation, but also impacted by the operation temperature. For the same battery with the same degradation degree, the discharging capacity is lower in cold temperature. The battery capacity at 298.15°K is usually defined as the rating capacity. The real discharging capacity or relative capacity at different temperatures are determined through experiments [49, 116]. Based on experimental data [63], the relative capacity percentage can be expressed as a function of temperature using polynomial regression as shown below with an R-square of 0.99:

$$Relative\% = (0.0099 \times T^2 - 5.1818 \times T + 762.05) \times 100\% \quad (17)$$

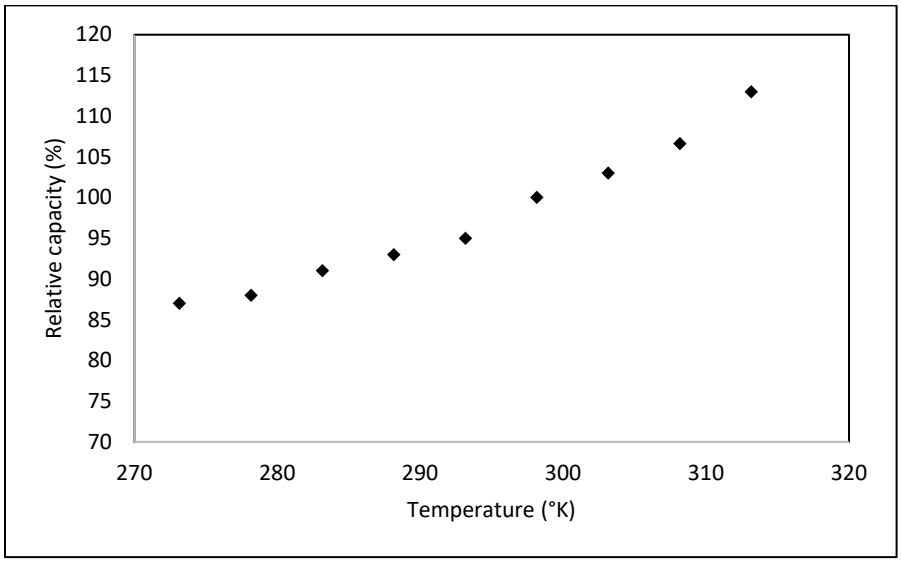

Figure 21. Relationship between Temperature and Relative Capacity

3.2 Simulation Structure

The economic benefits of the BESSs at various BESS sizes, utility data, operation temperatures, and operation strategies are simulated to investigate the effects of capacity sizing, operating temperature, battery degradation and utilization rate. Key factors and parameters used in the simulations and result analysis are:

1. Net present value (NPV) and net present value of unit BESS (NPVU). The cut off condition of the simulation is the lifetime of the BESS, which is 10 years according to the warranty of the vendor [117]. To evaluate the lifetime economic benefit of the BESS, the NPV considering both real discount rate and electricity price escalation rate are utilized. The rates used in our calculation are from US Department of Commerce as shown in Table 6 [118]. The NPVU is defined as the NPV of unit kWh of BESS.

Table 6. Economic Related Values [118]

Variable	Value
Real discount rate	3%
Average industrial electricity price index (***EI***)	Increase from 1.00 to 1.08 from 2018 to 2027

2. Normalized size percentage (NSP). The electricity demand profiles of various electricity accounts are different with each other. The absolute battery size cannot be used to equally compare the economic performance across different accounts. To get unbiased comparisons of the system performances, the NSP is defined as the ratio between “Size of BESS” and “Average Peak Demand”.

3. Utilization rate (UR). To quantitatively investigate how often the BESS is used, the utilization rate is defined as the ratio between “Discharging Time” and “Total on-peak Time”.

4. Simulation conditions and key parameters. To use the battery model introduced above, it is assumed the BESSs in this dissertation are all made from the same battery cell. The charging/discharging of the Li-ion battery can cause the battery degradation and capacity loss [119]. To reduce the battery degradation, the charging/discharging is usually controlled with ΔSOC lower than 100%, which is limited to 80% in all simulations [90, 120]. As the BESS is usually kept in air-conditioned space to avoid extreme temperatures, the simulation temperature range is set between 0°C and 40°C [121]. Only part of the energy stored in the batteries can be used to do useful work. Based on literature data [122], the average one-way charge/discharge efficiency (Eff_c and Eff_d) of 85% is used. Because the peak demand is measured monthly, the BESS capacity is calculated at the beginning of each month to determine the target peak demand reduction.

The overall simulation flow chart is shown in Figure 22. It is composed by three core sections: calculate target demand, obtain BESS operation status, and calculate economic benefit.

First, target demand calculation. Target demand is the proposed electricity peak demand of a facility with BESS installed. It is a key factor in the proposed simulation structure. Target demand determines the charge/discharge operation and hence influence the savings results. In each 15-minute interval during on-peak time, the BESS is designed to discharge to the facility whenever the electricity demand is higher than the calculated target demand. The discharge of the BESS yields demand reduction and is the major source of savings. In order to maximize the economic benefit, the goal is to use the least BESS to achieve the most demand reduction. Therefore, we

always minimize target demand for each scenario to get optimized savings. The target demand is determined by BESS capacity, operation temperature, and history utility data. BESS capacity is a variable which continue changes with time, cycling and operation condition. The nominal capacity rating of the BESS can be calculated using the battery model described in the battery modeling section. A BESS is usually composed of hundreds or even thousands of battery cells, therefore:

$$E_{rate,BESS} = \boldsymbol{N} \times Ah_{rate,cell} \times V_{cell}/1000 \quad (18)$$

where, $E_{rate,BESS}$ is the nominal capacity rating of the BESS, N is the number of battery cells, $Ah_{rate,cell}$ =1.5Ah is the capacity rating of the battery cell, and V_{cell} =3.7V is the nominal voltage rating of the battery cell. Not all the energy stored in BESS can be used for peak shaving. It is related with operation temperature, discharge efficiency, and discharge capacity limitation. The total available capacity also decreases with the increase of battery degradation. Therefore, at certain temperature:

$$E_{i,available,BESS} = \begin{cases} E_{rate,BESS} \times \Delta SOC \times Eff_d \times Relative\%, & i = 1 \\ Q_{i-1,loss,\%} \times E_{i-1,available,BESS}, & i = 2,3,4, \ldots \end{cases} \quad (19)$$

where, $E_{i,available,BESS}$ is the total available BESS capacity at the beginning of "i" month. With $E_{i,available,BESS}$ and history electricity demand profile known, the minimum target demand $D_{i,target}$ for each month can be determined. Under typical control strategy, the BESS is only charged at off-peak time and discharged at on-peak time. To investigate the influence of utilization rate, the benefit of charging battery at on-peak time is also analyzed in the simulations. Therefore, the target demands are calculated for two scenarios: with on-peak time charging and without on-peak time charging.

Second, obtain BESS operation status. The charge/discharge status of the BESS can be determined based on the target demand and utility data. The major purpose of this step is to

calculate battery capacity loss during operations and charge/discharge rates. As shown in equation 4, capacity loss is needed to calculate available capacity at the beginning of each month. Based on the battery model in equation 1, the average C rate and Ah throughput are needed for the calculation of $Q_{i,loss,\%}$. The average C rate can be calculated using the average discharge power and power rating of the BESS, as shown in:

$$I_{i,cell} = I_{rate,cell} \frac{\sum_{i=1}^{i=i} EC_i / \sum_{i=1}^{i=i} H_i}{E_{rate,BESS}/(1h)}, \quad i = 1,2,3 \cdots \tag{20}$$

where, $I_{rate,cell}$ is the rating C rate, which is 1.5A based on the specification of the cell used in this thesis, EC_i is total energy discharged from the BESS during on-peak time, H_i is discharge hours of each month. Both H_i and EC_i are obtained by applying the target demand to the utility data. The Ah throughput is the total discharge energy divided by the cell number and cell voltage:

$$Ah_{i,throughput,cell} = \frac{\sum_{i=1}^{i=i} EC_i}{NV_{cell}}, \quad i = 1,2,3, \cdots \tag{21}$$

Finally, the NPV of the cost savings is calculated based on the peak demand reduction, electricity consumption and utility rate. When the BESS is operated without on-peak time charging, the NPV of each month is:

$$NPV_i = \frac{(DR_i \times R_d + R_{e,p} \times EC_i - R_{e,o} \times EC_i/(Eff_d \times Eff_c)) \times EI_y}{(1+0.03)^y}, \quad i = 1,2,3 \cdots, \mathrm{y} = 1,2,3 \cdots \tag{22}$$

where, "y" is the year number of month "i", DR_i is peak demand reduction of each month, R_d is peak demand rate, $R_{e,p}$ is on-peak electricity rate, $R_{e,o}$ is off-peak electricity rate, EI_y is the average industrial electricity price index of year "y". When operated with on-peak time charging, the NPV of each month should be:

$$NPV_i = \frac{(DR_i \times R_d + R_{e,p} \times (EC_i - ECO_i \times (Eff_d \times Eff_c)) - R_{e,o} \times (EC_i/(Eff_d \times Eff_c) - ECO_i)) \times EI_y}{(1+0.03)^y},$$

$$i = 1,2,3\cdots, \mathrm{y} = 1,2,3\cdots \quad (23)$$

where, ECO_i is the on-peak time charging energy consumption.

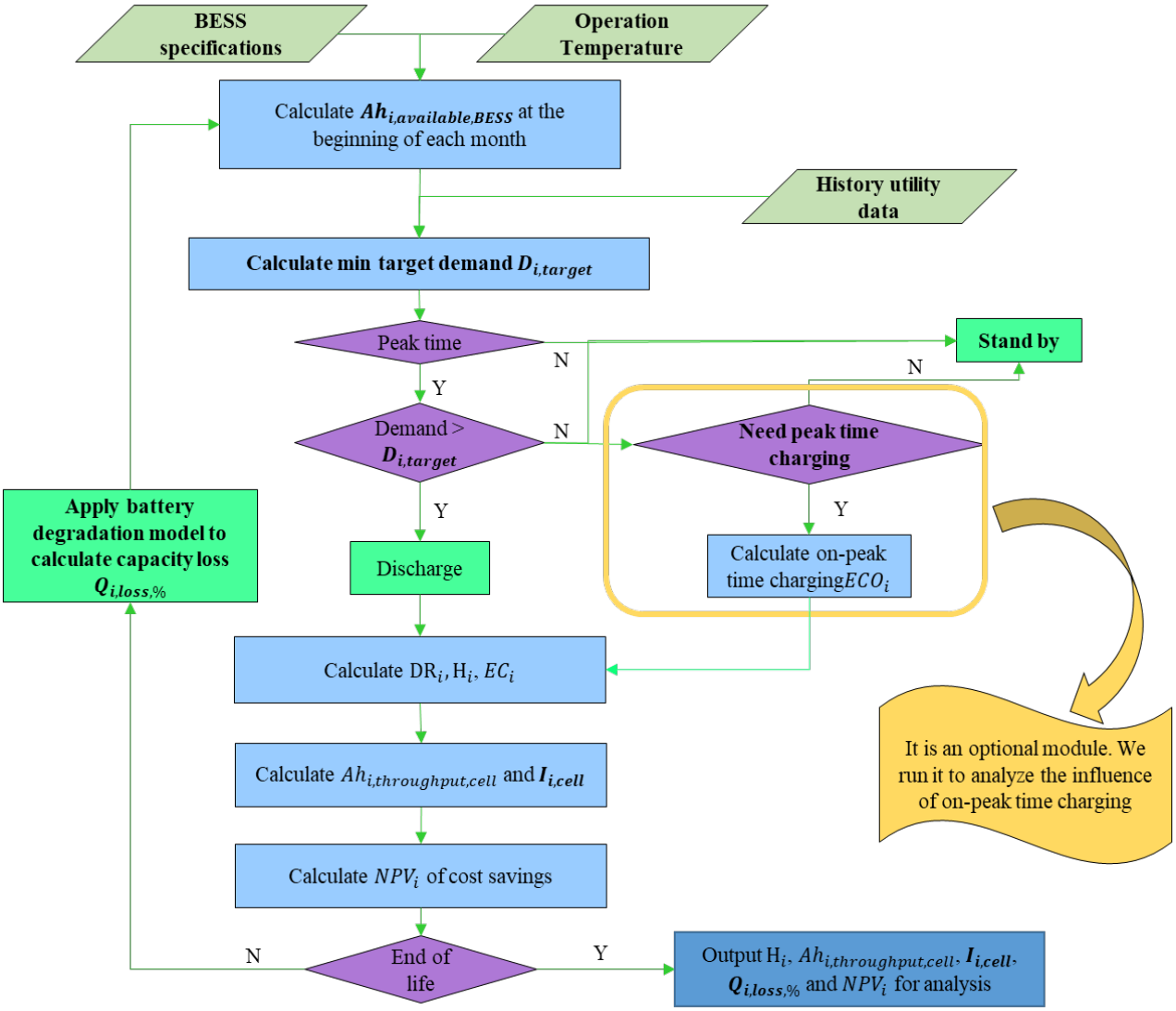

Figure 22. Simulation Flow Chart

3.3 Simulation Results and Discussion

3.3.1 Utility Rates and BESS Cost

Rate structure of utility company and the cost of BESS significantly impact the economic benefit of the BESS. There are two major BESS-friendly electricity rate structures, namely, Demand Charge rate and TOU rate. Demand Charge rate is typically designed for medium and big commercial and industrial (C&I) customer. Peak demand is usually the monthly maximum power (kVa or kW) calculated in certain time interval during on-peak period. Peak demand charges billed to customers could vary monthly based on the equipment utilization schedule [123]. TOU rate is the most common pricing structure used for residential and small C&I customer. It encourages the usage during off-peak time and reduces peak demand load for the grid. The price usually varies two to four times a day per the peak demand occurrence periods. Typically, the electricity rate for consumers served under TOU program has a lower cost at night and a higher cost during daytime. Some utility companies offer an intermediate rate for early morning or late afternoon [124]. Table 7 illustrates the rate structures of two selected utility companies.

Due to the focus of this section is peak demand reduction, the Demand Charge Rate is used in all simulations. One-year 15-minutes utility data from seven small industrial facilities in Wisconsin was collected. The average monthly peak demand of each facility is shown in Table 8. It is assumed the electricity consumption profiles are the same for every year when simulating. Because “Cg3” tariff in Table 8 is the most common rate structure in the surveyed facilities, it is employed for all simulations to eliminate the influence of utility rate. The purpose of this thesis is to investigate the maximum potential of the BESS, therefore, all the simulations are based on perfect electricity demand prediction, which is also the assumptions made in [42, 59].

Table 7. Rate Structures for Different Utility Companies [125, 126]

State/Utility Company	Rate Type	Seasons	On-peak ($/kWh)	Off-peak ($/kWh)	Demand ($/kW)	On-peak Periods	Criteria
Wisconsin/We-Energies	Residental-TOU (Rg 2)	All seasons	$0.1968	$0.0896	N/A	Weekdays: 7 a.m. to 7 p.m. Or 8 a.m. to 8 p.m. Or 9 a.m. to 9 p.m. Or 10 a.m. to 10 p.m	Annual usage > 60,000 kWhs.
	General Secondary Service (Cg 3)	All seasons	$0.0784	$0.0562	$13.80	Weekdays: 9 a.m. to 9 p.m.	Daily usage > 986 kWhs for any 3 out of 12 month period.
Arizona/Salt River Project	General Service TOU (E-32)	Summer	$0.1521	$0.0528	$4.32	Weekdays: 2 p.m. to 7 p.m.	May, June, September and October. Shouder-peak rate is $0.1030/kWh for 11 a.m. to 2 p.m. and 7 p.m. to 11 p.m. in weekdays.
		Summer Peak	$0.1671	$0.0538	$6.65	Weekdays: 2 p.m. to 7 p.m.	July and August. Shouder-peak rate is $0.1093/kWh for 11 a.m. to 2 p.m. and 7 p.m. to 11 p.m. in weekdays.
		Winter	$0.1151	$0.0512	$4.06	Weekdays: 5 a.m. to 9 a.m.	November through April. Shouder-peak rate as $0.1036/kWh for 5 p.m. to 9 p.m. in weekdays.

Table 8. Average Peak Demand Data of Each Facility

Facility number	Facility 1	Facility 2	Facility 3	Facility 4	Facility 5	Facility 6	Facility 7
Average peak demand (kW)	172	433	202	85	181	523	812

The high price of Li-ion battery is a major factor that limits its utilization as an energy storage. The industry-wide cost of EV Li-ion battery is around $410/kWh in 2014 [39]. The Powerwall from Tesla designed for home and small business application is about $437/kWh. It is also equipped together with some support hardware and a Bi-Directional high-efficiency inverter which cost additional $300/kW. Based on available research [42] and online quote system, the unit

costs of the BESS including installation is expressed as a function of the battery size and the inverter size [117]:

$$\text{Unit Cost} = \frac{437\times\text{Battery Size}+300\times\text{Inverter Size}+1000}{\text{Battery Size}} \quad (24)$$

where, the units of battery size and inverter size are kWh and kW respectively. The capacity of the BESS includes energy capacity determined by the battery pack size and power capacity determined by the inverter/converter size. The capacity of the BESS in this research is mainly about the energy capacity because it is the major factor that limits the BESS capability [45]. When used for peak shaving, the optimized inverter power is at the same level with the battery size [48]. There will be economic benefits to optimize the power capacity and try to have a smaller inverter. However, a small investor would limit the power output of the BESS in extreme cases. The smaller inverter size also limits the expansion capability of the BESS. Moreover, the unit price of the inverter is much less than that of the battery. Therefore, it is assumed the inverter size is the same with the battery size when calculating the BESS cost.

3.3.2 Sizing Effect

Due to the high cost of BESS, it is critical to properly size BESS for each application. The system NPV and NPVU are used as economic indicators to compare the sizing effect. The operation temperature is set to be 20°C during sizing analysis.

To obtain the maximum economic potential of the BESS in each facility, the NPVs of the BESSs with various NSPs were calculated for all seven facilities. The results are shown in Figure 23. The NPVs for seven facilities are totally different with each other. Because all the other simulation factors are the same, the only explanation is that the NPV highly depends on the utility data. The best NPV changes from negative to more than $35,000. There is no payback for facility

4 no matter what size we choose. A positive NPV can be obtained for facility 6 even more than 30% NSP is chosen. The NPVs of the BESSs will become negative if the NSPs are larger than critical values. The critical NSPs for every facility are also different. In most cases, the critical NSPs are less than 15%. Overall, the average NPV is largest when the NSP is around 4%.

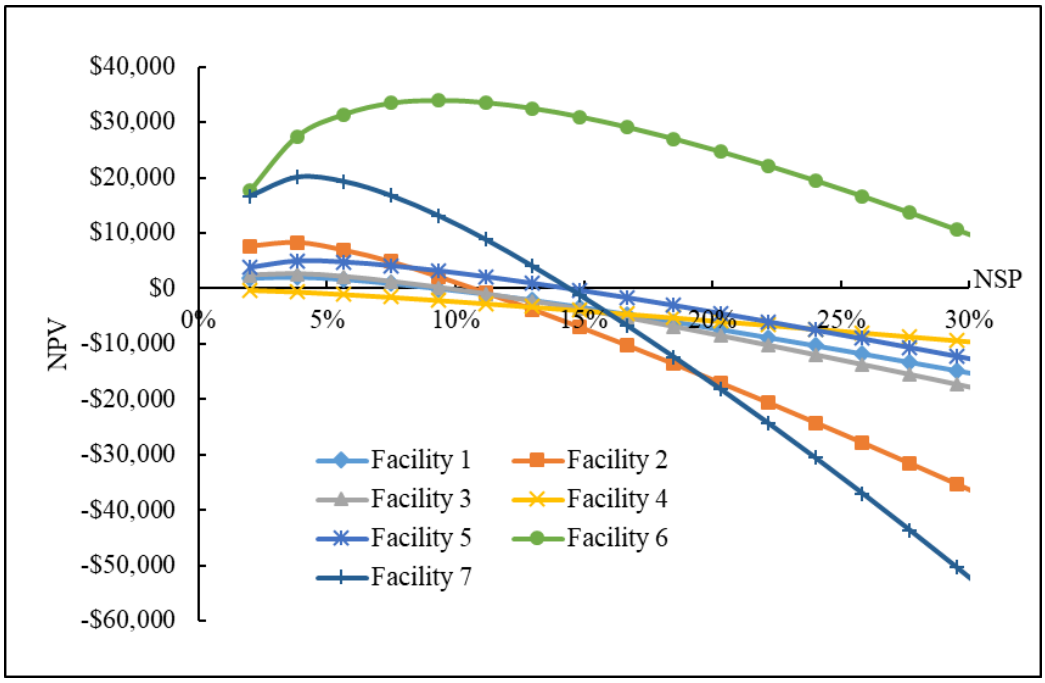

Figure 23. Influences of NSP on NPV

The NPV of the whole system is closely related to the absolute size of the BESS. The facility with higher demand requires larger BESS size and more investment. To obtain the economic benefit of unit size BESS, the NPV of unit BESS (NPVU) is calculated and shown in Figure 24. The results show a smaller NSP is always better for the NPVU. The NPVUs are positive when the NSPs are lower than 9% excepting facility 4. Utility data clearly impacts NPVU. However, the NPVU is not totally proportional to the facility demand. Such as the electricity demands of Facility 7 and Facility 5 are ranked first and fifth, but their NPVUs are ranked third and second respectively.

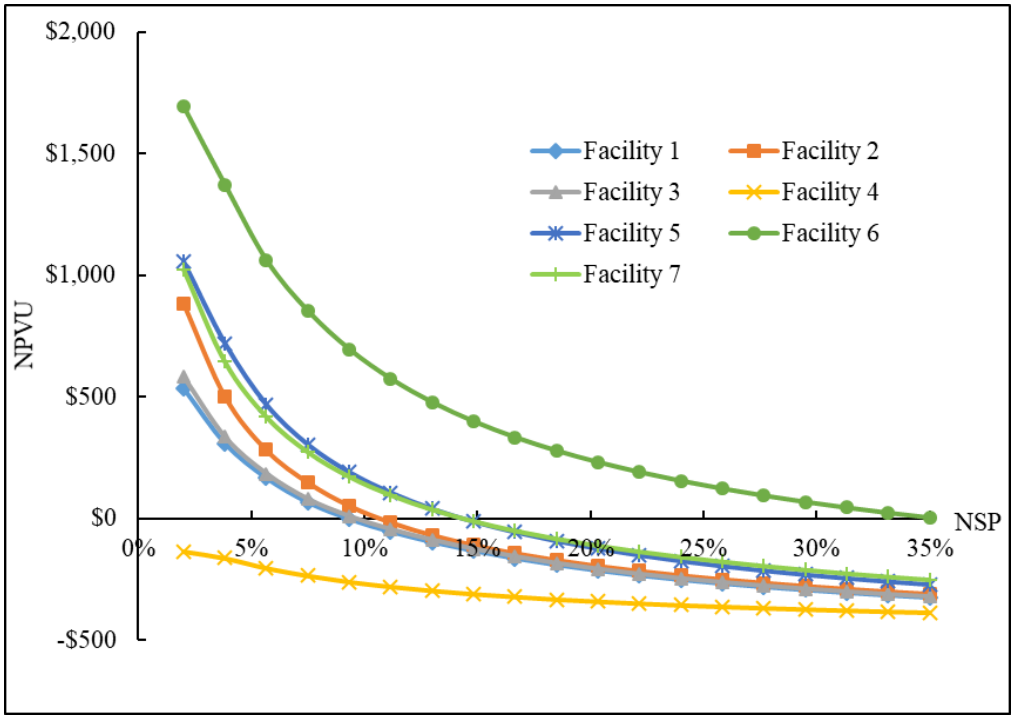

Figure 24. Influences of NSP on NPVU

Overall, the benefit of optimizing the size of the BESS is limited by the best NPV. The NPVU is negatively related with NSP and highly depended on the utility data. In order to have better economic profit, the size of the BESS needs to be very small. Similar results have been drawn from other research. Simulations for 98 facilities showed the smaller BESSs had better NPVs in [47]. The optimized battery size is between 16kWh and 20kWh for a facility with higher than 600kW demand in [48]. With necessary data in hand, the companies can choose the proper NSP based on their own preferences using the proposed method. The obtained figures are only an estimate based on the case study data and subject to uncertainty. The detailed relationship is highly dependent on the BESS cost and the utility data.

3.3.3 Degradation and Temperature Effects

Battery degradation significantly influences the overall system performance. Due to degradation, the available capacity of BESS declines during each operation cycle and all the standby time. Its peak demand shaving potential also decreases day by day. According to battery model, temperature is a key factor that impacts battery degradation. Temperature also influences battery relative capacity. Because of their close interaction with each other, the effects of degradation and temperature are analyzed in the same section. Degradation is determined by C rate, Ah throughput and temperature. C rate and Ah throughput are highly dependent on the NSP and utility data. Therefore, two groups of simulations are carried out.

First, keep the temperature as constant (use 20°C), the NSP changes from 2% to 35%. Simulations are done for all seven facilities. Results are illustrated in. The capacity loss is around 38.6% after ten years of operation. The differences of the final capacity losses for all cases are less than one percent, which means the C rate and Ah throughput nearly have no influence on the battery degradations in all case studies. This is can be explained by the super low cycling loss. According to the results, the average monthly operation hour and C rate are only 9.2hours and 0.174 respectively. The utilization rate is calculated to be 3.6%. These results are comparable to the results from [47], in which the optimized operation hours of the BESS is between 30 and 40minutes per day. [58] suggested to use the BESS around 1.5% of the time to maximize the savings. The extremely low utilization rate results in less than one percent overall cycling loss difference. Therefore, the degradation is mainly caused by calendar loss, which is dominated by temperature. The BESS needs to be maintained at a proper temperature to minimize the calendar loss and prolong battery life.

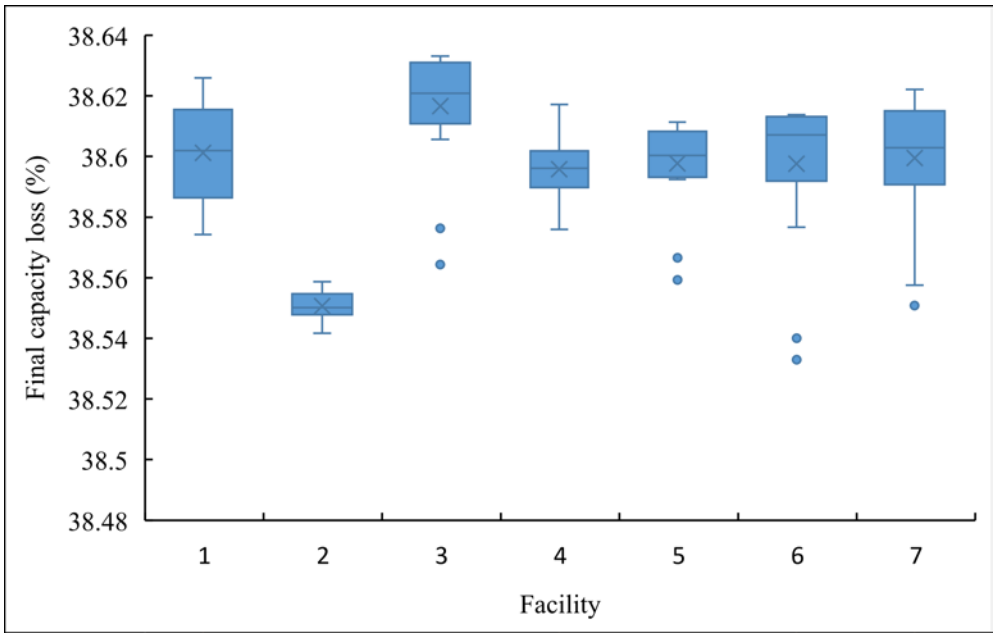

Figure 25. Final Capacity Losses of Every Facility at Various NSP

Second, keep the NSP as constant (use 10%), the temperature changes from 0°C and 40°C. The results are shown in Figure 26. NPVU slightly declines with the increase of the temperature in all scenarios. The final capacity loss steadily increases from 19.3% to 73.2% when the temperature increases from 0°C to 40°C. The final available battery capacity is less than 50% of the rated capacity if operated at 30°C or higher. The average NPVU at 0°C and 25°C is $147.4 and $111.4 respectively, which represents a 24.4% savings difference. When the temperature increases from 25°C to 40°C, the average NPVU decreases by 67.4%, which means the savings reduction is more than doubled in less temperature increase compared with that of changing the temperature from 0°C to 25°C. Therefore, temperature greatly impacts battery degradation. To prolong battery life, higher than 25°C operation temperature should be avoided. This result is consistent with the analysis from [127], in which the degradation rates of all components of the battery were found to increase when the temperature was higher than 25°C. The contiguous United States average temperature is 12.4°C in 2015 [128]. When lowering the temperature from 12.4°C to 0°C, the

NPVU is increased by 7.8%, which is the average potential savings improvement by optimizing the operation temperature.

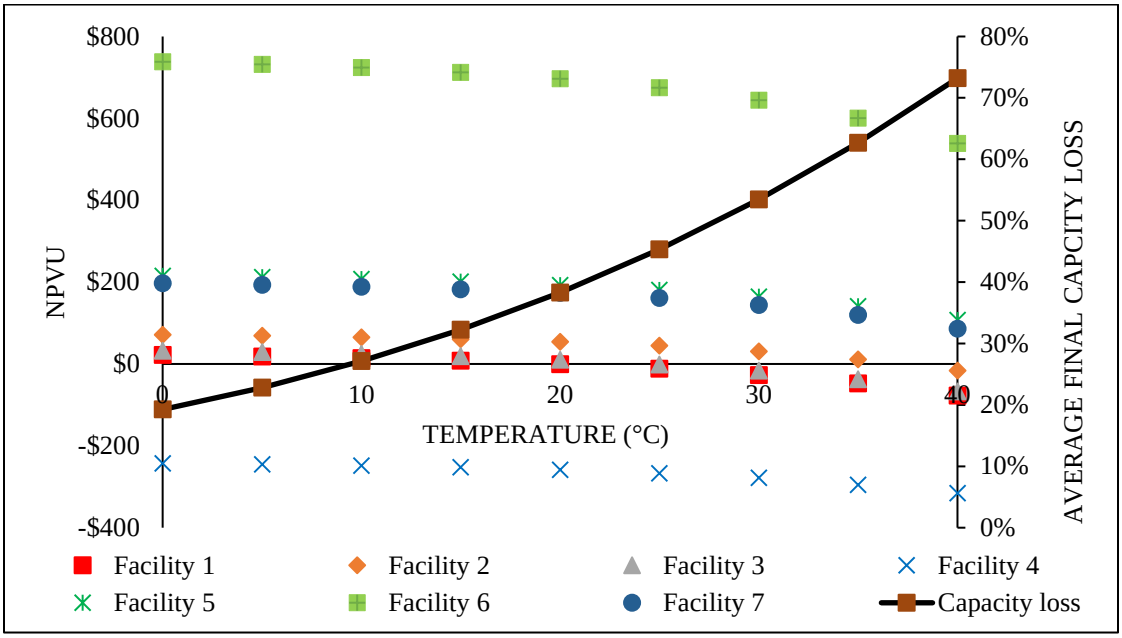

Figure 26. Impact of Temperature on The NPVU and Capacity Loss

In conclusion, the cycling loss of the BESS is super low when used for peak shaving due to the low operation hours. The temperature related calendar loss is the major capacity loss. The NPVU can be maximized by adopting optimized operation temperature, but the average savings improvement is only about 7.8%. Currently, the mainstream industrial scale BESS is designed to be placed in a container with integrated HVAC system. It is costly to maintain the temperature at a specific set point all through the year. Therefore, the aim of the thermal management system should be trying to maintain the temperature at an optimized range and to avoid extreme operation temperatures which may cause serious battery damages or system failures. The extra heating is important in cold climate region such as great lake area to keep the environmental temperature above the freezing point. The air condition cooling is necessary in warm area such as sunbelt region to cool down the environmental temperature to below 25°C. It is necessary to take the cost of

thermal management systems into account and propose the regionally optimized operation temperature ranges for different locations in the future.

3.3.4 Utilization Rate Effect

When used for peak shaving, the BESS only discharges when the "peak demand" reaches the target demand. The so called "peak demand" doesn't happen all the time in a facility. As descripted in the above section, the average discharging time is only 9.2hours in some cases. The cycling loss is less than one percent due to the extremely low utilization rate. A typical peak shaving effect of one month is simulated and illustrated in Figure 27. It is shown the BESS is operated at standby mode for most of the time. Therefore, it is critical to investigate the impact of utilization rate on NPVU. As an important approach to increase the utilization rate, on-peak time charging strategy is studied in this research.

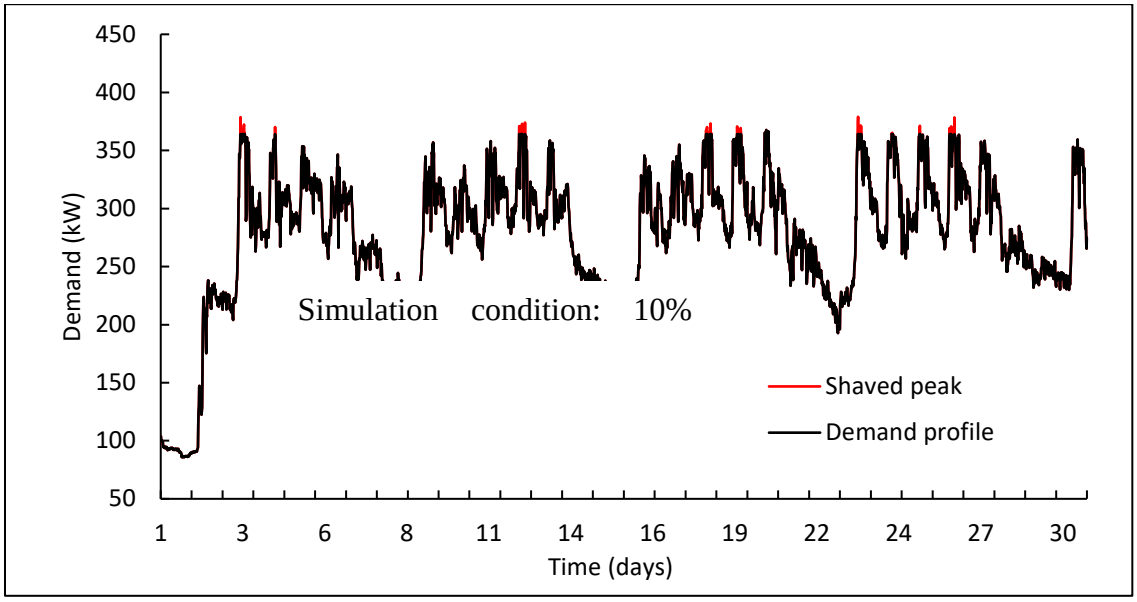

Figure 27. Illustration of Demand Reduction Effect in One Month

When used for load shifting, the BESS can only be charged at off-peak time and discharged at on-peak time to avoid paying high electricity prices. However, due to the much higher price of

electricity demand, the on-peak time charging is possible if the BESS is used for peak shavings. According to research, the economic savings of demand charges can easily offset the higher energy cost [47]. As shown in Figure 28, the electricity stored in the BESS may be exhausted during A1 area without on-peak time charging. Therefore, the target demand cannot be achieved because there is no available capacity left in the BESS. Nonetheless, if the BESS can be charged during A3, it would be capable to support A2 area and thereby provide more demand reduction potential. This on-peak time charging can effectively increase the utilization rate of the BESS.

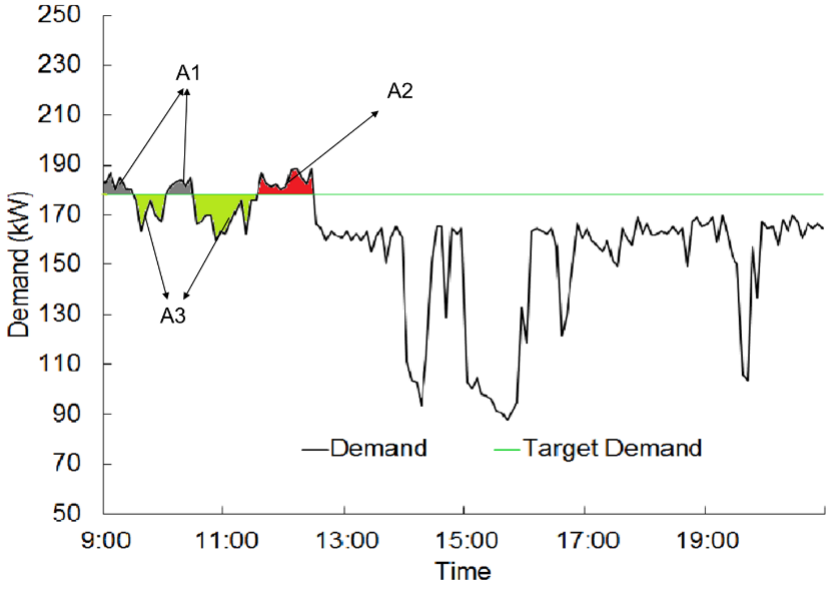

Figure 28. On-peak Time Charging Effect Illustration Using One Day's Electricity Profile

Simulations were carried out assuming the batteries can be charged whenever the real demands were lower than the target demands and the batteries were not fully charged. The simulation conditions are 20°C operation temperature and 2%-11% NSP (this is the NSP range where most of the BESS may have positive NPVU). The increase of NPVU by adopting on-peak

time charging is illustrated in Figure 29. In general, $117.3 to $491.7 more NPVU can be obtained using on-peak time charging. The average increase is $241.5 for all scenarios, which represents a significant 69.9% increase compared to the NPVU of without on-peak time charging.

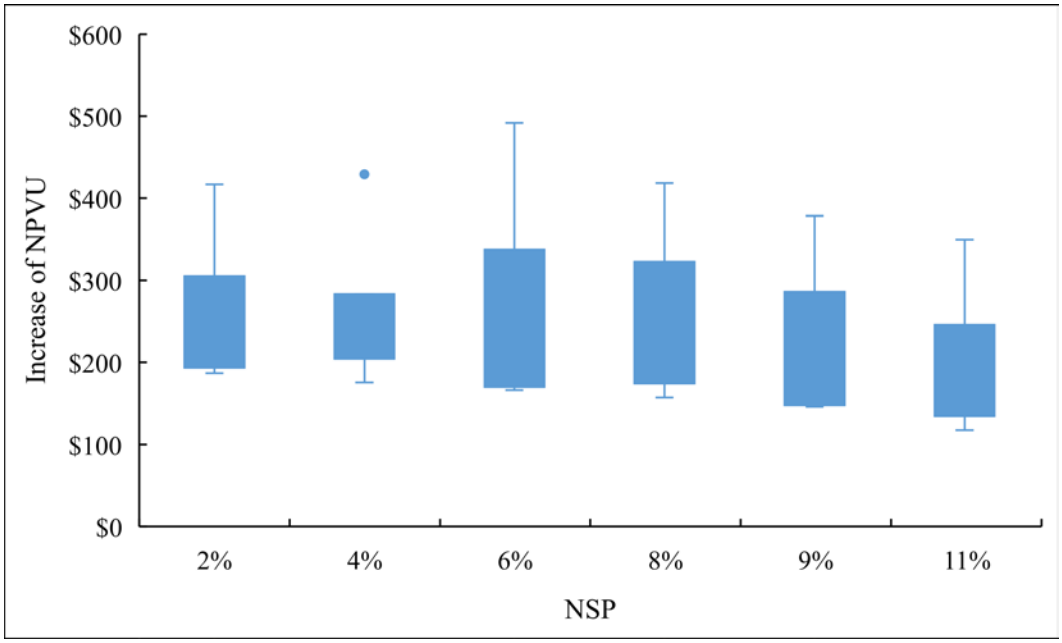

Figure 29. Increase of NPVUs at Various NSPs

The saving improvement is more critical when the customer is pursuing a larger BESS. The comparison of NPVUs using 10% NSP and 20°C temperature is shown in Figure 30. With on-peak time charging, the NPVUs of facility 1 to 3 are increased from nearly zero to about $200, which can change the projects from nearly non-profitable into economically feasible. Because all the other conditions are the same, the improvement from on-peak time charging is mainly caused by the increase of system utilization. According to the simulations, the utilization rate, and average C rate and Ah throughput are increased by 35.2%, 18.1%, and 59.8% respectively. One concern of using on-peak time charging is the increase of cycling number may hurt the battery life. However, the final capacity losses are only less than one percent more than that of without on-peak time charging in all scenarios. The reasons are the extremely low lifetime Ah throughput and

average C rate. According to the research [115], the cycling loss of 300Ah throughput at 0.5C is less than 1%. The overall average C rate and average Ah throughput with on-peak time charging are 0.21C and 544Ah in the simulations. Hence, their values are still too low to obviously impact the battery cycling degradation. The calendar loss which remains the same is the major capacity loss in any cases. Therefore, with the increase of utilization rate resulted from on-peak time charging, NPVU of the BESS is greatly boosted with nearly no sacrifice of the battery life. These results are similar with the conclusion from [81], in which the utilization rate of the BESS is increased by sharing BESS among consumers. The NPV of the BESS is almost doubled and a larger BESS becomes profitable.

Compared with choosing proper sized BESS, reducing battery degradation and optimizing operation temperature, the benefits of increasing utilization rate are obvious. The benefit from optimizing the size of the BESS is limited by relatively low NPV because only very small NSP can be chosen. The optimized NSP also highly depends on the utility data and the preference of the customer which subjected to uncertainty. The cycling loss of the BESS used for peak shaving is ignorable because of the low utilization rate. Therefore, an effective approach to reduce battery degradation is to maintain the storage temperature at the optimized level to limit the calendar loss. The average NPVU can only be increased by 7.8% by optimizing the operation temperature and reduce the battery degradation in the case studies. Nonetheless, the average NPVU is increased by 69.9% with the application of on-peak time charging. The utilization rate of the BESS is only about 5.6% in this situation. There is still a great potential to optimize the operation structure of the BESS to further increase its utilization rate. The possible approaches include integrating the BESS with other demand response system, sharing one BESS among multiple electricity accounts, and

combining the BESS with renewables etc. [58]. Therefore, the utilization rate is recognized as the most important factor that impacts the economic benefit of the BESS.

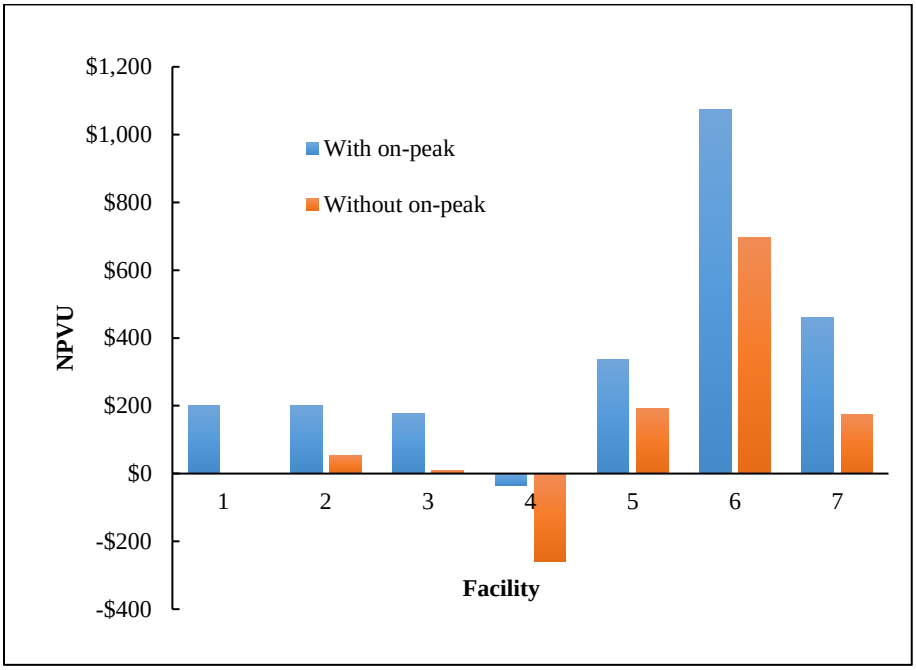

Figure 30. Comparison of NPVUs at 10% NSPs

3.3.5 Spatially Potential in the US

To provide a guideline about the application of BESS, the cost savings for each state in the US is estimated using the real electricity rates. The electricity consumption data of 30 big C&I sites form 2012 from Open Data [129] is used for simulation. The data includes building types of education, light industrial, food sales & storage, and commercial property, which makes it a good representative for all kinds of C&I consumers. Because the EIA doesn't report peak demand rate for each state, the rates from major energy suppliers are collected and applied to the BESS model (no on-peak time charging, 10% size percentage, 20°C, 10years lifetime), the lifetime cost savings

per unit BESS is illustrated in a map as shown in Figure 31. Considering the overall system cost of over $600/kWh including invertor, the BESS is only economically feasible in limited states.

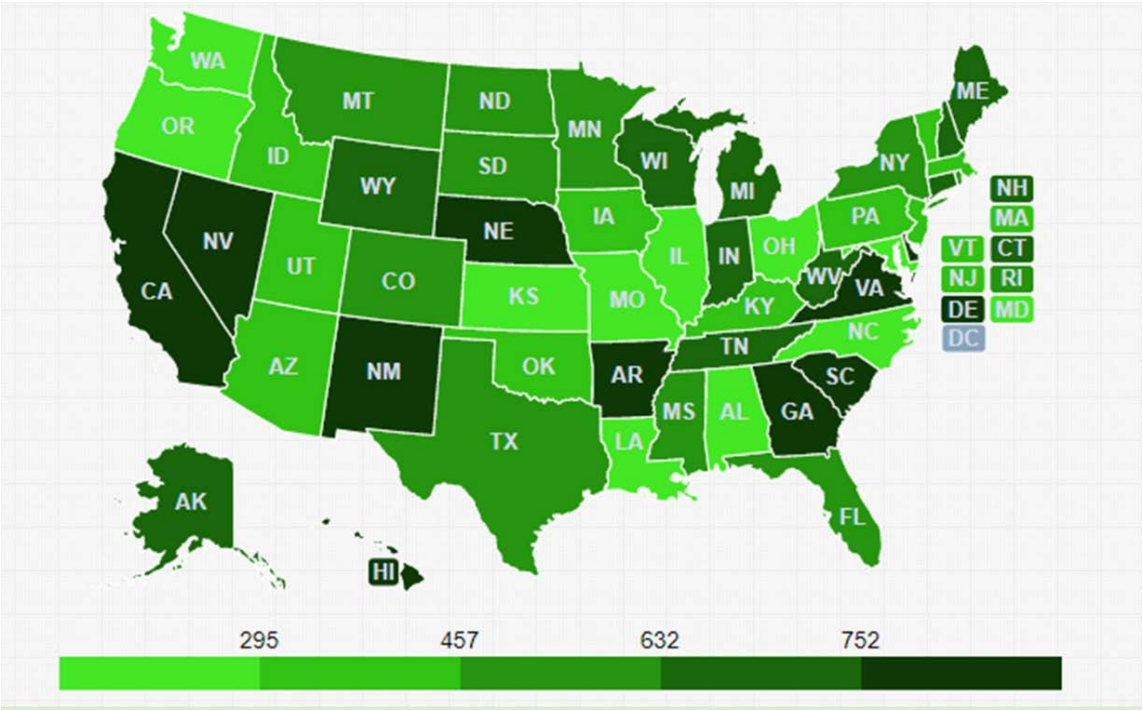

Figure 31. NPVU of BESS Used for Peak Shaving in Each State ($/kWh)

Due to the complexity of modeling process, it is hard for individual consumers to estimate their potential savings from using BESS. A simple estimate approach is proposed by using the standard deviation. Theoretically, there would be no demand reduction if the consumption is constant during the on-peak time. The fluctuation of the consumption is the source of demand reduction. Therefore, the relationship between standard deviation and demand reduction in 30 big C&I consumers is analyzed and shown in Figure 32**.** 10% BESS size percentage is used in the simulations. A clear parabolic relationship is observed with an R^2 of 0.8671. The demand reduction can be expressed as:

$$DR = 0.0062Std^2 - 0.2358Std + 5.8848 \quad (25)$$

where, DR is demand reduction, Std is standard deviation. The consumer can use this simple expression to estimate the possible demand reduction with utility data in hand.

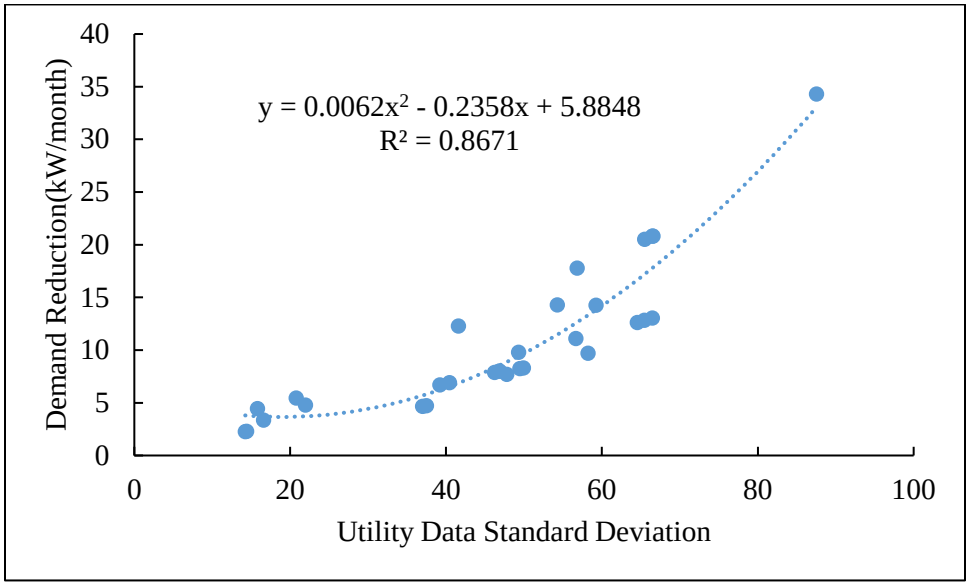

Figure 32. Relationship between Standard Deviation and Demand Reduction

4. Comprehensive Demand Side Management (DSM) System

According to the analysis of the PTL/T system in the second chapter, its cost savings needs to be greatly boosted to make it economically feasible in most of the cities. During the initial calculation of electricity cost savings, only electricity consumption cost was counted in the financial savings. The peak demand reduction was not considered due to the intermittent behavior of the sunlight. Daylighting systems need to be integrated with artificial lightings to provide consistent lighting. The short period operation of the artificial lightings still results in the increase of the on-peak electricity demand. The demand charge is a big part of the total utility bill. Therefore, it is essential to reduce both electricity consumption and peak demand using PTL/T system, which can be achieved by integrating with BESS. The economic feasibility of using BESS for electricity peak shaving is better than PTL/T system but its simple payback period is still relatively long. The low utilization rate of the BESS is the key factor that draws back its economic benefits. Based on analysis in [51], the BTM energy storage can provide up to 13 services for all stakeholders simultaneously. However, its economic benefits for utility services and ISO/RTO services are hard to be quantified and collected by the end-use customer. This thesis only focuses on the savings that can directly benefit the customers. Therefore, two DSMs based on sharing strategy are investigated in this chapter to maximize the cost savings and the reliability of both PTL/T and BESS: a) Simple sharing. Under this methodology, one BESS is shared among several customers for single service, to reduce the peak demand with its best savings potential; b) Comprehensive sharing, which is to share one BESS to provide multiple services such as peak demand reduction, TOU bill management, integration of PTL/T, and power quality control etc.

4.1 Simple Sharing

The core value of the sharing economy involves unlocking the value of unused or low utilized assets for monetary, environmental, social or other benefits. The low utilization rate and high cost of the BESS make it a great potential candidate for sharing economy. Considering many small and medium C&I customers are located together in many places, it is proposed to simply share one BESS in multiple C&I buildings for peak shaving. An optimized sharing structure is introduced to maximize demand reduction. Case studies are carried out to investigate the possible savings increase and reliability improvement.

4.1.1 System Structure in Simple Sharing

The same BESS model and utility database in Chapter 3 are used in this section. The overall design and operation of the simple sharing network are illustrated through Figure 33. The shared BESS works similar to a cloud service. Each consumer buys certain capacity of storage, which is certain percentage of its average peak demand in the case studies. The optimized target demands can be calculated for all customers based on the overall history utility data and the size of BESS. During on-peak time, the customer can request discharge from BESS whenever the demand from the smart meter is higher than the designed target demand. At off-peak time, the consumer needs to charge the BESS according to the electricity it withdraws, which should include efficiency compensation during charge/discharge. Because the BESS is BTM energy storage, it is not necessary owned by the utility company. It can be owned and maintained by the community based on their requested share of capacity. A certain number of sites can be selected to participate the sharing network. Considering the restriction of both geometry and market, it is better to limit the number of customers in each case, which is set to change from one to six in the simulations. To get reliable results, ten sets of simulations are designed for each scenario.

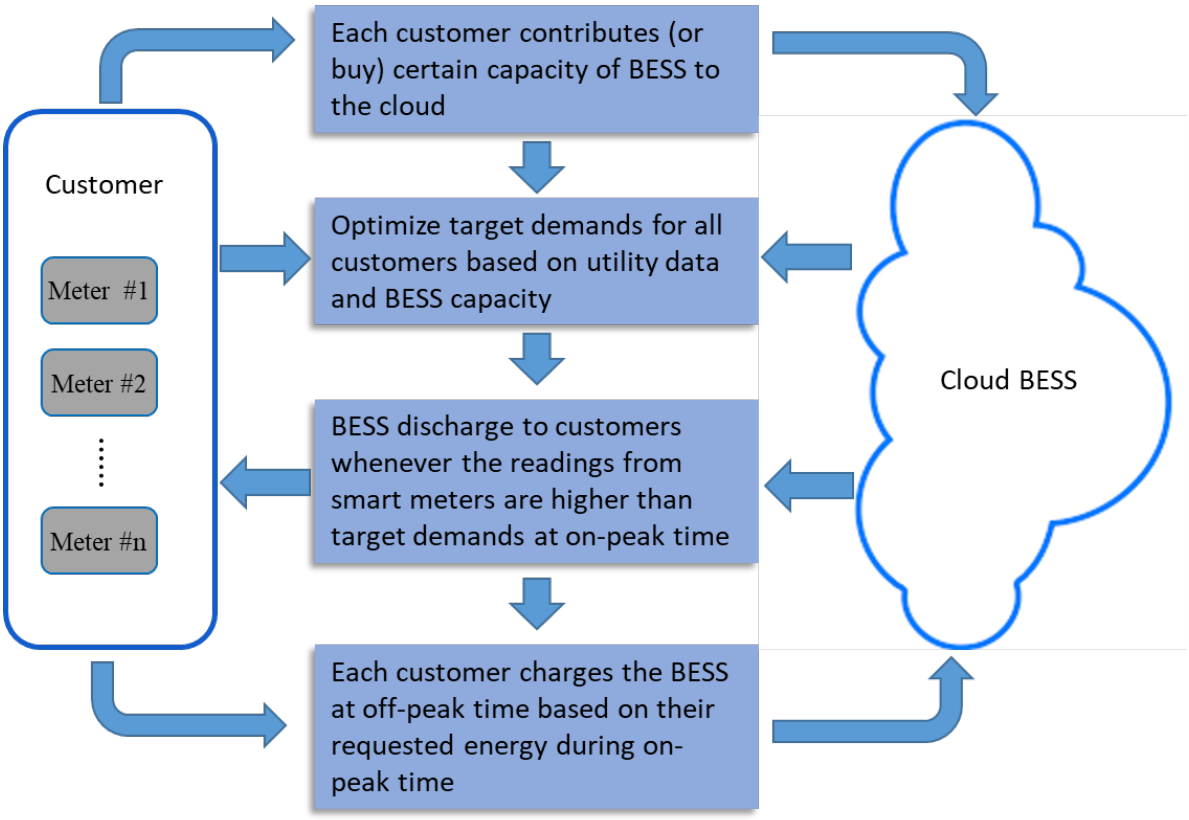

Figure 33. System Structure of Simple Sharing Network

It is worth to mention although the on-peak time charging can greatly boost the savings from BESS, it is not used in the simple sharing network. The reasons are: 1) electricity sell among end-use-customers are not allowed by most of the utility companies, 2) the frequently charge/discharge among different customers is hard to be controlled.

4.1.2 Optimization of the Target Demands

Suitable target demand for each site is necessary, otherwise there maybe not enough capacity left when needed or too much capacity wasted by idling. Considering the characteristic of peak demand charge, a single miss in one month means no savings at all. Hence, the optimized target demand calculation is the core part in this simulation. Due to the uncertainty of the utility data, no function can be presented to accurately describe the electricity consumption. Therefore,

search-and-test method is used to find the optimized target combination in each scenario. Because Genetic Algorithm (GA) works well to solve the problems with flexible efficient solution, or with no set function well defined, it is used to search the combined minimum target demand in the proposed structure.

GA is an adaptive heuristic search method inspired by the mechanism of biological evolution. It is efficient to be used to solve both constrained and unconstrained optimization problems [130]. Benefiting from the development of computer technologies and maturing of the computational algorithms, GA was firstly introduced in early 1970s to help researchers to search the optimized solutions in changing environment. Some biological terms are adapted to introduce the process of genetic algorithm. Chromosome, which consists of genes at particular locations and serves as the "blueprint" for all living organisms, is typically referred as a candidate solution for the problem. A set of solutions is called population. To create the next generation of solutions, recombination, or crossover of randomly selected chromosomes occurs. Mutations, which consist of gene change at random location, also occurs at random frequency. The degree of goodness for each chromosome is evaluated by a fitness function at each generation. The fitness value is used as the criteria to select the chromosomes for next generation. Since the chromosomes with high fitness values are more possible to stay in the population, the new generation of chromosomes tends to have higher average fitness value than those of the old generation. This screening process is then repeated until the termination condition is satisfied [130, 131]. GA discovers and combines good "genes" of solutions in a highly parallel fashion. It is an excellent tool to search for optimal solutions in complex environment or among large spaces of possible solutions [132]. Therefore, GA is a good fit to find the optimized target demand for each consumer in the sharing plan.

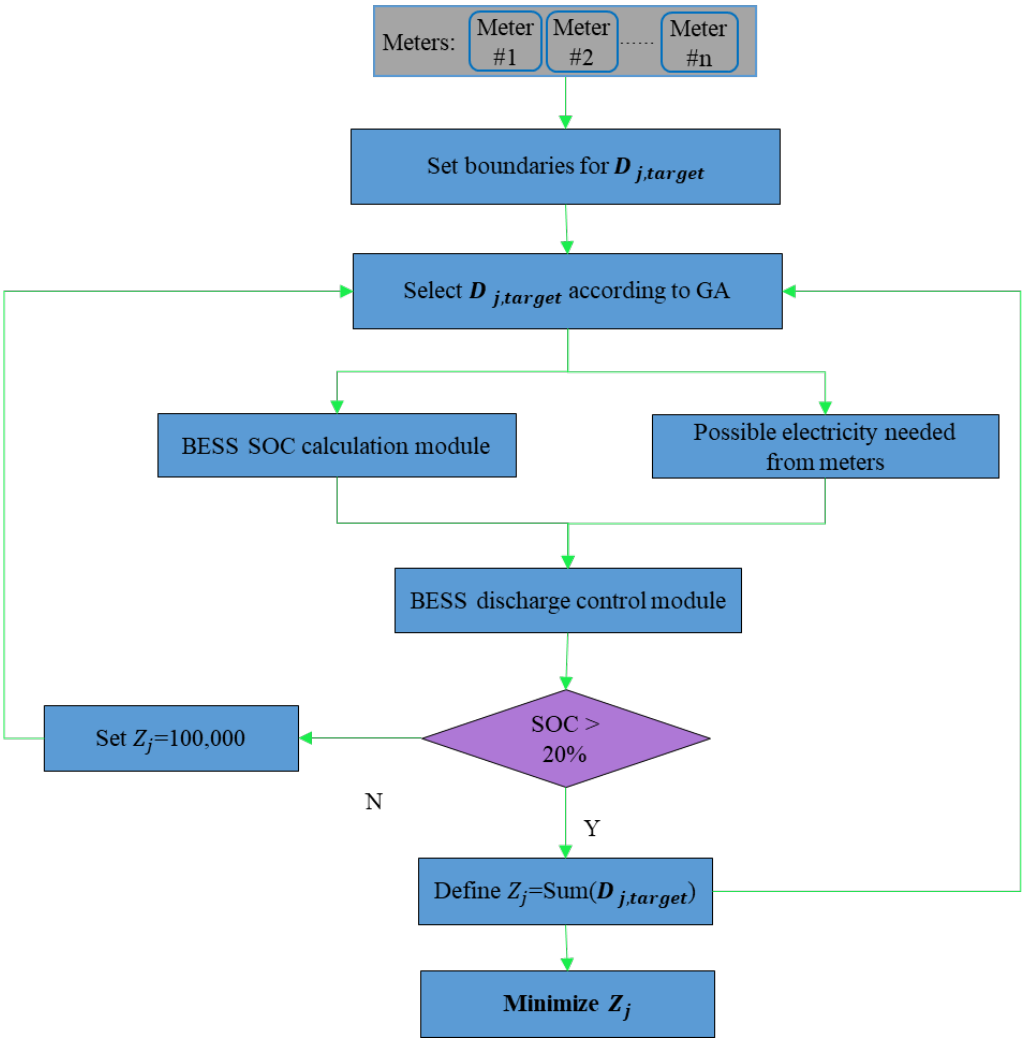

Figure 34. Target Demand Minimization Process

The overall target demand minimization procedure is shown in Figure 34. The basic simulation conditions are: 20°C temperature, 10% sizing percentage, and 10-years lifetime. SOC calculation module is based on the battery model from chapter 3. BESS discharging is based on the target demand selected by GA. During on-peak time, set Z to a large number whenever the SOC is less than 20%, which means a failure. The calculation of target demand is a constrained minimization problem. The control function is:

$$F_n = \text{Min}\,(Z_j) = \text{Min}\,(\text{Sum}\,(D_{i,j,target})) \quad (26)$$

where, Z_j is the proposed target demand for month "j", $D_{i,\,j,target}$ is the target demand for consumer "i" at month "j". GA optimization tool in Matlab is used to search proper $D_{i,j,target}$ which fulfills the requirement of minimizing Z_j. By participating the sharing plan, the consumer certainly is expecting more savings. Therefore, the target demand for single customer application (under the same simulation condition) is set as upper boundary, which ensures more DR can be achieved for each consumer. It is also not fair to provide too much DR for one consumer. A 15% DR is set as lower boundary to prevent overdraw from single consumer. The other important GA parameters are obtained based on convergence speed and quality during simulation tests, which are listed in Table 9.

Table 9. Key Parameters of GA Optimization

Parameters	**Values and Conditions**
Population size	200
Creation function	Constraint dependent
Scaling function	Rank
Selection function	Stochastic uniform
Crossover fraction	0.85
Mutation and Crossover	Constraint dependent
Generation	150
Stall Generations	100

4.1.3 Results Analysis

As described in system structure section, six sets of simulations were carried out to investigate the impact of simple sharing strategy. Constant operation temperature of 20°C was used in all simulations. Because low system utilization rate and high initial equipment cost are the major barriers for the application of BESS's application, BESS utilization and economic benefit are used as the key indicators to demonstrate the advantage of simple sharing strategy.

4.1.3.1 BESS Utilization Analysis

As concluded in Chapter 3, the low utilization rate is the most significant factor that impacts the economic benefit of BESS. The simulation results of the simple sharing strategy reveal great utilization rate and average operation hours improvement as shown in Figure 35. The utilization rate increases from 4.08% to 11.45%, while the average operation hours increase from 10.5 hours/month to 29.4 hours/month. More importantly, the increased charge/discharge cycle does not significantly impact the battery life. The absolute capacity loss only increases by less than 2% as shown in Figure 36. The reason is the average C rate and Ah throughput of the battery cell are still relatively low. At the scenario of six customers, the C rate and Ah throughput are 0.38C and 1123Ah respectively, which means less than eight full cycles per month. Calendar loss still dominates the battery degradation.

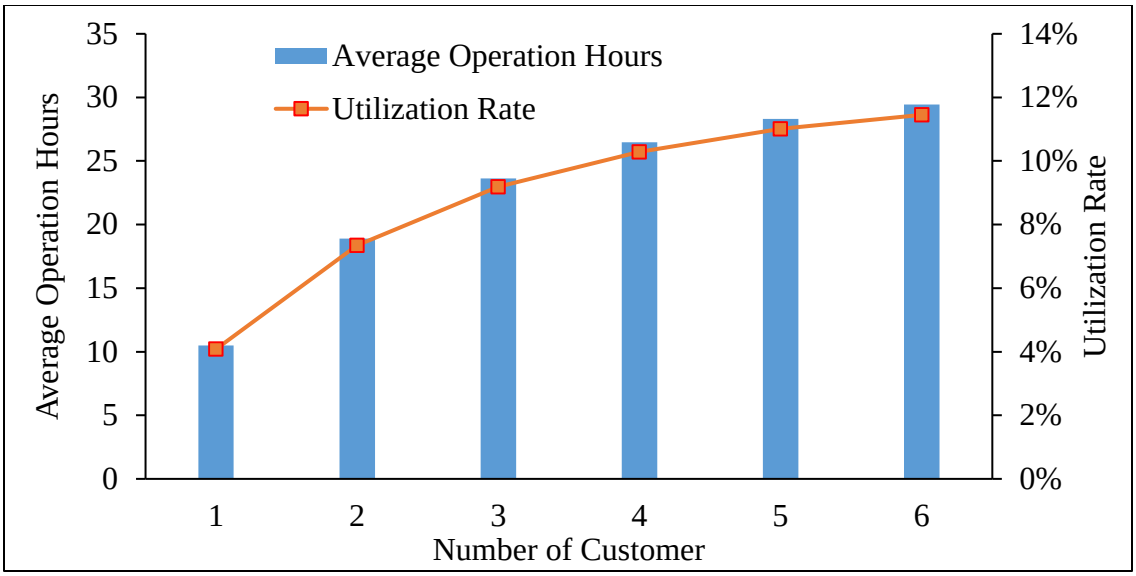

Figure 35. Utilization of BESS in Simple Sharing Network

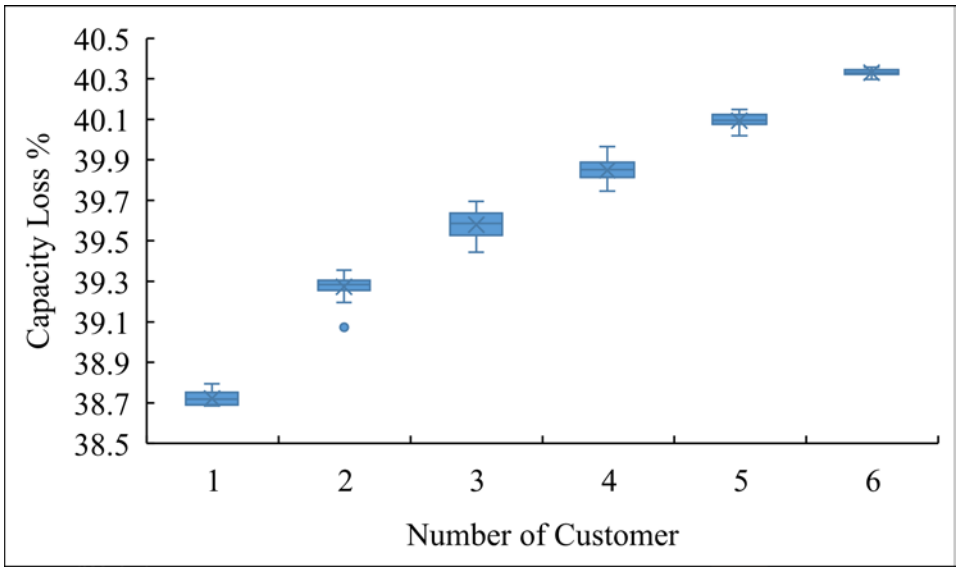

Figure 36. Capacity loss of BESS in Simple Sharing Network

4.1.3.2 Economic Benefit Analysis

At first, results show a larger size of BESS is generally allowed in the simple sharing network. As introduced in Chapter 3, the NSP of the BESS typically needs to be less than 10% to achieve a positive NPV. This NSP is called maximum NSP, which is increasing steadily with the number of customer under simple sharing strategy. It is higher than 18% in the scenario of six customers as shown in Figure 37. Similar results were obtained for the optimized NSP, which is about 4% for single application. The small optimized NSP severely limits the size of BESS and potential savings. With simple sharing, it reaches 8.1% as shown in Figure 38. These NSPs increase mean relatively larger BESS can be applied, hence a higher total NPV can be obtained.

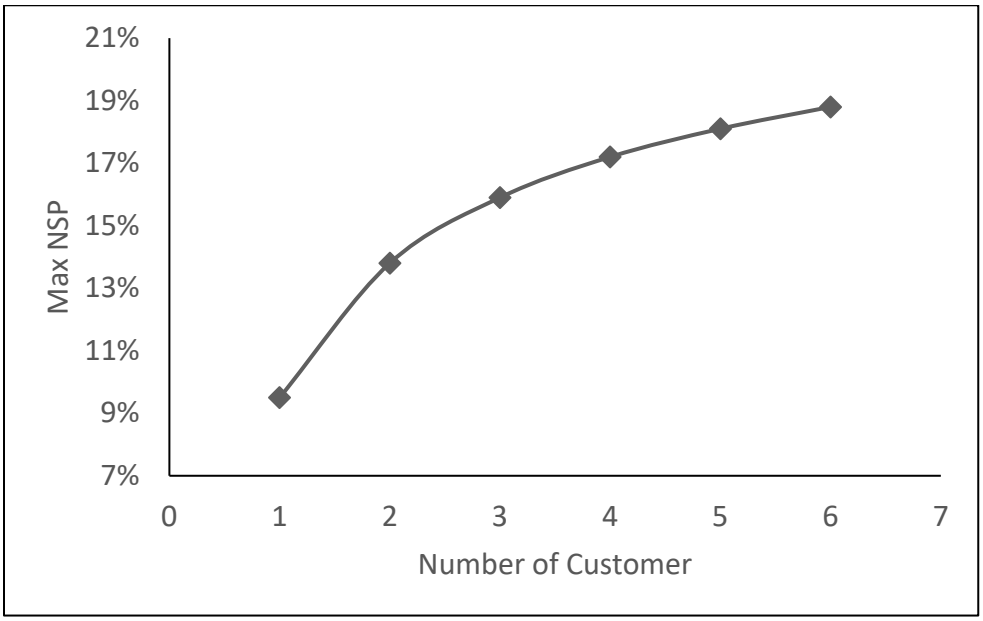

Figure 37. Maximum NSP in Simple Sharing Strategy

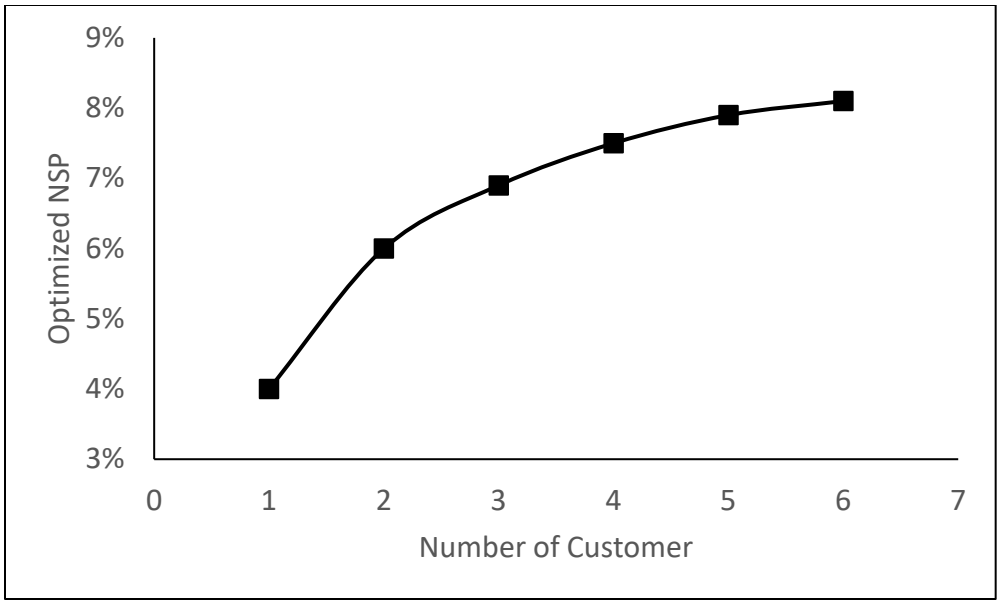

Figure 38. Optimized NSP in Simple Sharing Strategy

Second, NPVU gradually increases with the number of customer. As shown in Figure 39, the average NPVUs are always better in the scenarios with more customers. For example, the average NPVU of single application with NSP of 8% is $85.8, while it is $527.7 in six-customer scenario, which represents 515% improvement. These results demonstrate the great economic potential of sharing strategy. The advantage of sharing is gradually fading with the increase of customer number. The improvement after the number reaches four is insignificant. This phenomenon can be explained more clearly through Figure 40. The relative improvement of adding one more customer decreases with the growing of customer number and is less than 10% when the customer number is higher than four. Because more customers lead to higher system complexity, the optimized customer number should be three or four. However, the number of customer is only the apparent reason of the observing improvements. The stagger peaks of different customers are the primary cause under the surface, which can be explained through analyzing the coincidence factor (CF) of all scenarios. CF is the ratio, expressed as a numerical value or as a percentage, of the simultaneous maximum demand of a group of electrical appliances or

consumers within a specified period, to the sum of their individual maximum demands within the same period. Therefore, lower CF means higher staggering possibility and better NPVU. As shown in Figure 41, the average CF decreases with the increase of customer number, which helps understand why the higher customer number generates more savings. Furthermore, the NPVU values in Figure 39 are average values. In some special cases as shown in Table 10, the NPVU of four-customers scenario with CF of 0.941 is less than that of three-customers scenario with CF of 0.935. This mismatch demonstrates that CF is a better indicator to estimate savings compared with the number of customer. Generally, the optimized CF is around 0.925 according to the simulation results. Moreover, the range of NPVU with more customers is much smaller as shown in Figure 42. There are ten sets of simulations for each scenario. The less diversity of NPVUs at higher customer number scenario indicates the savings are more promising. Therefore, the system reliability is improved with the proposed simple sharing network.

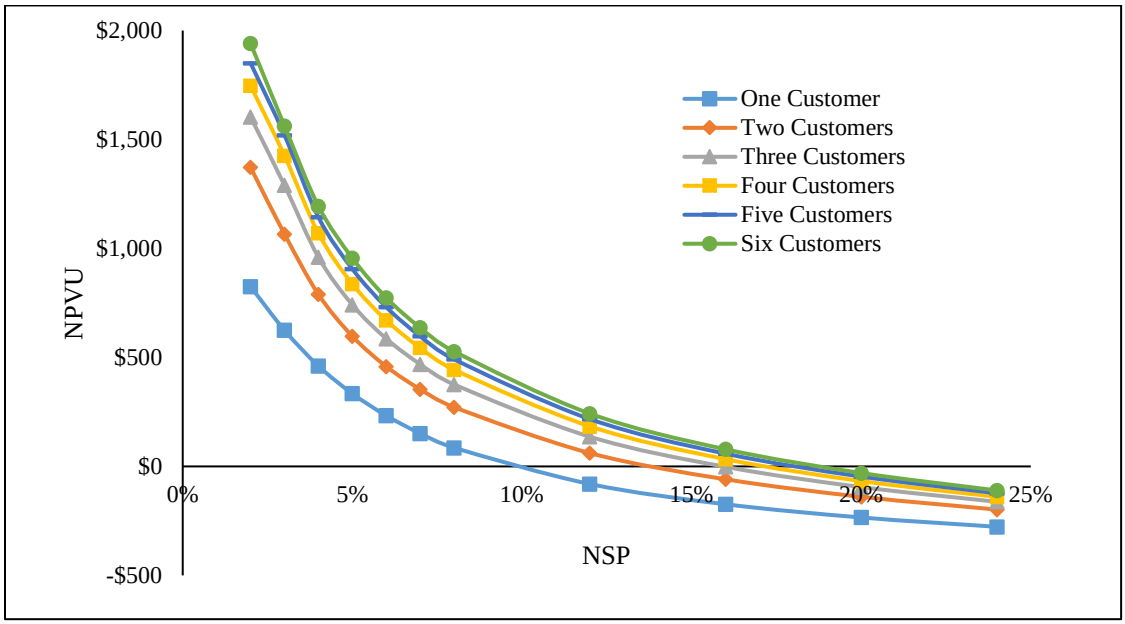

Figure 39. NPVU of the BESS with Different NSP in All Six Scenarios

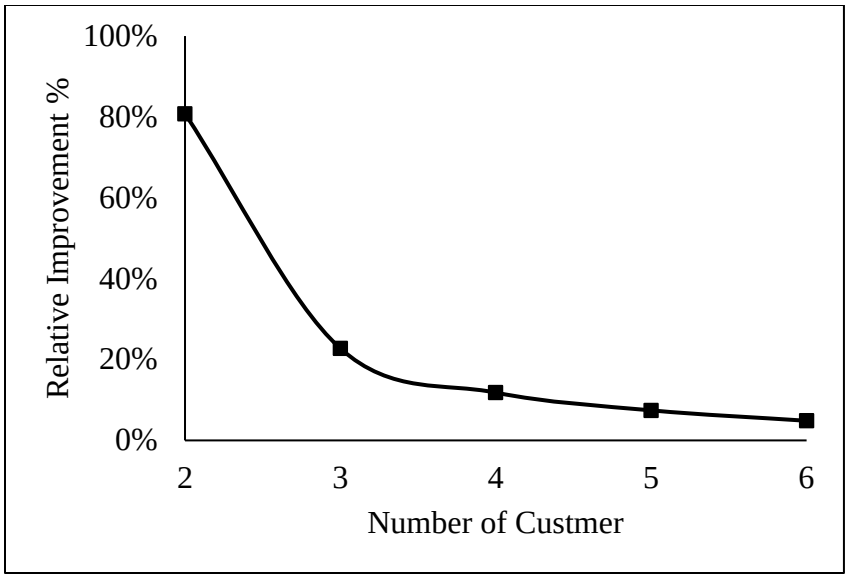

Figure 40. Relative Improvement Percentage with The Increase of Customer Quantity

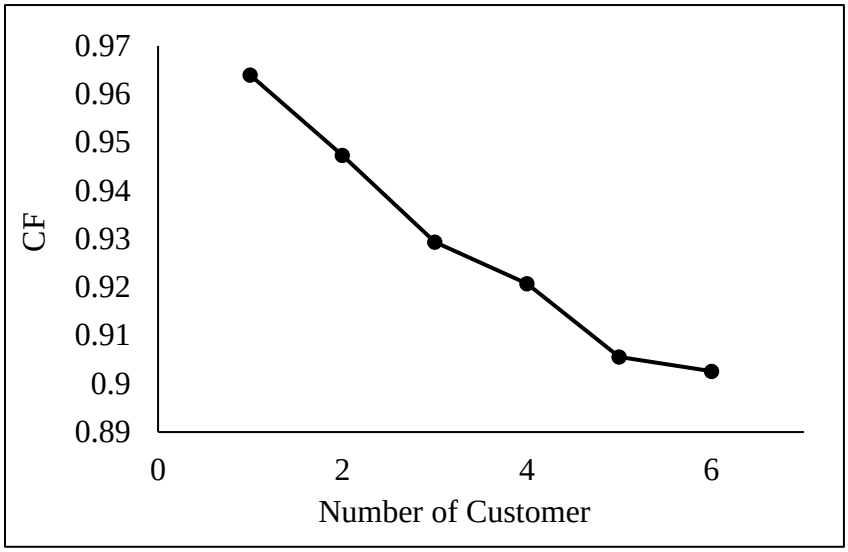

Figure 41. Relationship between Average CF and Number of Customer

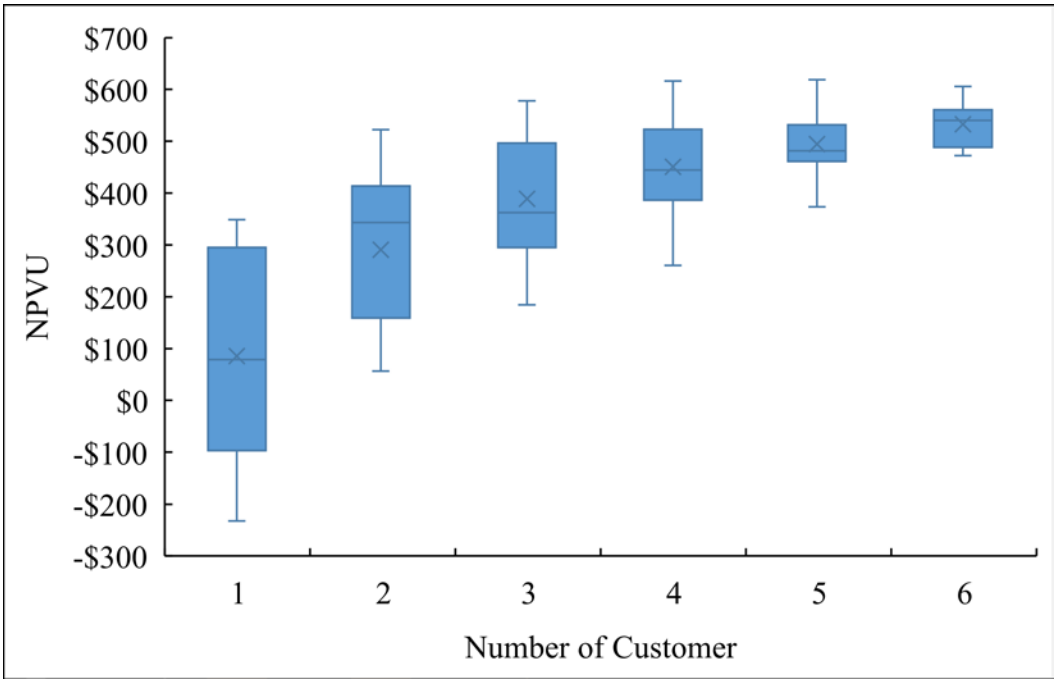

Figure 42. NPVU at Different Scenarios with NSP of 10%

Table 10. Special Cases about CF and Number of Customer

	Scenario 1	Scenario 2
Number of customer	3	4
CF	0.935	0.941
NPVU	$524	$456

4.2 Comprehensive Sharing

Although the simple sharing of BESS is already attractive with improved savings and reliability, it is a challenge to clearly define the ownership. To achieve the best savings, it is better to have three or four customers in one network. Due to the flux of energy consumption, it is hard

to obtain best demand reduction for everyone. Therefore, an improved comprehensive sharing strategy is proposed in this section.

4.2.1 System Structure

As shown in introduction section, the BESS economics can be greatly improved when sharing one battery for several services. However, the utility company and grid are free-riders for the energy storage. Although the BESS can help to achieve distribution and transmission deferral, and energy arbitrage etc., the customer lacks the ability to collect corresponding savings from the other stakeholders. Therefore, the objective of the proposed comprehensive sharing is to simplify the ownership and maximize the sharing. We only include the direct savings for the customers themselves in the calculations. The overall system structure is shown in Figure 43. The whole system is supposed to have modularized operation. Peak shaving is the base function because of its best savings capability. The core optional modules include: TOU application, integration with PTL/T and other possible services. The interaction between each model will be simulated using the BESS model in Chapter 3. All the basic system specifications are the same with the previous sections. The savings improvement potential of each module and the combined benefits will be quantified using case studies.

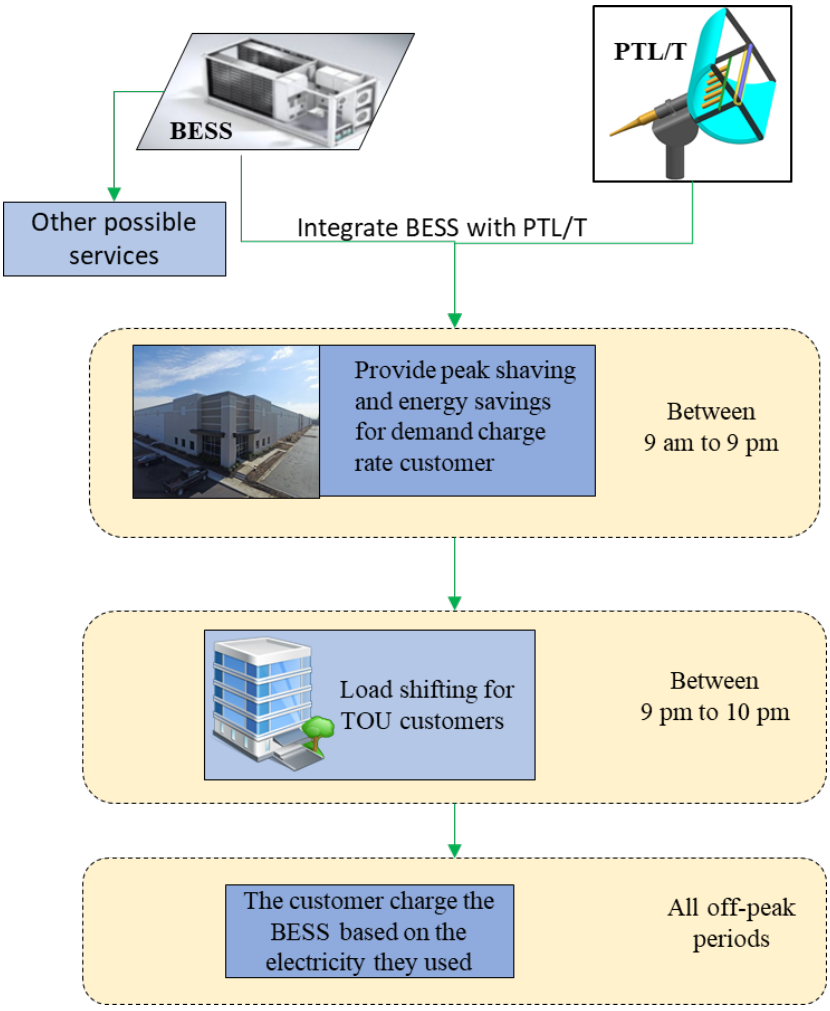

Figure 43. Comprehensive Sharing System Structure

4.2.2 TOU Peak Load Shifting Application

Only demand reduction or peak demand shaving is analyzed in the previous sections. In all the simulations, the BESS is designed and optimized to reduce the peak demand charge of the consumer. Although the electricity rates during on-peak and off-peak are different for the demand charge rate customer, its difference is too low to contribute significant amounts of savings. This situation would change when using BESS for peak load shifting, in which, the savings only comes from utility rate difference between on-peak time and off-peak time. Most of the applications for residential and small commercial buildings fall into this category. Typically, the kWh rate in this

situation is much higher than that of big C&I customer. The control and savings calculation of the BESS in this situation is relatively simple and can be concluded by:

1. Charge the BESS at off-peak hours and discharge to the customer at on-peak hours. The capacity of the BESS is always 100% utilized during on-peak period. There is no direct economic benefit to share BESS for load shifting in multiple customers.
2. The savings is directly linear with the capacity of the BESS and on-peak/off-peak utility rate difference:

$$Unit\ Savings = R_{e,p} \times Eff_d - R_{e,o}/Eff_c \quad (27)$$

where, Unit Savings is the savings per unit BESS ($/kWh). A typical savings estimate is listed in Table 11.

Table 11. Typical Savings from Peak Load Shifting

On-peak rate ($/kWh) [133]	0.20101
Off-peak rate ($/kWh)	0.09137
One-way charge/discharge efficiency	85%
Savings ($/kWh/cycle)	0.063364
Cycling times in ten years	2550
Total lifetime savings	162

It is shown that the savings ($162 per kWh BESS) from load shifting is very low. The simple payback is longer than the lifetime of the BESS, which makes it economically impossible to install BESS for load shifting alone. However, the important advantages of this application are its flexibility and reliability. The BESS can be discharged any time on request as long as it is on-peak time. When the capacity of the BESS is smaller than the total electricity consumption, it can

shift certain amount of electricity usage for each on-peak period without any other constrains. These valuable advantages make the load shifting a perfect complimentary application for peak shaving. It is possible to design a scenario as shown in Figure 43. The BESS is connected to a community transformer to provide load shifting service. Typically, the TOU consumers have the right to choose the peak time schedule for themselves [125]. The options are: 7am to 7pm, 8am to 8pm, 9am to 9pm, and 10am to 10pm. Due to the peak time for demand charge rate is from 9am to 9pm, the 10am to 10pm peak time for TOU rate is chosen for staggering purpose. In this way, the remaining capacity of the BESS can be used for load shifting after 9pm, which provides reliable additional savings without extra initial battery cost. On the other hand, this load shifting does come with a cost of extra battery degradation, which reduces the peak shaving potential. Trade-off between capacity loss influence and load shifting savings is necessary. Therefore, the combined savings was evaluated through case study to demonstrate its feasibility.

At first, the load shifting capacity needs to be calculated. According to the simulation in chapter 3, there is 93% capacity left for the BESS used for peak shaving as shown in Figure 44. The average demand of the 30 big C&I accounts in the database is 211.9kW. Using 80% ΔSOC and 85% discharge efficiency, the remining usable capacity of the BESS after 9pm is about 13.4kWh. On the other hand, the average electricity consumption of 30 TOU accounts between 9pm and 10pm on regular weekdays is calculated to be 10.2 kWh. It means at least two TOU customers is needed under the connected transformer, which is true in most cases in the US. Therefore, all the remained capacity after 9pm should be able to be used for load shifting for TOU customer.

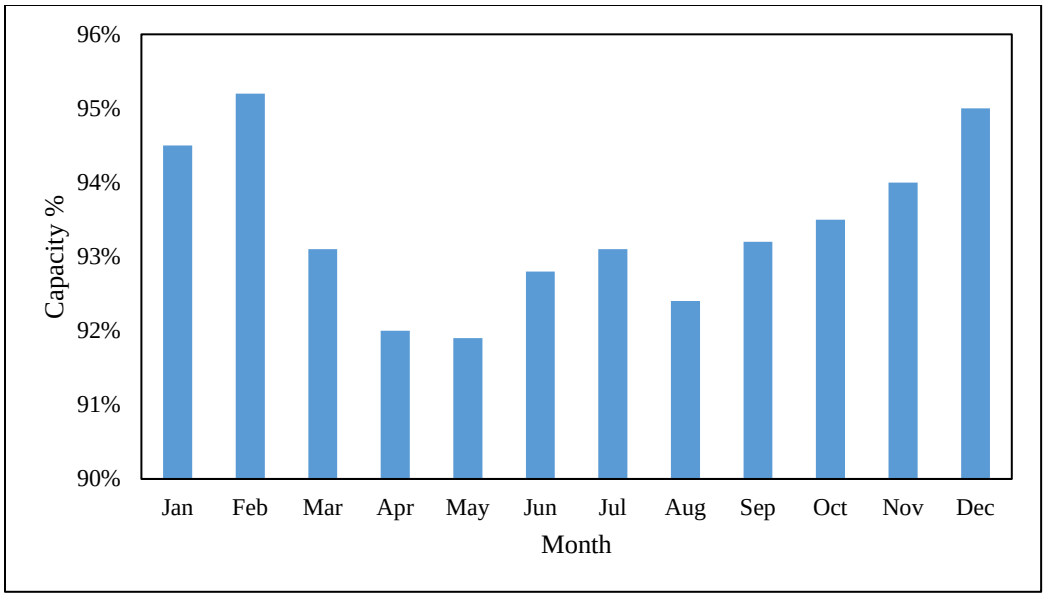

Figure 44. Average Remaining Capacity Percentage of BESS Used for Peak Shavings

Second, simulations were carried out for three sizes of BESSs at the constant 20°C operation temperature to calculate the combined savings. The results are shown in Table 12. Generally, the NPVUs of the BESS are improved in all scenarios. Load shifting can generate considerable positive cash flow for the sharing network. The advantage is more significant for larger NSP due to its small baseline NPVU value. The additional savings from load shifting is relatively stable with an average value of $96. The reason is the savings from load shifting are nearly constant which is only related with BESS itself and utility rate. The extra battery capacity loss caused by load shifting does not significantly reduce the peak demand reduction. With 79.4% NPVU improvement at 10% NSP, the load shifting is a valuable service that can be included in the proposed comprehensive sharing network, especially when the size of the BESS is large. Moreover, the savings from load shifting is almost guaranteed and not influenced by the fluctuation of peak demand, which improves the reliability of the overall system.

Table 12. NPVU Improvement of Adding Load Shifting Function

	NPVU		
Parameters	4% NSP	8% NSP	10% NSP
Only Peak Shaving	$570	$235	$126
Peak Shaving + Load Shifting	$662	$331	$226
Improvement	**16.1%**	**40.9%**	**79.4%**

At last, it is worth mentioning that the proposed load shifting also significantly benefits utility companies because of the "Duck Curve" phenomenon, which represents the imbalance between supply and consumption due to solar energy [134]. As shown in Figure 45, the demand increasingly occurs during the early evening hours after the sun has set, which requires utility company to steeply ramp up generation using peak power plants. This is an increasingly severe challenge due to the rapid development of solar energy. Therefore, the load shifting between 9pm and 10pm is of more special importance for utility companies.

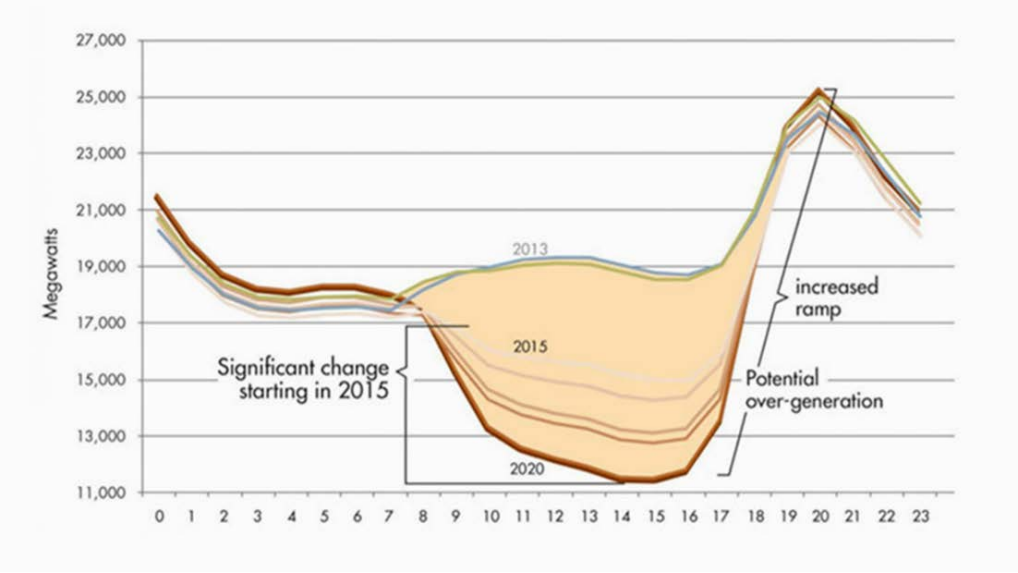

Figure 45. Duck Curve Effect from CAISO [134]

4.2.3 Integration with PTL/T

As presented in introduction section, the benefits of both BESS and renewables can be increased by integrating them together. Therefore, similar advantage should be available for PTL/T system. This section aims to simulate the combination effect of those two systems and evaluate the possible performance improvement. Different with previous sections, NPV is not suitable to be compared herein due to: 1) the NPVUs of BESS and PTL/T have different units. The economic performance of BESS is much better than PTL/T. To optimize the combined NPV will eliminate PTL/T directly; 2) it is hard to distribute the additional savings to each individual system, which makes the separate NPV evaluation difficult. Therefore, the improvement percentage of total cost savings is selected as the performance indicator. Case studies of seven facilities in Wisconsin are carried out.

The simulation structure is shown in Figure 46. At first, to calculate the electricity savings from PTL/T, the optimized unit equipment size and efficiency from Chapter 2 are used directly. The hourly average direct normal irradiance data in Wisconsin is applied. Second, combine the calculated hourly electricity savings and original utility data from customer, a new set of utility data can be generated, which can be used to simulate cost savings using the model presented in Chapter 3. Third, the size of both systems need to match with each other to maximize the improvement. A two-factor three-level experiment is designed to investigate their main impacts, as shown in Table 13. Simulations are carried out for nine scenarios in all seven facilities. The results are compared with the situations when no PTL/T applied to get the improvement percentage of total cost savings.

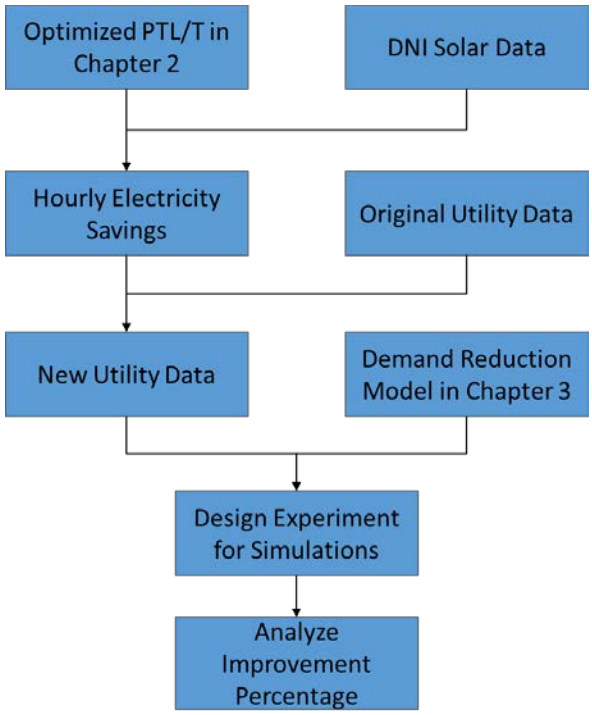

Figure 46: Simulation Structure of Integrating PTL/T with BESS

Table 13: Experiment Design for the Integration of BESS and PTL/T

Factors	Level 1	Level 2	Level
NSP of BESS	4%	8%	12%
Number of PTL/T	3	6	9

Simulation results show a positive relationship between the size of PTL/T and the improvement percentage. The average improvement increases from 14.8% to 35.7%. This can be explained by the higher electricity savings due to the larger solar collector. Although the solar energy is not consistent and subjected to change frequently, its operation time is highly coincident with peak time, which helps to reduce peak demand in general. On the other side, the improvement

percentage decrease with the increase of NSP. The reason is: when NSP increases, the BESS is capable to achieve more demand reduction and cost savings; due to the fact that the combined demand savings does not increase as quick as the baseline demand savings, a negative relationship exists. It means a small BESS should be enough to support PTL/T system to achieve optimized demand reduction. This phenomenon can be further illustrated through the main effects plot as shown in Figure 47. The line for the size of PTL/T is steeper, which indicates it is a more significance impact factor. Overall, simulation results show 12.4% to 43.5% cost savings improvement by combining PTL/T and BESS for peak demand reduction.

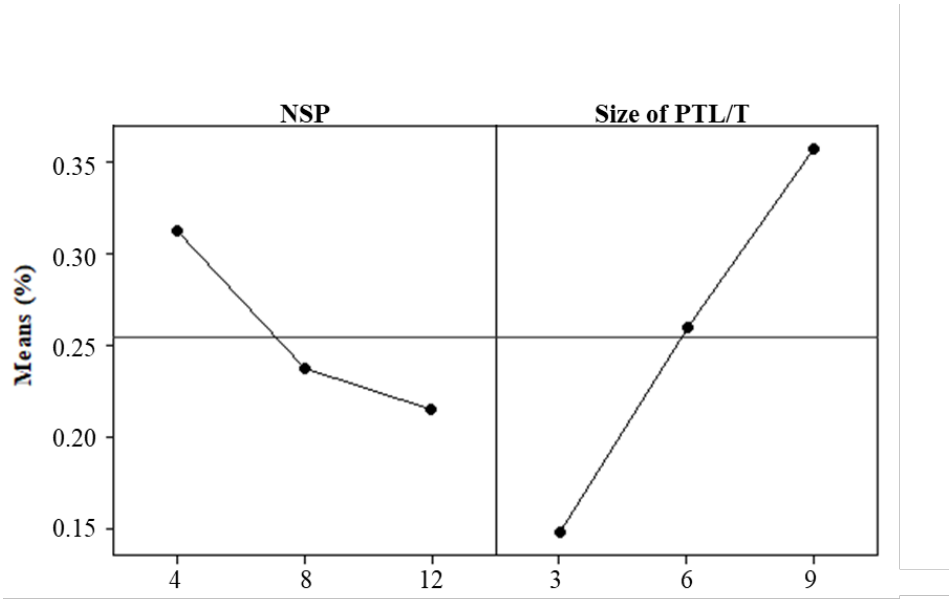

Figure 47: Main Factor Effects Plot for Improvement Percentage

4.2.4 Additional Potential

4.2.4.1 Power Factor Correction

Power Factor (PF) is the ratio between the “active power” that the system uses to produce useful work (in W or kW) and the “apparent power” that the utility company deliveries to the

system (in VA or kVA). It is universally expressed using power triangle as shown in Figure 48. The difference of the apparent power and the active power is known as the reactive power (VAR or kVAR), which is a non-productive power and not recorded by the power meter. Low PF and high reactive power mean less delivered power is used to do productive work. The uncorrected PF of an industrial facility is typically around 80% [135]. The plant with low power factor would need larger transformers and conductors to ensure the adequate power supply for the equipment. Large amount of reactive power could deteriorate the voltage stability of power grids and may cause power outages if the generated power couldn't match what is consumed [136]. To discourage this bad practice, many utility companies charge penalties to low power factor customers and provide incentives for power factor correction projects. Power factor correction usually brings in savings for both the utility companies and the end-use consumers. For utility companies, the benefits include stabilizing the system voltage, mitigating the risk of power outages, and avoiding immediate system upgrades etc. As to the consumers, the benefit is directly reflected on the reduced utility bills through avoided penalties and received incentives.

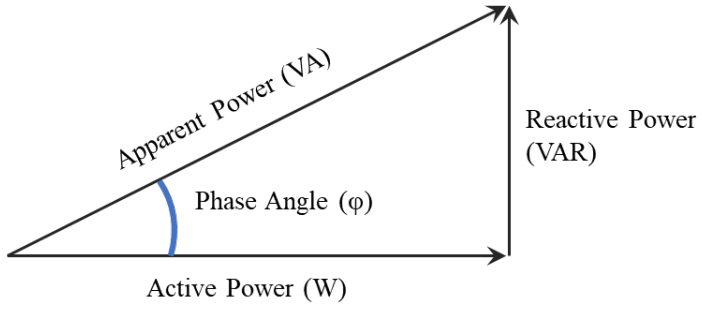

Figure 48. Power Factor Triangle

Traditionally, capacitor banks are used for PF correction. Capacitor banks can be installed at various locations to offset the inductive impact and reduce the excess reactive power. Due to the popularity of solar energy and electric vehicles (EV), using smart bi-directional inverters,

power factor compensation has been proposed and analyzed by researchers. In a smart PV system, the inverter can be configured to produce more reactive power and bring the factory to a unity power factor [137]. In this process, the reactive power capacity of the inverter is used similar to a fast-acting capacitor [138]. The V2G connected bi-directional EV charger is capable of fulfilling reactive power compensation with/without battery power consumption [139]. Specially designed EV inverters can provide optimized PF correction [140, 141]. The basic reason is the existence of a big capacitor in the invertor as shown in Figure 49 [139]. When equipped with proper control module, the inverter can work as well as a separate capacitor bank. Considering the extremely low utilization rate of BESS, its inverter is suitable to be used for PF compensation most of the time. Therefore, it is proposed to include PF correction in the shared network when the power factor is low.

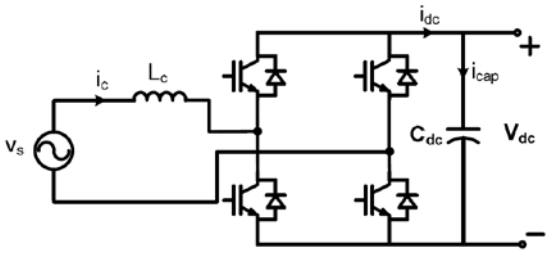

Figure 49. Typical Bi-directional Invertor Structure [139]

The additional potential savings can be calculated using a case study. According to PF policy of We Energies [133], the penalty and incentive can be calculated through:

$$\mathrm{BD}_{0.85} = Actual\ peak\ demand \times [1 + 0.65 \times (0.85 - PF_{uncorrected})] \quad (25)$$

$$\mathrm{BD}_{0.95} = Actual\ peak\ demand \times [1 - 0.5 \times (PF_{corrected} - 0.85)] \quad (26)$$

As introduced in TOU peak load shifting section, the average peak demand of 30 big C&I accounts is 211.9 kW. Using typical uncorrected PF of 0.80 and NSP of 10%, the smart inverter will add $367.3 NPVU for the system as calculated in Table 14.

Table 14. Power Factor Savings Calculation

	Actual Demand (kW)	Inverter Capacity (kVAR)	Power Factor	Billed Demand (kW)	Demand Cost
Existing	211.9	0	0.80	218.8	$3,019.3
Proposed	211.9	21.19	0.84	213.3	$2,943.2
Monthly Savings					$76.0
NPVU increase					**$ 367.3**

4.2.4.2 Combine Meter Effect

To simplify the ownership and operation, the best option is to have single ownership. In this way, the BESS can be solely managed by one shareholder. Nonetheless, single customer doesn't necessarily mean single electricity account. According to the assessment data from IAC in UW-Milwaukee, about 40% of the audited facilities have two or more electricity accounts in the same site. It is the results of organization expansion in the past decades, which is very common in the entire US. Thereby, a sharing network specially designed for this situation is proposed as shown in Figure 50. According to the simple sharing calculation, sharing between two accounts is not enough to get optimized savings but the improvement is impressive. More importantly, sharing one BESS between two accounts owned by one shareholder can achieve "Combining Two Electricity Accounts" effect. Typically, each electricity account is used to determine peak demand during a billing period and the customer is billed for summation of two peak demands. Based on IAC data, this demand charge can be reduced by about 5% through simply combining two accounts. However, due to the extremely high cost of new transmissions when combining accounts, most of

these multi-account facilities feel reluctant to invest on this. If shared between two accounts with on-peak time charging, the BESS is capable of spreading peak demand between two accounts, which helps achieve similar demand reduction as combing meters.

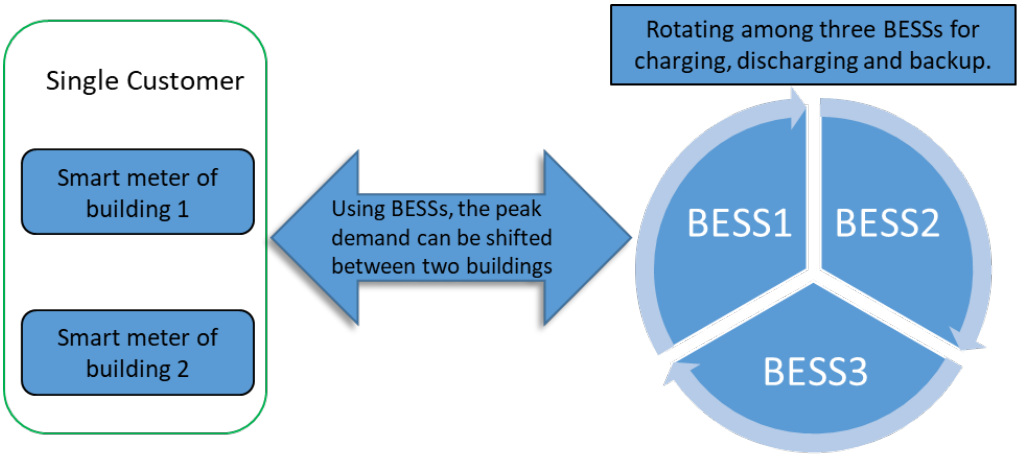

Figure 50. Using BESS to Achieve Combining Meters Benefits

The economic benefit of this special application is simulated through an IAC assessment in Wisconsin. The basic information of the customer is shown in Table 15. The demand reduction results are shown in Figure 51. Compared with using the same BESS for simple sharing without on-peak time charging, the average demand reduction was increased by 85.6%. Meanwhile, the NPVU, the utilization rate and $\sum Ah_i$ were increased by 45.6%, 106.3% and 123.2% respectively, which indicated a great promotion of the savings and utilization. The discharging time is 39.0hours per month in this case, which is already longer than simple sharing one BESS among six customers. The final capacity loss is 42.6%. Therefore, this special sharing situation provides best economic benefit in all scenarios analyzed in the comprehensive sharing network.

Table 15. Basic accounts information

Parameters	Values
Account 1 average peak demand (kW)	172.2
Account 2 average peak demand (kW)	433.2
Average peak demand by combining accounts (kW)	566.1
Peak demand rate ($/kW)	13.8

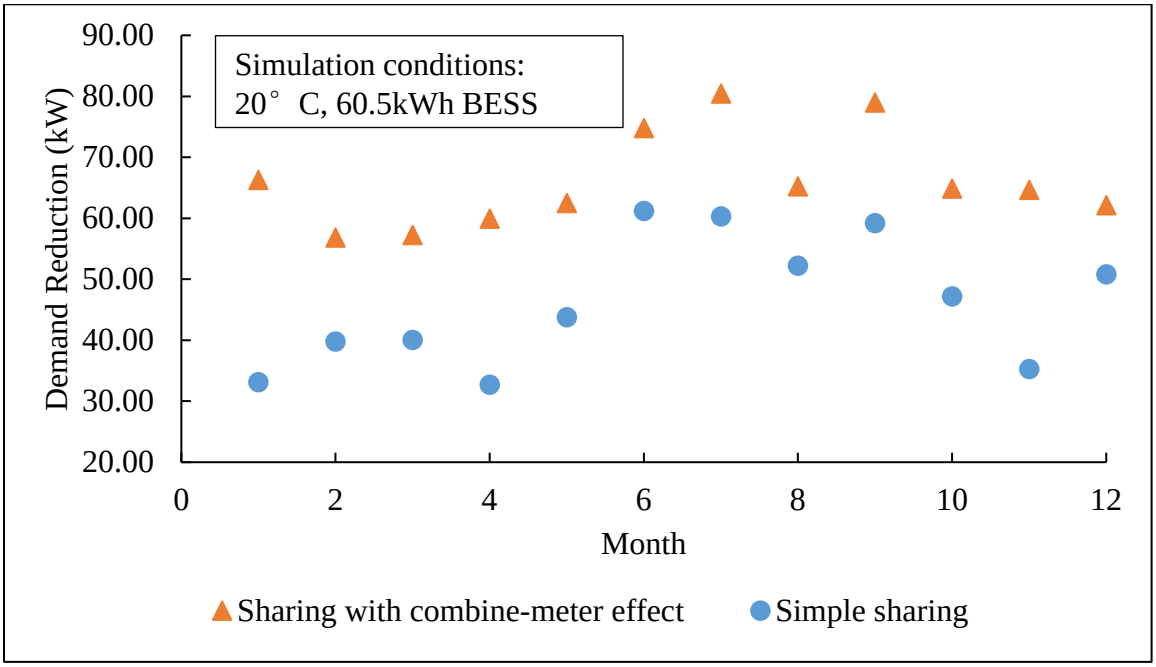

Figure 51. Demand Reduction Improvement in Sharing with Combine-Meter Effect

5. Conclusions

Electricity demand needs to be appropriately managed due to the increasing imbalance between supply side and consumption side. Because of its tremendous advantages compared with traditional demand response system, BESS based DSM for end use customer is thoroughly research in this dissertation.

5.1 Main Contributions to Knowledge

In this thesis, a novel PTL/T system is proposed to increase the solar energy utilization efficiency, the economic characteristic of using battery energy storage system (BESS) for peak demand reduction is evaluated, several new DSMs based on sharing economy are proposed to increase the economic benefits of the BESS, the comprehensive demand reduction potential of combining daylighting and BESS is calculated. The main contributions are summarized as follows:

1. The most significant innovation of PTL/T is the utilization of PTC for daylighting and the combination of daylighting with heat generation. In the proposed system, solar light is split into visible light and IR. The visible light is delivered for indoor lighting and the IR is used for heat generation. The critical components of the proposed system are optimized. The cost of illuminating unit area is expressed as a function of illumination space dimensions and critical components efficiency. The size of the PTL/T module can be optimized on economical basis when applying some basic component specification parameters to the proposed function. The final optimized system specifications were obtained by a case study.

2. According to the case study, the optimized PTL/T is to use a module with $8m^2$ PTC to illuminate $500m^2$ office areas. A 7-fiber bundle composed by 3mm diameter fiber is adopted. The fiber ends are polished in hexagon shape to eliminate heat generation in the entrance of fiber. For the PTC, the aperture is 2,26m, the length is 3.54m, and the rim angle is 90^o. The illumination area is divided into 4 sections. The fiber lengths for each section are 8.6m, 14.2m, 19.8m, and 25.4m respectively. The average combined fiber efficiency is 49%. The overall utilization efficiency of the solar energy is 39.4%. The maximum energy savings and simple payback period of PTL/T are calculated when applying in residential, commercial and industrial sector for different cities. The result shows the commercial sector is the best candidate for the proposed system. The cost savings potential of unit PTL/T in each state is expressed in the map to demonstrate its economic benefit in the US.
3. The economic benefits of using BESS for peak shavings in have been modelled. Detailed battery model is included in the proposed simulation structure. Real utility data from facilities and commercial available equipment data are used for calculations. The impacts of system capacity, battery degradation, environmental temperature and utilization rate are quantified and compared through case studies for the first time. The best NPV of BESS can be obtained when the NSP is around 4%, after which, the NPV decreases with the increase of NSP. Therefore, the benefit of optimizing the size of the BESS is limited by the best NPV. The system is only economically feasible when the NSP is less than 15%. The NPVU is negatively correlated with NSP and highly depends on the utility data. The battery degradation is significant after ten years' operation. Due to the low utilization rate and C rate, the cycling loss is only less than one percent. Therefore, the battery lifetime can only be prolonged by reducing the calendar loss through optimizing the operation temperature.

Higher than 25°C temperature should be avoided because the acceleration of both battery degradation and NPVU reduction. Because the average environmental temperature is right in the range of proper operation temperature, the benefit of optimizing the temperature is only about 7.8% in the US.

4. When used for peak shavings, the utilization rates of the BESS are extremely low when operated at traditional control strategy. The average discharging time is less than ten hours per month. To evaluate the effect of increasing utilization factor, on-peak time charging strategy has been studied. The simulation results show the utilization rate is promoted from 3.6% to 5.6%. The average NPVU are increased by 69.9% with nearly no increase of the battery degradation. Additionally, larger BESS becomes profitable with the increase of utilization rate. Compared with the uncertain impact of NSP and 7.8% limitation from reducing battery degradation, the utilization rate clearly has the most significant impact on the NPVU. Considering there is still great potential of increasing the utilization rate, it is recognized as the dominant factor that impacts the economic benefit.

5. A simple sharing DSM is proposed to increase the utilization rate of the BESS when solely used for peak demand reduction. The demand reduction among all customers is optimized through GA method. Simulation results show larger size of BESS can be applied using the new strategy. The max NSP and optimized NSP reaches 18.8% and 8.1% respectively in six-customer scenario. The NPVU is more than doubled in most cases. According to the trade-off between reliability and savings improvement, three or four customer number should be included in one sharing network.

6. To simplify ownership and maximize savings, a comprehensive sharing DSM is proposed to share one BESS for multiple services. Using peak demand reduction as baseline function,

the TOU peak load shifting application is approved to be a reliable addition to the system with average increase of $96 in NPVU. The demand reduction can be improved by combining daylighting and BESS together because they complement each other. The integration of PTL/T is capable to add another 12.4% to 43.5% more savings. Due to the proposed three services don't significantly interact with each other, they can be simply combined in one network to maximize the total savings.

7. Two extra special opportunities are evaluated for the comprehensive DSM. The smart bi-directional inverter of the BESS can provide PF compensation with extra built in control module, which can add extra $367.3 NPVU to the system. A special operation strategy is designed for the customer who has multiple accounts. According to a case study, combine-meter effect can be achieved with 45.6% increase in NPVU by sharing the BESS with on-peak time charging.

5.2 Future Research Direction

The proposed PTL/T system is still pure theory calculations. Although the economic benefits of the BESS and PTL/T can be improved by a large margin through the sharing strategies proposed in this dissertation, there are still several major barriers for its application. For example, the optimized battery size is still relatively small, which limits the total savings. The uncertainty of electricity consumption causes extra difficulty for the control algorithm. The future work should focus on:

1. Build a prototype of PTL/T system. The feasibility of the proposed structure was already approved. The similar system is being followed by other research team [142]. Integrating PTL/T and LED to provide uniform illumination should be the next step. A prototype needs to be developed to demonstrate its advantage.

2. The proposed peak demand reduction system based on BESS needs to be integrated with building energy management system (EMS). Typically, the EMS is capable to response to peak demand by adjusting the operation of the energy consumption equipment. Therefore, modelling the entire building and integrating the proposed system with EMS is capable to achieve better demand reduction and more reliable control.

3. All the services provided by the BESS in the proposed sharing network are for the customers themselves. The benefits for utility companies and ISO/RTO services are still unclear. It is necessary to evaluate the cost savings for the other stakeholders. The knowledge of this will help the utility companies to design incentive programs to popularize the installation of BESS.

References

1. Balijepalli, V.M., et al. *Review of demand response under smart grid paradigm*. in *Innovative Smart Grid Technologies-India (ISGT India), 2011 IEEE PES*. 2011. IEEE.
2. Nguyen, H.K., J.B. Song, and Z. Han, *Distributed demand side management with energy storage in smart grid.* IEEE Transactions on Parallel and Distributed Systems, 2015. **26**(12): p. 3346-3357.
3. Administration, U.S.E.I., *International Energy Outlook 2016*. 2016.
4. Administration, U.S.E.I. [cited 2018 3/10]; Available from: http://www.eia.gov/tools/faqs/faq.cfm?id=99&t=3.
5. Werring, C.G., *Design and application of fiber optic daylighting systems*. 2009, Kansas State University.
6. Boubekri, M., *Daylighting, architecture and health*. 2008: Routledge.
7. Shi, L. and M.Y.L. Chew, *A review on sustainable design of renewable energy systems.* Renewable and Sustainable Energy Reviews, 2012. **16**(1): p. 192-207.
8. Imenes, A. and D. Mills, *Spectral beam splitting technology for increased conversion efficiency in solar concentrating systems: a review.* Solar energy materials and solar cells, 2004. **84**(1): p. 19-69.
9. Himawari. [cited 2018 3/26]; Available from: http://www.himawari-net.co.jp/e_page22.htm.
10. Beshears, D.L., et al. *Solar Energy, Collected, Concentrated, Transported, and Distributed as Light With No Energy Conversion Via a Hybrid Solar Lighting System*. in *ASME 2007 Energy Sustainability Conference*. 2007. American Society of Mechanical Engineers.
11. Sapia, C., *Daylighting in buildings: Developments of sunlight addressing by optical fiber.* Solar Energy, 2013. **89**: p. 113-121.
12. MAYHOUB, M. and D. CARTER. *Decision making in selecting the best matching hybrid lighting system*. 2011. PLEA.
13. Shen, X., et al. *Analysis of a hybrid cost-effective solar lighting system*. in *SPIE Optical Engineering+ Applications*. 2009. International Society for Optics and Photonics.
14. Kandilli, C., K. Ulgen, and A. Hepbasli, *Exergetic assessment of transmission concentrated solar energy systems via optical fibres for building applications.* Energy and Buildings, 2008. **40**(8): p. 1505-1512.
15. Oh, S.J., et al., *Computational analysis on the enhancement of daylight penetration into dimly lit spaces: Light tube vs. fiber optic dish concentrator.* Building and environment, 2013. **59**: p. 261-274.
16. Ullah, I. and S.-Y. Shin, *Development of optical fiber-based daylighting system with uniform illumination.* Journal of the Optical Society of Korea, 2012. **16**(3): p. 247-255.
17. Shao, L. and J. Callow, *Daylighting performance of optical rods.* Solar energy, 2003. **75**(6): p. 439-445.
18. Couture, P., et al. *Improving passive solar collector for fiber optic lighting*. in *Electrical Power and Energy Conference (EPEC), 2011 IEEE*. 2011. IEEE.
19. Tekelioglu, M. and B.D. Wood, *Solar light transmission of polymer optical fibers.* Solar Energy, 2009. **83**(11): p. 2039-2049.
20. Tekelioglu, M. and B.D. Wood, *Prediction of light-transmission losses in plastic optical fibers.* Applied optics, 2005. **44**(12): p. 2318-2326.

21. Liang, D., et al., *Fiber-optic solar energy transmission and concentration.* Solar Energy Materials and Solar Cells, 1998. **54**(1): p. 323-331.
22. Cheadle, M., *A Predictive Thermal Model of Heat Transfer in a Fiber Optic Bundle for a Hybrid Solar Lighting System*. 2005, University of Wisconsin-Madison.
23. Mayhoub, M.S., *Hybrid lighting systems: performance, application and evaluation*. 2011, University of Liverpool.
24. Price, H. *A parabolic trough solar power plant simulation model*. in *ASME 2003 International Solar Energy Conference*. 2003. American Society of Mechanical Engineers.
25. Patnode, A.M., *Simulation and performance evaluation of parabolic trough solar power plants*. 2006, University of Wisconsin-Madison.
26. Acciona. [cited 2018 3/26]; Available from: http://www.acciona.us/projects/energy/concentrating-solar-power/nevada-solar-one/.
27. Rolim, M.M., N. Fraidenraich, and C. Tiba, *Analytic modeling of a solar power plant with parabolic linear collectors.* Solar Energy, 2009. **83**(1): p. 126-133.
28. Zhang, H. and H. Li, *An energy factor based systematic approach to energy-saving product design.* CIRP Annals-Manufacturing Technology, 2010. **59**(1): p. 183-186.
29. Hu, P., et al., *Optical analysis of a hybrid solar concentrating photovoltaic/thermal (CPV/T) system with beam splitting technique.* Science China Technological Sciences, 2013. **56**(6): p. 1387-1394.
30. Coventry, J., *Simulation of a concentrating PV/thermal collector using TRNSYS.* Made available in DSpace on 2011-01-05T08: 29: 09Z (GMT). No. of bitstreams: 4 simulation_solar_2002. pdf. jpg: 3287 bytes, checksum: a2b51fe8db9ea3d661210f2757a0f49d (MD5) 1783-01.2003-07-23T03: 45: 47Z. xsh: 366 bytes, checksum: 1449b829fb382c7aed977aca29e11bea (MD5) simulation_solar_2002. pdf: 1291404 bytes, checksum: 99c063414faefc0f28f09fc5c94e6649 (MD5) simulation_solar_2002. pdf. txt: 19573 bytes, checksum: 4e356a709071736961f768c2ec69e468 (MD5) Previous issue date: 2004-05-19T13: 00: 51Z, 2002.
31. Carpinelli, G., et al. *Optimal operation of electrical energy storage systems for industrial applications*. in *Power and Energy Society General Meeting (PES), 2013 IEEE*. 2013. IEEE.
32. U.S. Department of Energy. [cited 2018 3/28]; Available from: https://iac.university/download.
33. Schoenung, S., *Energy storage systems cost update.* SAND2011-2730, 2011.
34. Divya, K. and J. Østergaard, *Battery energy storage technology for power systems—An overview*. Electric Power Systems Research, 2009. **79**(4): p. 511-520.
35. Oudalov, A., R. Cherkaoui, and A. Beguin. *Sizing and optimal operation of battery energy storage system for peak shaving application*. in *Power Tech, 2007 IEEE Lausanne*. 2007. IEEE.
36. McLaren, J., et al., *Battery Energy Storage Market: Commercial Scale, Lithium-ion Projects in the US*. 2016, National Renewable Energy Lab.(NREL), Golden, CO (United States).
37. Eller, A. and D. Gauntlett, *Energy Storage Trends and Opportunities in Emerging Markets.* International Finance Corporation (IFC), 2017.

38. Tan, X., Q. Li, and H. Wang, *Advances and trends of energy storage technology in Microgrid.* International Journal of Electrical Power & Energy Systems, 2013. **44**(1): p. 179-191.
39. Nykvist, B. and M. Nilsson, *Rapidly falling costs of battery packs for electric vehicles.* Nature Climate Change, 2015.
40. McLaren, J.A. and S. Mullendore, *Identifying Potential Markets for Behind-the-Meter Battery Energy Storage: A Survey of US Demand Charges*. 2017, National Renewable Energy Laboratory (NREL), Golden, CO (United States).
41. DOE, U. *Global Energy Storage Database*. 2018; Available from: http://www.energystorageexchange.org/projects/data_visualization.
42. Neubauer, J., *Battery Lifetime Analysis and Simulation Tool (BLAST) Documentation*. 2014, NREL/TP-5400-63246. Golden, CO: National Renewable Energy Laboratory. http://www. nrel. gov/docs/fy15osti/63246. pdf.
43. Dong, X., et al., *Optimal Battery Energy Storage System Charge Scheduling for Peak Shaving Application Considering Battery Lifetime*, in *Informatics in Control, Automation and Robotics*. 2012, Springer. p. 211-218.
44. Zanoni, S. and B. Marchi, *Optimal Sizing of Energy Storage Systems for Industrial Production Plants*, in *Advances in Production Management Systems. Innovative and Knowledge-Based Production Management in a Global-Local World*. 2014, Springer. p. 342-350.
45. Lu, C., et al., *Optimal Sizing and Control of Battery Energy Storage System for Peak Load Shaving.* Energies, 2014. **7**(12): p. 8396-8410.
46. Bayram, I.S., et al., *Energy Storage System Sizing for Peak Hour Utility Applications.* arXiv preprint arXiv:1406.4726, 2014.
47. Neubauer, J. and M. Simpson, *Deployment of behind-the-meter energy storage for demand charge reduction.* Golden, CO, 2015.
48. Nataf, K. and T.H. Bradley, *An economic comparison of battery energy storage to conventional energy efficiency technologies in Colorado manufacturing facilities.* Applied Energy, 2016. **164**: p. 133-139.
49. Perez, A., et al., *Effect of Battery Degradation on Multi-Service Portfolios of Energy Storage.* IEEE Transactions on Sustainable Energy, 2016. **7**(4): p. 1718-1729.
50. Greenwood, D.M., et al., *A Probabilistic Method Combining Electrical Energy Storage and Real-Time Thermal Ratings to Defer Network Reinforcement.* IEEE Transactions on Sustainable Energy, 2017. **8**(1): p. 374-384.
51. Fitzgerald, G., et al., *The Economics of Battery Energy Storage: How multi-use, customer-sited batteries deliver the most services and value to customers and the grid.* Rocky Mountain Institute, 2015.
52. Alias, N. and A.A. Mohamad, *Advances of aqueous rechargeable lithium-ion battery: A review.* Journal of Power Sources, 2015. **274**: p. 237-251.
53. Smith, A., et al., *Synergies in blended LiMn2O4 and Li [Ni1/3Mn1/3Co1/3] O2 positive electrodes.* Journal of The Electrochemical Society, 2012. **159**(10): p. A1696-A1701.
54. Fergus, J.W., *Recent developments in cathode materials for lithium ion batteries.* Journal of Power Sources, 2010. **195**(4): p. 939-954.
55. Chiu, K.-C., et al., *Cycle life analysis of series connected lithium-ion batteries with temperature difference.* Journal of Power Sources, 2014. **263**: p. 75-84.

56. Burns, J., et al., *Predicting and Extending the Lifetime of Li-Ion Batteries.* Journal of The Electrochemical Society, 2013. **160**(9): p. A1451-A1456.
57. Lu, L., et al., *A review on the key issues for lithium-ion battery management in electric vehicles.* Journal of power sources, 2013. **226**: p. 272-288.
58. Leadbetter, J. and L. Swan, *Battery storage system for residential electricity peak demand shaving.* Energy and Buildings, 2012. **55**: p. 685-692.
59. Peterson, S.B., J. Whitacre, and J. Apt, *The economics of using plug-in hybrid electric vehicle battery packs for grid storage.* Journal of Power Sources, 2010. **195**(8): p. 2377-2384.
60. Bradbury, K., L. Pratson, and D. Patiño-Echeverri, *Economic viability of energy storage systems based on price arbitrage potential in real-time US electricity markets.* Applied Energy, 2014. **114**: p. 512-519.
61. Masih-Tehrani, M., et al., *Optimum sizing and optimum energy management of a hybrid energy storage system for lithium battery life improvement.* Journal of Power Sources, 2013. **244**: p. 2-10.
62. Yuksel, T. and J.J. Michalek, *Effects of Regional Temperature on Electric Vehicle Efficiency, Range, and Emissions in the United States.* Environmental science & technology, 2015. **49**(6): p. 3974-3980.
63. Pesaran, A., S. Santhanagopalan, and G. Kim, *Addressing the impact of temperature extremes on large format Li-Ion batteries for vehicle applications.* National Renewable Energy Laboratory, 2013.
64. Gelazanskas, L. and K.A.A. Gamage, *Demand side management in smart grid: A review and proposals for future direction.* Sustainable Cities and Society, 2014. **11**: p. 22-30.
65. Strbac, G., *Demand side management: Benefits and challenges.* Energy policy, 2008. **36**(12): p. 4419-4426.
66. Gelazanskas, L. and K.A. Gamage, *Demand side management in smart grid: A review and proposals for future direction.* Sustainable Cities and Society, 2014. **11**: p. 22-30.
67. Chiu, W.-Y., H. Sun, and H.V. Poor, *Energy imbalance management using a robust pricing scheme.* IEEE Transactions on Smart Grid, 2013. **4**(2): p. 896-904.
68. Warren, P., *A review of demand-side management policy in the UK.* Renewable and Sustainable Energy Reviews, 2014. **29**: p. 941-951.
69. Lund, P.D., et al., *Review of energy system flexibility measures to enable high levels of variable renewable electricity.* Renewable and Sustainable Energy Reviews, 2015. **45**: p. 785-807.
70. Palensky, P. and D. Dietrich, *Demand side management: Demand response, intelligent energy systems, and smart loads.* IEEE transactions on industrial informatics, 2011. **7**(3): p. 381-388.
71. Gellings, C.W. 2017 [cited 2017 7/5]; Available from: www.puc.state.pa.us/electric/.../EPRI's%20Energy%20Efficiency%20Initiative.ppt.
72. GTM. *Tesla, Greensmith, AES Deploy Aliso Canyon Battery Storage in Record Time*. 2017 [cited 2018 3/19]; Available from: https://www.greentechmedia.com/articles/read/aliso-canyon-emergency-batteries-officially-up-and-running-from-tesla-green#gs.hH9NroA.
73. Nick Esch, J.F., Brenda Chew, Madison Lynch, *2017 Utility Energy Storage Market Snapshot*. 2017, Smart Electric Power Alliance.
74. Commission, C.P.U. *Self-Generation Incentive Program*. [cited 2018 3/19]; Available from: http://www.cpuc.ca.gov/sgip/.

75. Kempener, R. and E. Borden, *Battery storage for renewables: Market status and technology outlook.* International Renewable Energy Agency, Abu Dhabi, 2015.
76. News, B. *Tesla mega-battery in Australia activated*. 2017 [cited 2018 3/19]; Available from: http://www.bbc.com/news/world-australia-42190358.
77. GTM. *Japan Plans to Pump $700 Million Into Energy Storage*. 2015; Available from: https://www.greentechmedia.com/articles/read/japan-pumps-cash-into-energy-storage#gs.vAaoLck.
78. Bayar, T. *Solar Storage Market Set for Rapid Growth*. 2013 [cited 2018 3/19]; Available from: http://www.renewableenergyworld.com/articles/print/volume-16/issue-2/solar-tech/solar-storage-market-set-for-rapid-growth.html.
79. Alliance, C.E.S. *Energy Storage Industry White Paper 2017*. Available from: https://static1.squarespace.com/static/55826ab6e4b0a6d2b0f53e3d/t/5965bf4e78d171a8390f0cfb/1499840365633/CNESA+White+Paper+2017+wm.pdf.
80. Fitzgerald, G., et al., *The economics of battery energy storage.* Rocky Mountain Institute, 2015.
81. Lombardi, P. and F. Schwabe, *Sharing economy as a new business model for energy storage systems.* Applied Energy, 2017. **188**: p. 485-496.
82. COOPERS, P., *The Sharing Economy. Consumer Intelligence Series*. 2015.
83. Rahbar, K., et al. *Shared energy storage management for renewable energy integration in smart grid*. in *Innovative Smart Grid Technologies Conference (ISGT), 2016 IEEE Power & Energy Society*. 2016. IEEE.
84. Liu, J., et al., *Cloud energy storage for residential and small commercial consumers: A business case study.* Applied Energy, 2017. **188**: p. 226-236.
85. Orehounig, K., R. Evins, and V. Dorer, *Integration of decentralized energy systems in neighbourhoods using the energy hub approach.* Applied Energy, 2015. **154**: p. 277-289.
86. Yao, J. and P. Venkitasubramaniam. *Optimal end user energy storage sharing in demand response*. in *Smart Grid Communications (SmartGridComm), 2015 IEEE International Conference on*. 2015. IEEE.
87. Mégel, O., J.L. Mathieu, and G. Andersson, *Scheduling distributed energy storage units to provide multiple services under forecast error.* International Journal of Electrical Power & Energy Systems, 2015. **72**: p. 48-57.
88. Wang, Z., et al., *Active demand response using shared energy storage for household energy management.* IEEE Transactions on Smart Grid, 2013. **4**(4): p. 1888-1897.
89. Rahbar, K., J. Xu, and R. Zhang, *Real-time energy storage management for renewable integration in microgrid: An off-line optimization approach.* IEEE Transactions on Smart Grid, 2015. **6**(1): p. 124-134.
90. Bortolini, M., M. Gamberi, and A. Graziani, *Technical and economic design of photovoltaic and battery energy storage system.* Energy Conversion and Management, 2014. **86**: p. 81-92.
91. Hamari, J., M. Sjöklint, and A. Ukkonen, *The sharing economy: Why people participate in collaborative consumption.* Journal of the Association for Information Science and Technology, 2016. **67**(9): p. 2047-2059.
92. Zervas, G., D. Proserpio, and J.W. Byers, *The rise of the sharing economy: Estimating the impact of Airbnb on the hotel industry.* Journal of Marketing Research, 2014.
93. DeMaio, P., *Bike-sharing: History, impacts, models of provision, and future.* Journal of Public Transportation, 2009. **12**(4): p. 3.

94. Benjaafar, S., et al., *Peer-to-peer product sharing: Implications for ownership, usage and social welfare in the sharing economy*. 2015.
95. Martin, C.J., *The sharing economy: A pathway to sustainability or a nightmarish form of neoliberal capitalism?* Ecological Economics, 2016. **121**: p. 149-159.
96. Wosskow, D., *Unlocking the sharing economy: An independent review*. 2014, Department for Business, Innovation and Skills. United Kingdom.
97. Fang, B., Q. Ye, and R. Law, *Effect of sharing economy on tourism industry employment.* Annals of Tourism Research, 2016. **57**: p. 264-267.
98. Lapsa, M.V., et al., *Hybrid solar lighting provides energy savings and reduces waste heat.* Energy Engineering, 2007. **104**(4): p. 7-20.
99. André, E. and J. Schade, *Daylighting by optical fiber*. 2002, MSc Thesis 2002: 260, Luleå University of Technology, Sweden.
100. Kalogirou, S., et al., *Design and performance characteristics of a parabolic-trough solar-collector system.* Applied energy, 1994. **47**(4): p. 341-354.
101. Güven, H.M. and R.B. Bannerot, *Determination of error tolerances for the optical design of parabolic troughs for developing countries.* Solar Energy, 1986. **36**(6): p. 535-550.
102. Kalogirou, S. and S. Lloyd, *Use of solar parabolic trough collectors for hot water production in Cyprus. A feasibility study*. Renewable Energy, 1992. **2**(2): p. 117-124.
103. Development, K.R.a. [cited 2018 3/26]; Available from: http://www.koluacik.com/.
104. Co., S.I.L. [cited 2017 12/15]; Available from: http://www.alibaba.com/product-detail/plastic-optic-fiber-for-Lighting_929186630.html.
105. Mayhoub, M. and D. Carter, *The costs and benefits of using daylight guidance to light office buildings.* Building and Environment, 2011. **46**(3): p. 698-710.
106. Muhs, J.D., *Hybrid solar lighting doubles the efficiency and affordability of solar energy in commercial buildings.* CADDET Energy Efficiency Newsletter, 2000(4): p. 6-9.
107. Moan, J., *7 Visible Light and UV Radiation.* Radiation, 2001: p. 69.
108. NREL. [cited 2018 3/26]; Available from: http://www.solarpowerworldonline.com/2010/09/nrel-says-skyfuels-parabolic-troughs-are-73-efficient/.
109. Brooks, M.J., *Performance of a parabolic trough solar collector*. 2005, Stellenbosch: University of Stellenbosch.
110. Stackhouse, P.W. and C. Whitlock, *Surface meteorology and Solar Energy (SSE) release 6.0, NASA SSE 6.0.* Earth Science Enterprise Program, National Aeronautic and Space Administration (NASA), Langley, http://eosweb. larc. nasa. gov/sse, 2008.
111. Administration, U.S.E.I. [cited 2018 1/29]; Available from: http://www.eia.gov/electricity/data.cfm.
112. Agency, U.S.E.P. [cited 2018 3/26]; Available from: http://www2.epa.gov/energy/egrid-subregion-representational-map.
113. *National Solar Radiation Data Base*, N.s.E.S. Center, Editor.
114. Safari, M. and C. Delacourt, *Aging of a commercial graphite/LiFePO4 cell.* Journal of the Electrochemical Society, 2011. **158**(10): p. A1123-A1135.
115. Wang, J., et al., *Degradation of lithium ion batteries employing graphite negatives and nickel–cobalt–manganese oxide+ spinel manganese oxide positives: Part 1, aging mechanisms and life estimation.* Journal of Power Sources, 2014. **269**: p. 937-948.
116. Sanyo. [cited 2018 3/3]; Available from: http://www.meircell.co.il/files/Sanyo%20UR18650W.pdf.

117. Tesla. [cited 2018 3/3]; Available from: https://www.teslamotors.com/powerpack.
118. Lavappa, P.D. and J.D. Kneifel, *Energy Price Indices and Discount Factors for Life-cycle Cost Analysis, 2016*. 2016: US Department of Commerce, National Institute of Standards and Technology.
119. Barré, A., et al., *A review on lithium-ion battery ageing mechanisms and estimations for automotive applications.* Journal of Power Sources, 2013. **241**: p. 680-689.
120. Battke, B., et al., *A review and probabilistic model of lifecycle costs of stationary batteries in multiple applications.* Renewable and Sustainable Energy Reviews, 2013. **25**: p. 240-250.
121. Yu, K., et al., *Thermal analysis and two-directional air flow thermal management for lithium-ion battery pack.* Journal of Power Sources, 2014. **270**: p. 193-200.
122. Sears, J., D. Roberts, and K. Glitman. *A comparison of electric vehicle Level 1 and Level 2 charging efficiency*. in *Technologies for Sustainability (SusTech), 2014 IEEE Conference on*. 2014. IEEE.
123. Hyman, L.S., *America's electric utilities: Past, present, and future.* 1994.
124. Ong, S., P. Denholm, and E. Doris, *The impacts of commercial electric utility rate structure elements on the economics of photovoltaic systems*. 2010: National Renewable Energy Laboratory.
125. Energies, W. [cited 2018 3/26]; Available from: http://www.we-energies.com/pdfs/etariffs/wisconsin/ewi_sheet40-42.pdf.
126. District, S.R.P.A.I.a.P. [cited 2018 3/26]; Available from: https://www.srpnet.com/prices/pdfx/BusE32.pdf.
127. Leng, F., C.M. Tan, and M. Pecht, *Effect of temperature on the aging rate of Li Ion battery operating above room temperature.* Scientific reports, 2015. **5**: p. 12967.
128. NOAA. [cited 2018 3/26]; Available from: https://www.ncdc.noaa.gov/sotc/national/201513.
129. Data, O. 2017.
130. Mitchell, M., *An introduction to genetic algorithms*. 1998: MIT press.
131. Kumar, M., et al., *Genetic algorithm: Review and application.* International Journal of Information Technology and Knowledge Management, 2010. **2**(2): p. 451-454.
132. Ooi, C. and P. Tan, *Genetic algorithms applied to multi-class prediction for the analysis of gene expression data.* Bioinformatics, 2003. **19**(1): p. 37-44.
133. Energies, W. 2018 [cited 2018 3/25]; Available from: http://www.we-energies.com/pdfs/etariffs/wisconsin/elecrateswi.pdf#pagemode=bookmarks.
134. ISO, C., *What the duck curve tells us about managing a green grid.* Calif. ISO, Shap. a Renewed Futur: p. 1-4.
135. Bhatia, A., *Power factor in electrical energy Management.* PDH online course E, 2012. **144**.
136. Hossain, J. and H.R. Pota, *Power system voltage stability and models of devices*, in *Robust control for grid voltage stability: high penetration of renewable energy*. 2014, Springer. p. 19-59.
137. CSES. *Power Factor and Grid-Connected Photovoltaics*. 2015 [cited 2018 3/25]; Available from: https://www.gses.com.au/wp-content/uploads/2016/03/GSES_powerfactor-110316.pdf.
138. Zuercher-Martinson, M., *Smart pv inverter benefits for utilities.* Renewable Energy World, 2012.

139. Kisacikoglu, M.C., B. Ozpineci, and L.M. Tolbert. *Examination of a PHEV bidirectional charger system for V2G reactive power compensation*. in *Applied Power Electronics Conference and Exposition (APEC), 2010 Twenty-Fifth Annual IEEE*. 2010. IEEE.
140. Kisacikoglu, M.C., B. Ozpineci, and L.M. Tolbert. *Effects of V2G reactive power compensation on the component selection in an EV or PHEV bidirectional charger*. in *Energy conversion congress and Exposition (ECCE), 2010 IEEE*. 2010. IEEE.
141. Yilmaz, M. and P.T. Krein, *Review of battery charger topologies, charging power levels, and infrastructure for plug-in electric and hybrid vehicles.* IEEE Transactions on Power Electronics, 2013. **28**(5): p. 2151-2169.
142. Ullah, I. and S. Shin, *Highly concentrated optical fiber-based daylighting systems for multi-floor office buildings.* Energy and Buildings, 2014. **72**: p. 246-261.

CURRICULUM VITAE

Tonghui Li

Education

Ph.D., University of Wisconsin Milwaukee, Mechanical Engineering, May 2018

Master of Science, Hebei University of Technology, Mechanical Engineering**,** Dec. 2010

Bachelor of Science, First Aeronautical College of Air Force, Mechanical Engineering**,** Jul. 2008

Awards and recognitions

Vice President, Association of Energy Engineers in UW-Milwaukee, 2015 to 2017

IAC Student Certificates

CEAS Dean's Scholarship, University of Wisconsin-Milwaukee, 2015

CGSA Mechanical Engineering Scholarship, 2012-2014

Publications

Li, Tonghui, and Chris Yuan. "An optimal design analysis of a novel parabolic trough lighting and thermal system." International Journal of Energy Research (2016).

Li, Tonghui, Fan Yang, and Chris Yuan. "A novel parabolic trough solar lighting and thermal system for building energy efficiency." 2013 IEEE International Conference on Automation Science and Engineering (CASE). IEEE, 2013.

Li, Tonghui, and Chris Yuan. "Numerical Modeling of Specific Energy Consumption in Machining Process." ASME 2013 International Manufacturing Science and Engineering Conference collocated with the 41st North American Manufacturing Research Conference. American Society of Mechanical Engineers, 2013.

Articles under Review and in Preparation

Tonghui Li, Yadan Zeng, Yelin Deng, Chris Yuan, “Battery energy storage system for peak shaving in industrial facility-A comparative economic analysis of key factors”. Ready for submission. Energy.

Conference Presentations

Manufacturing & Processing session, The 8th ASME 2013 Manufacturing Science and Engineering Conference, MSEC2013, Madison, WI, Jun. 10-14, 2013.

2013 IEEE International Conference on Automation Science and Engineering, CASE 2013, Madison, WI, Aug. 17-20, 2013.

Attended Conferences

WEEC World Energy Engineering Congress, Washington, DC, Sep.21-23 2016.

WEEC World Energy Engineering Congress, Orlando, FL, Sep.30th-Oct.1st, 2015.

West Coast Energy Management Congress (EMC), Seattle, WA, June25-26, 2014.